

**Effects of amyloidogenic peptides on the phosphorylation state of
the τ -protein and on the expression of the $\alpha 7$ subunit of the
nicotinic acetylcholine receptor *in vitro***

Inaugural-Dissertation

zur

Erlangung des Doktorgrades

der Mathematisch-Naturwissenschaftlichen Fakultät
der Universität zu Köln

vorgelegt von

Enzo Lain

aus Vicenza

Köln, 2004

Berichterstatter:

Prof. Dr. H. Schröder

Prof. Dr. S. Waffenschmidt

Prof. Dr. S. Korsching

Tag der mündlichen Prüfung: 26.05.2004

ABSTRACT

In Alzheimer's disease, the possible correlation between abnormal deposition of proteins like hyperphosphorylated τ and β -amyloid, cytoskeletal alterations and the deficit in the cholinergic neurotransmission remains to be clarified. In order to investigate the possible links connecting β -amyloid accumulation, τ -hyperphosphorylation and nicotinic receptor expression, embryonic primary hippocampal cultures were incubated with amyloidogenic peptides. $A\beta_{1-42}$, the β -amyloid form with the highest fibrillogenic potential, was used for the experimental approach in this study. Additionally, a shorter form of the peptide, $A\beta_{31-34}$, was employed to investigate its putatively protective action against the impact of $A\beta_{1-42}$.

$A\beta_{1-42}$ caused retraction of dendrites, shrinkage of cell bodies and a decrease in the total amount of MAP2b, without affecting the total number of neurons and their viability. No impact on the τ -phosphorylation sites Ser-202 (antibody AT8), Thr-231 / Ser-235 (antibody AT180), Ser-262 (antibody 12E8) and Ser-396 / Ser-404 (antibody AD2) and on the expression of the $\alpha 7$ -nAChR subunit protein was found. The total number of homomeric $\alpha 7$ -nAChRs and their affinity for [125 I] α -Bgt remained also unaltered.

Upon $A\beta_{31-34}$ incubation cell bodies were swollen in the region of the apical dendrite. These morphological alterations, different from those elicited by $A\beta_{1-42}$, did not involve MAP2 expression changes. In contrast to $A\beta_{1-42}$, the shorter fragment caused a massive hyperphosphorylation of the τ -protein at Ser-202 and at Ser-396 / Ser-404. The expression of the $\alpha 7$ -nAChR subunit, the total number of homomeric $\alpha 7$ -nAChRs and their affinity for [125 I] α -Bgt were unaffected.

As regards the colocalization of the receptor subunit with hyperphosphorylated τ -protein, the $\alpha 7$ -nAChR subunit was present in all AT8- and AD2-positive neurons under $A\beta_{31-34}$ incubation.

In conclusion, the present results show a toxic effect of $A\beta_{1-42}$ on the cytoskeletal structure at concentrations normally present in Alzheimer brains, but raise some doubts about the role of $A\beta_{1-42}$ fibrils as a direct trigger of τ -hyperphosphorylation. As regards $A\beta_{31-34}$, it can not be considered protective with regard to cell morphology. Although it prevents the $A\beta_{1-42}$ -induced retraction of dendrites, it shows own toxic properties.

TABLE OF CONTENTS

1. INTRODUCTION	1
1.1 Key features of Alzheimer's disease	1
1.2 Neuronal nicotinic acetylcholine receptors (nAChRs)	2
1.2.1 Structure	3
1.2.2 Cholinergic innervation, nAChR distribution and function	4
1.2.3 nAChRs and Alzheimer's disease	5
1.3 β-amyloid	6
1.3.1 β -amyloid formation	6
1.3.2 β -amyloid, neurodegeneration and Alzheimer's disease	7
1.3.3 β -amyloid and nAChRs	8
1.4 τ-protein	9
1.4.1 Structure and functions	9
1.4.2 τ -protein and Alzheimer's disease	10
1.5 Hippocampal primary cultures as a model for Alzheimer's disease	11
1.6 Aim of the project	13
2. MATERIALS AND METHODS	14
2.1 Antibodies	14
2.1.1 Primary antibodies	14
2.1.2 Secondary antibodies and markers	15
2.2 Media and buffers	15
2.2.1 Cell culture	15
2.2.2 Electrophoresis and Western blot	16
2.3 Radioactive material	16
2.4 Technical equipment	17
2.4.1 Microscopes	17
2.4.2 C.A.S.T.-Grid system	17
2.5 Cell culture	17
2.5.1 Dissection of the hippocampus	
2.5.2 Preparation of the cell suspension	17
2.5.3 Cell plating	18

2.5.4 Medium change	19
2.5.5 Incubation	19
2.5.6 Fixation	19
2.6 Cytotoxicity assay	20
2.7 Immunocytochemistry	20
2.7.1 Immunoperoxidase staining	20
2.7.2 Immunofluorescence	21
2.7.3 Assessment of neuron numbers	21
2.7.4 Immunoreactive area measurement	22
2.8 Cell extract	23
2.9 Protein estimation	23
2.10 Electrophoresis	24
2.11 Western blot	24
2.12 Receptor binding assay	24
2.13 Data bank search	25
2.14 Statistical evaluation	25
3. RESULTS	26
<hr/>	
3.1 Neuron labeling in cell culture	26
3.2 $\alpha 7$- and $\beta 2$-nAChR subunit immunoreactivity in cultured neurons	27
3.3 Effect of Ab₁₋₄₂ on cultured neurons	28
3.3.1 Neuron morphology and number	28
3.3.2 LDH determination	30
3.3.3 Morphological measurements	31
3.3.4 Quantitative determination of MAP2 isoforms	31
3.4 Effect of Ab₁₋₄₂ on the phosphorylation state of the τ-protein	34
3.4.1 Immunocytochemistry	34
3.4.2 Western blot analysis	38
3.5 Effect of Ab₁₋₄₂ on the expression of the $\alpha 7$-nAChR subunit	42
3.5.1 Immunocytochemical findings	42
3.5.2 Quantitative determination	42
3.5.3 Receptor binding assay	44
3.6 Effect of Ab₃₁₋₃₄ on cultured neurons	46
3.6.1 Neuron morphology and number	46

3.6.2 LDH determination	47
3.6.3 Morphological measurements	48
3.6.4 Quantitative determination of MAP2 isoforms	49
3.7 Effect of Ab₃₁₋₃₄ on the phosphorylation state of the t-protein	50
3.7.1 Immunocytochemistry	51
3.7.2 Western blot analysis	54
3.8 Effect of Ab₃₁₋₃₄ on the expression of the α7-nAChR subunit	58
3.8.1 Immunocytochemical findings	58
3.8.2 Quantitative determination	59
3.8.3 Receptor binding assay	60
3.9 Colocalization of the α7-nAChR subunit with hyperphosphorylated t-protein	61
3.10 Summary of results	62
Results: Appendix	63
4. DISCUSSION	64
4.1 Effects of Ab₁₋₄₂	64
4.1.1 Cell morphology	65
4.1.2 Phosphorylation state of the τ -protein	66
4.1.3 α 7-nAChRs	68
4.2 Effects of Ab₃₁₋₃₄	69
4.2.1 Cell morphology	70
4.2.2 Phosphorylation state of the τ -protein	70
4.2.3 nAChRs	71
4.2.4 Possible mechanisms of action of A β ₃₁₋₃₄	71
4.3 Colocalization of the α7-nAChR subunit with hyperphosphorylated t-protein	72
4.4 Conclusions	72
5. ZUSAMMENFASSUNG	74
6. REFERENCES	76

ABBREVIATIONS

Ach	acetylcholine
AD	Alzheimer's disease
APP	amyloid precursor protein
A β	β -amyloid
α -Bgt	alpha-bungarotoxin
BSA	bovine serum albumin
C.A.S.T.	computer assisted stereological toolbox
CNS	central nervous system
Cy	cyanine
DMSO	dimethyl sulfoxide
DTT	dithiothreitol
E18, E19	embryonic day 18, 19
EDTA	ethylenediaminetetraacetic acid
HEPES	N-2-hydroxyethylpiperazine-N'-2-ethanesulfonic acid
IgG	immunoglobulin G
-ir	immunoreactive
LDH	lactate dehydrogenase
Kd	dissociation constant
MAPs	microtubule associated proteins
mRNA	messenger ribonucleic acid
MW	molecular weight
nAChRs	nicotinic acetylcholine receptor
NADH/NAD ⁺	nicotinamide adenine dinucleotide (reduced / oxidized)
NFTs	neurofibrillary tangles
P10	post-natal day 10
PBS	phosphate buffered saline
PHFs	paired helical filaments
PMSF	phenylmethyl sulphonyl fluoride
Pro	proline
Pr-IGLL	propionyl-(Isoleucine-Glycine-Leucine-Leucine)
PS	presenilin
RT	room temperature

R _{TOT}	total number of binding sites
SEM	standard error of the mean
SDS	sodium dodecyl sulfate
Ser	serine
TBS	Tris buffered saline
Thr	threonine
Tris	tris-(hydroxymethyl) aminomethane
TTBS	0.1% Tween 20 / Tris buffered saline

1. INTRODUCTION

1.1 Key features of Alzheimer's disease

Although in the last twenty years a plethora of knowledge about Alzheimer's disease (AD) has been accumulated and an exponentially increasing amount of data has been produced, many crucial questions about its neuropathology remain open. The absence of early diagnostic tools and the lack of animal models, which have only recently become available, are the main problems that scientists have been facing in the investigation of the possible mechanisms leading to neuronal dysfunction in AD.

Historically, the characterization of the disease had been based on post-mortem histopathological observations, which point to (1) extracellular deposition of β -amyloid ($A\beta$) and (2) intracellular formation of neurofibrillary tangles (NFTs) as the hallmarks of the Alzheimer's pathology (for review see Drouet et al., 2000).

(1) $A\beta$, generated by proteolytic cleavage of the ubiquitous expressed amyloid precursor protein (APP) (Kang et al., 1987), is the major constituent of mature plaques, in which it is surrounded by dystrophic neurites and infiltrates of reactive astrocytes and microglia (Busciglio et al., 1995). $A\beta$ is either directly toxic to cultured neurons or able to increase their vulnerability to excitatory neurotoxins (Koh et al., 1990; Mattson et al., 1993). Several groups agree that there is a strong correlation between the toxicity and the aggregation state of the peptide: the neurodegeneration seems in fact to require the formation of fibrils, while the amorphous aggregates would not be toxic (Arriagada et al., 1992; Lorenzo and Yankner, 1994; Busciglio et al., 1995; Lorenzo et al., 2000).

(2) Neurofibrillary tangles are composed of self-aggregated hyperphosphorylated tau protein (τ), a member of the group of the microtubule associated proteins (MAPs), and their spreading throughout the brain correlates with the severity of the disease (Grundke-Iqbal et al., 1986).

The identification of a precise sequence of events connecting $A\beta$ deposition and tangle formation would obviously play a key role in the understanding of the pathology, but nobody has so far provided such evidence, even though some studies have already shown the capability of $A\beta$ to induce and increase τ -phosphorylation in cultured neurons (Takashima et al., 1993; Busciglio et al., 1995), and to accelerate the formation of neurofibrillary tangles (NFTs) when injected in transgenic mice expressing the P301L mutant human τ -protein (Götz et al., 2001).

The most prominent clinical change in AD patients is a cognitive deficit caused most likely by the degeneration of cholinergic fibers arising from the forebrain and projecting to the cortex (Whitehouse et al., 1981; Rosser et al., 1982). Therefore many attempts have been made in order to restore the cholinergic activity in patients affected by the disease. At first the attention was focused on choline acetyltransferase (ChAT) and particularly on acetylcholinesterase (AChE), which are the enzymes responsible for acetylcholine (ACh) synthesis and breakdown, respectively. The treatment with cholinesterase inhibitors showed palliative effects on symptoms and some trend to slow the progression of the disease (Nordberg and Svensson, 1998; Giacobini, 2000; Van den Berg et al., 2000). Only later, as it was noticed that the administration of nicotine to experimental animals (Levin, 1992; Blondel et al., 2000; Grottick and Higgins, 2000) and to non-diseased human subjects (Wesnes and Warburton, 1983) improves attention and memory-related tasks, nicotinic acetylcholine receptors (nAChRs) began to attract the interest of scientists as possible therapeutical targets (Newhouse et al., 1997; Lloyd et al., 1998; for review see Wevers and Schröder, 1999). It is therefore of great interest to understand if, and eventually how, A β and hyperphosphorylated τ -protein may influence the cholinergic system at the level of nAChRs.

In this study attention will be focused on the effect of amyloidogenic peptides on τ -protein phosphorylation state and on nAChR distribution and expression, in order to get new insights into possible correlations between these events.

1.2 Neuronal nicotinic acetylcholine receptors (nAChRs)

Transmitter-gated ion channels, like nAChRs, are transmembrane receptor proteins allowing the propagation of electric signals between nerve cells and their targets at the level of the chemical synapse. Neurotransmitters released from the nerve terminal interact with the ligand-binding domain of the receptor on the cell surface, thus triggering transient conformational changes in the structure that result in the opening of the gate in the membrane-spanning pore (for review see Sine, 2002). Although much information has been obtained about the relative positions of individual amino acids in the membrane-spanning segments of nAChRs and about their roles in affecting ion transport, the first successful attempts to determine the detailed three-dimensional structure of the receptor and the conformational change mechanisms leading to the ion-influx have only recently been carried out (Miyazawa et al., 2003).

1.2.1 Structure

nAChRs belong to the superfamily of ligand-gated ion channels which includes γ -aminobutyric acid A ($GABA_A$), glycine, and serotonin 3 (5-HT₃) receptors. They exist as a variety of subtypes in the mammalian brain, formed as pentamers from different combinations of genetically distinct subunits. Nine distinct alpha subunits ($\alpha 2$ - $\alpha 10$) and three beta ($\beta 2$ - $\beta 4$) have been shown to assemble to a pentameric structure so far, but not all the possible combinations were found (Lustig et al., 2001; for reviews see Role, 1992; Sargent, 1993). Nucleotide and amino acid sequences are similar in all nAChR subunits: each subunit consists of an N-terminal extracellular domain, four transmembrane domains (M1-M4), with an extended intracellular loop between the third (M3) and the fourth (M4) of them, and of an extracellular C-terminal tail. The amino acid sequence of the cytoplasmic loop represents the unique feature of the individual nAChR subunits, while the second transmembrane domain of every subunit forms the channel pore (for review see Lindstrom et al., 1995) (Fig.1).

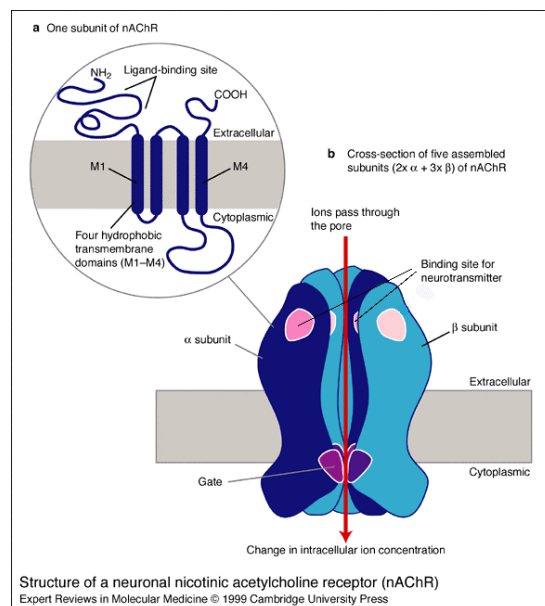


Fig.1: Schematic view of a nicotinic acetylcholine receptor (nAChR). Five subunits, inserted into the membrane structure, form the channel complex (b). The neurotransmitter binding sites are located in the α -nAChR subunits. In (a), a single subunit with its N-terminal large hydrophilic domain, its four transmembrane domains and the loop is represented.

The $\alpha 7$ -nAChR subunit is the only subunit in the human central nervous system (CNS) able to form homomeric pentameric receptors, whereas the other subunits are always assembled in heteromeric combinations. Such a variety of nAChR subunits results in a

great diversity of functional nAChRs expressed throughout the CNS, which show distinct pharmacological and biophysical properties (for review see Albuquerque et al., 1997).

There is strong evidence that transmembrane receptors are associated with lipid microdomains called lipid rafts, enriched in sphingolipids and cholesterol (Simons and Ikonen, 1997), which avoid the lateral diffusion of receptors in the membrane phospholipidic bilayer. nAChRs are also thought to be inserted in this environment, as already shown for the $\alpha 7$ -nAChR subunit (Brusés et al., 2001).

1.2.2 Cholinergic innervation, nAChR distribution and function

The cholinergic system provides diffuse innervation to practically all parts of the brain and a small number of cholinergic nuclei send input to different brain areas (for reviews see Kasa, 1986; Woolf, 1991). Three major cholinergic projection subsystems can be identified. The first one arises from neurons in the pedunculo-pontine tegmentum and the laterodorsal pontine tegmentum and provides innervation to the thalamus, midbrain areas and also to the brain stem. The second one arises in the basal forebrain and sends projections mainly throughout the cortex, while the third one comes from the septum and innervates the hippocampus. A relatively low number of cholinergic neurons can in general give rise to projections reaching broad areas and can consequently influence a relatively high number of neuronal structures (for review see Dani, 2001).

In neurons, nAChRs are located pre- and postsynaptically. Their prominent presynaptic role is to modulate the release of neurotransmitters - nAChRs are in fact able to increase the release of almost all examined neurotransmitters (McGehee et al., 1995; Gray et al., 1996; Wonnacott, 1997; Li et al., 1998; Radcliffe et al., 1999) - while at the postsynaptic side they are responsible for direct excitation. Although the glutamatergic system is overwhelming in this way, nicotinic transmission can modulate the excitability of groups of neurons in different brain areas: besides their direct synaptic role, nAChRs can therefore influence neuronal circuits in a broader sense (for review see Dani, 2001).

As regards the individual subunit composition, the $\alpha 4\beta 2$ and $\alpha 7$ receptor subtypes are numerically the most abundant ones in the mammalian CNS (Lukas et al., 1999). Mapping studies indicate that nAChRs are present throughout the hippocampus (Perry et al., 1993), which plays a central role in learning and memory, and *in situ* hybridization shows that the $\alpha 7$ - and $\beta 2$ -nAChR subunits in particular are highly expressed in this area (Zarei et al., 1999).

When two molecules of ACh interact with their binding sites, located in the α -subunits of the receptor complex (Fig.1), the ion channel opens up for several milliseconds, allowing cations to enter the cell. The resulting ion influx can lead to a local depolarization of the membrane and produce an intracellular ionic signal. Sodium and potassium are the cations carrying most of the nAChR current, but calcium can also play a significant role. nAChR-mediated calcium entry can assume biological importance because it is different from the calcium influx through voltage-gated calcium channels or through the N-methyl-D-aspartate (NMDA) subtype of glutamate receptors. Compared with the latter two, which require membrane depolarization to pass current freely, nAChR-mediated calcium influx can exhibit a different voltage dependence: nAChRs do function at negative potential, thus providing a strong voltage force driving cations into the cell. The distribution of the incoming calcium depends on the location of nAChRs on the cell surface (for review see Dani, 2001).

1.2.3 nAChRs and Alzheimer's disease

The role of nAChRs becomes of main importance when considering the pathogenesis of the disease. Biological changes may lead to neurotransmitter release alterations and circuit excitability abnormalities (for review see Dani, 2001). In AD patients, measurements of the nAChR binding sites using nicotinic ligands have repeatedly shown a decrease in their number (Newhouse et al., 1997; for review see Wevers and Schröder, 1999). The loss of binding sites in diseased brains was confirmed by autoradiography of [3 H]nicotine, showing decreased binding in all cortical layers, particularly in the deepest ones (Nordberg and Winblad, 1986; Whitehouse et al., 1988). Looking at individual nAChR subunits, a remarkable decrease in the amount of α 4-nAChR protein, analyzed by quantitative immunohistochemistry (Wevers et al., 2000) and Western blotting (Burghaus et al., 2000), has already been demonstrated by our group in the cerebral cortex of AD patients in comparison with age-matched controls, while the α 7-nAChR protein shows a minor reduction. Although the most common type of central nervous nAChRs is represented by the association of the β 2- with the α 4-nAChR subunit, as previously mentioned (see 1.2.2), the level of the β 2-nAChR subunit seems, in contrast to the α 4-nAChR findings, not to be altered (Guan et al., 2000). The fact that the nAChR mRNA distribution and the density of neurons expressing the nAChR transcripts in AD cortices did not show significant differences in comparison to controls suggests that the decrease in the number of nAChRs may be the result of post-translational events (Wevers et al.,

1999; for review see Wevers and Schröder, 1999). Colocalization studies and in situ hybridization showed that the $\alpha 4$ - and $\alpha 7$ -nAChR subunit proteins and their transcripts exhibit a different behavior as to their histotopographical relation with regard to plaques and tangles: while both proteins and transcripts are still present in close vicinity or even inside of amyloid plaques, they disappear from almost all tangle-bearing neurons (Wevers et al., 1999; Wevers et al., 2001).

1.3 b-amyloid

1.3.1 β -amyloid formation

A β originates from the amyloid precursor protein (APP), which is a single transmembrane polypeptide. APP is expressed in a number of cell types, most notably in neurons, but its function remains unknown, although it is thought to be involved in many cellular mechanisms, including neurotrophic activity, synaptogenesis, modulation of neuronal excitability, protection against toxic insults and signal transduction functions. The extracellular N-terminal domain of APP represents the longest part of the structure, ranging between 590 and 680 amino acids, while the C-terminal cytoplasmic domain has normally only 47 amino acid residues. Approximately one half of the A β_{1-42} sequence lies extracellularly, while the other half, containing hydrophobic residues, lies within the phospholipidic bilayer. APP, during normal cellular metabolism, is processed by at least three different enzymes. These enzymes, indicated as α -, β - and γ - secretases, cut the protein sequence at distinct positions. A β_{1-42} is formed, together with A β_{1-40} , when γ -secretase APP-cleavage follows the β -cleavage, while the α -secretase pathway, cutting the A β sequence in the middle, prevents its formation (for review see Mattson, 1997) (Fig.2). The γ -secretase-mediated proteolytic cleavage of the APP C-terminal fragment seems to be influenced by presenilin-1 (PS1), a highly conserved transmembrane protein, point mutations of which are a major cause of familial Alzheimer's disease (De Strooper et al., 1998).

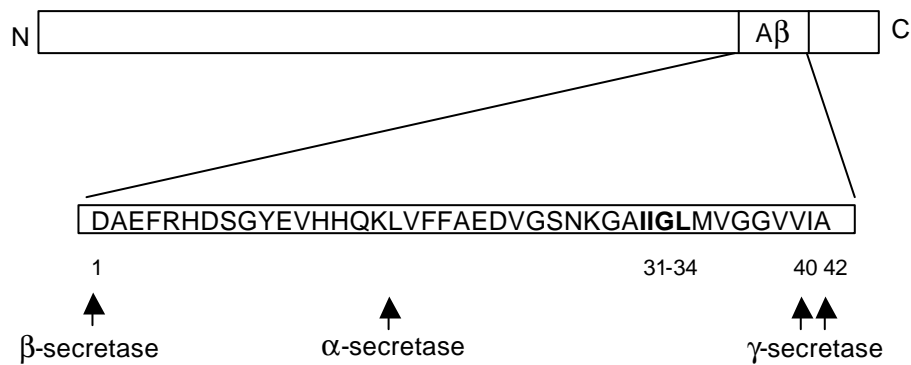


Fig.2: a-, b- and g-secretase are the enzymes involved in APP cleavage. a-secretase cleaves the sequence at position 17 of the A β fragment, which can, consequently, not be released in its entire form. The release of A β_{1-40} and/or A β_{1-42} occurs when the action of g-secretase, acting at position 40 and/or 42 of A β , follows the b-secretase cleavage, which takes place at position 1 (Small and McLean, 1999).

1.3.2 β -amyloid, neurodegeneration and Alzheimer's disease

A β is cleared from the brain under normal conditions, but during aging, and to a much greater extent in AD, its propensity to form fibrils prevails. Several mechanisms can be involved in A β toxicity. The peptide can not only suppress neuronal signaling by affecting receptor transduction and/or transmitter production, but also increase cell vulnerability to different metabolic and excitotoxic insults. In fact, in cell culture it has been demonstrated that the formation of A β fibrils may be accompanied by generation of oxyradicals, membrane damage, impairment of membrane transport systems and disruption of ion homeostasis (for review see Mattson, 1997).

As regards AD, some observations suggest that A β , besides its role as a pathological hallmark (amyloid plaques), is directly involved in the neurodegenerative process.

The first observation is that mutations of the APP gene on chromosome 21 may lead to AD, and that individuals carrying an extra copy of this chromosome due to trisomy 21 (Down's syndrome) present a higher number of plaques when compared with non-diseased subjects if they live beyond their thirties. Furthermore, other early onset AD mutations, including presenilin-1 (PS1) and presenilin-2 (PS2), are associated with increased A β production (Carter and Lippa, 2001).

In comparison with the short-tailed A β_{1-40} , A β_{1-42} is more neurotoxic, has a lower solubility and a greater tendency to form fibrils (Busciglio et al., 1995). A β_{1-42} can also act as a

“seed” for A β ₁₋₄₀ fibril formation. Early diffuse amyloid plaques and age-related plaques in cognitively normal subjects are composed predominantly of A β ₁₋₄₂ (Carter and Lippa, 2001; for review see Mattson, 1997).

A great number of A β -related peptides have been studied to get hints about the mechanisms of amyloid cytotoxicity. Among these peptides, which exhibit different levels of toxicity, the synthetic peptide propionyl-IIGL (Pr-IIGL), an analogue of the region 31-34 of A β (see Fig.2), was in contrast reported to protect cultured astrocytes from A β ₁₋₄₂-induced changes in calcium metabolism (Laskay et al., 1997).

1.3.3 β -amyloid and nAChRs

Amyloid plaques, as already mentioned, are extracellular deposits. The extracellular accumulation of the peptide could, however, be a secondary step in the progression of events and follow its internalization, as recent studies have shown (Gouras et al., 2000). It has been hypothesized that the α 7-nAChR subunit might play a fundamental role in the intracellular accumulation of A β ₁₋₄₂ (Nagele et al., 2002). The first hints in this direction came from the high binding affinity of A β ₁₋₄₂ for the receptor subunit (Wang et al., 2000). Subsequently, it was noticed that the internalization seems to take place particularly in those cells, like the pyramidal neurons, which are rich in the α 7-nAChR subunit (Nagele et al., 2002). Moreover, it was demonstrated that cells transfected with the α 7-nAChR subunit exhibit a lower viability after A β incubation in comparison with their non-transfected counterparts, and that α 7-nAChR subunit inhibitors (e.g. α -bungarotoxin) prevent intracellular A β accumulation (Nagele et al., 2002). By contrast, other authors reported a possible protective action of α 7-nAChRs against A β cytotoxicity, as selective antagonists of this receptor subtype reduce the protective effect of nicotine on A β cytotoxic effects (Shimohama and Kihara, 2001). Although these findings are contradictory, they all suggest an interplay between the α 7-nAChR subunit and A β , which may represent a crucial step in the series of events leading to the A β -induced cellular damage. A further investigation of this possible interaction is therefore required to extend the knowledge about the mechanisms of A β cytotoxicity.

1.4 τ -protein

1.4.1 Structure and functions

In the human brain, one single gene gives rise to six τ -protein isoforms by alternative splicing. These isoforms, which range from 352 (fetal form) to 441 amino acids, differ in the presence of none, one or two 29 amino acid inserts encoded by exons 2 and 3 (the insert encoded by exon 3 is never present without the insert encoded by exon 2) in the N-terminal domain, in combination with either 3 (R1, R3 and R4) or 4 (R1-R4) repeats in the C-terminal domain (R2 encoded by exon 10) (Fig.3).

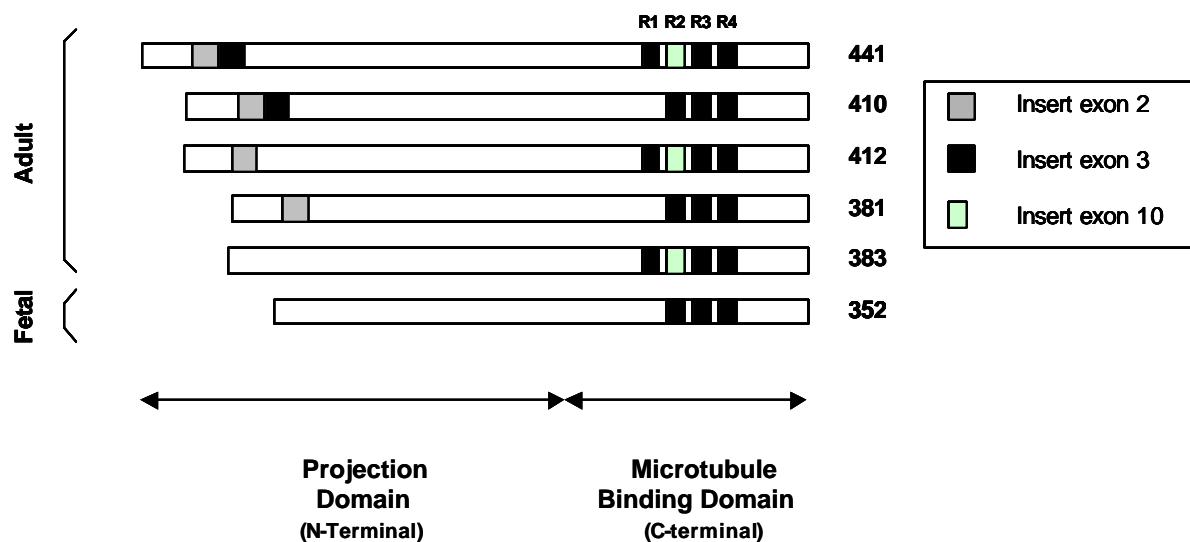


Fig.3: Representation of the six τ -protein isoforms expressed in the human brain, deriving from alternative splicing of a single gene (Buée et al., 2000).

The C-terminal portion (repeats plus flanking regions) represents the “microtubule binding domain”, while the N-terminal portion of the protein is indicated as “projection domain” and determines the spacing between microtubules (Friedhoff et al., 2000; for review see Buée et al., 2000).

As regards the amino acid composition, τ -protein residues are mostly charged and hydrophilic and the protein displays a natively unfolded structure. τ -protein, which is usually enriched in axons (Binder et al., 1985), normally stabilizes microtubules for their role in the development of cell processes, establishment of cell polarity and intracellular transport (Drewes et al., 1998).

1.4.2 τ -protein and Alzheimer's disease

In AD, the normal balance between τ -kinases and τ -phosphatases seems to be disturbed and the phosphorylation state of the τ -protein therefore abnormal (for reviews see Mandelkow et al., 1995; Trojanowski and Lee, 1995). τ -protein distribution correlates with its phosphorylation state (Li and Black, 1996; Mandel and Banker, 1996) and in AD it mislocalizes from the axon to the somatodendritic compartment of neurons (Braak et al., 1994). Hyperphosphorylated τ -protein can in fact lose its capability to bind microtubules and aggregate into paired helical filaments (PHFs), which subsequently assemble to form NFTs. The phosphorylation at the C-terminal microtubule assembly domain seems to play an important role in this process. At least thirty phosphorylation sites have been described in the τ -protein structure, mainly localized outside the microtubule binding domain. They can be broadly subdivided into two classes: several Ser-Pro or Thr-Pro motifs occur in both regions flanking the internal repeats and are targets of different enzymes (for review see Mandelkow and Mandelkow, 1998) (Fig.4).

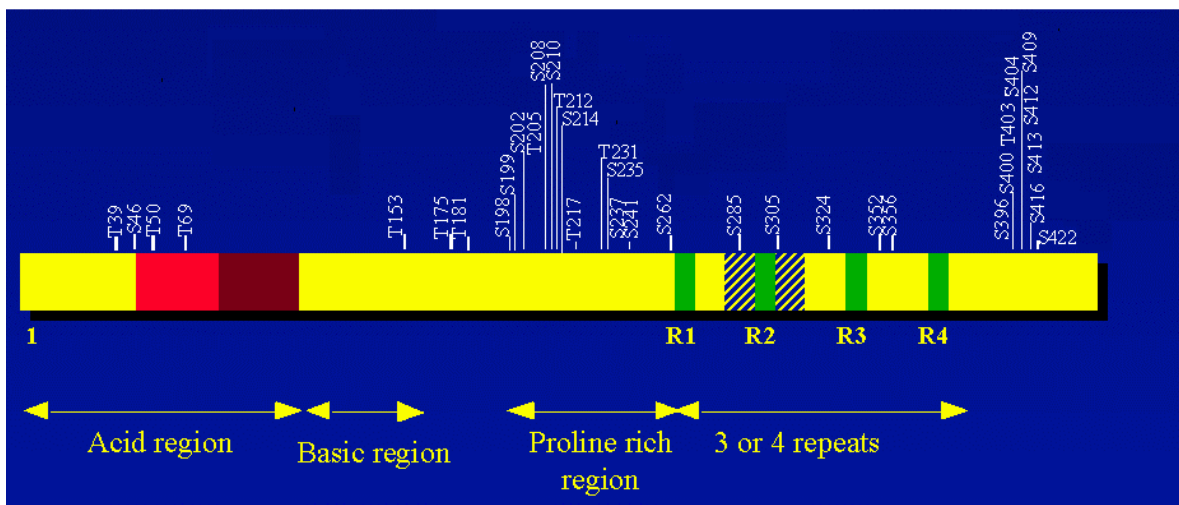


Fig.4: Phosphorylation sites are distributed along the entire structure of the τ -protein. Different enzymes are responsible for the phosphorylation in different regions of the sequence (Mandelkow and Mandelkow, 1998).

Mitogen activated protein kinase (MAPK), glycogen synthase kinase 3 (GSK-3), protein kinase A (PKA), τ -tubulin kinase, Ca^{2+} /calmodulin-dependent protein kinase type II (CaMKII) and cyclin-dependent kinases including cdc2 and cdk5 have been proven to be involved in the phosphorylation of the τ -protein (Pei et al., 1998; Bennecib et al., 2001; for review see Buée et al., 2000). It has also been shown that distinct enzymes target

different τ -phosphorylation sites. It is therefore very important to know at what sites the possible $A\beta$ -induced phosphorylation may be prominent in order to understand what mechanisms are responsible for this effect. So far, most studies in this field have been performed on brain slices. In the present study, the use of primary cultures will allow to investigate the involvement of these pathways at the cellular level.

τ -protein interacts not only with microtubules and other cytoskeletal elements, but also with the plasma membrane (Hirokawa et al., 1988; Brandt et al., 1995), where nAChRs are located. τ -phosphorylation can modulate the properties of τ -protein and influence its functions. Alterations of the τ -protein phosphorylation state could therefore provoke changes at the membrane level, although it is still completely unknown whether this event may also have an impact on the nAChR subunit distribution within the phospholipidic bilayer. Moreover, cytoskeletal changes induced by τ -hyperphosphorylation can affect the transport of vesicles and of organelles along the microtubules, leading to various problems, e.g. energy deficits and vulnerability against oxidative stress (Ebner et al., 1998; Trinczek et al., 1999; Stamer et al., 2002).

1.5 Hippocampal primary cultures as a model for Alzheimer's disease

In this study, rat embryonic hippocampal neurons in low-density culture have been used as an *in vitro* model to study the expression of nAChRs and τ -phosphorylation state under conditions which mimic certain aspects of AD.

The hippocampus is a source of a rather homogeneous population of neurons with well-characterized properties typical of CNS neurons in general (Goslin et al., 1998). Pyramidal-like neurons, the principal cell type in the hippocampus, have been estimated to account for 85% to 90% of the total neuronal population and they are similar to each other in many fundamental respects, even if they can differ from one another in some of their aspects (Goslin et al., 1998). In E18 to E19 fetal rats, from which our culture is prepared, the generation of pyramidal neurons is essentially complete, while the generation of dentate granule cells has scarcely begun (Schlessinger et al., 1978).

An advantage of this model is that the low density facilitates the quantitative and morphological analysis (Goslin et al., 1998). Moreover, strong similarities between neurite dystrophy in AD and $A\beta_{1-42}$ -induced neurite dystrophy in hippocampal neuronal cultures have been observed (Pike et al., 1992). On the other hand, a limitation in the study of AD is constituted by the fact that the formation of amyloid plaques from fibrillogenic $A\beta$ and

the aggregation of hyperphosphorylated τ -protein into neurofibrillary tangles are long lasting processes which do not occur spontaneously *in vitro* and may require additional age-related factors not present in fetal cell cultures (Busciglio et al., 1995). The standardized experimental conditions mimic to some extent the first stages of the Alzheimer's disease, where $A\beta$ fibrils start to aggregate but the formation of plaques has not begun (Busciglio et al., 1995). Using this model it is therefore possible to analyze selectively the impact of $A\beta$ and/or conditions leading to τ -protein hyperphosphorylation on properties of the cytoskeleton and nAChR expression.

1.6 Aim of the project

In Alzheimer's disease, the possible correlation between abnormal deposition of proteins like hyperphosphorylated τ and β -amyloid, cytoskeletal alterations and the deficit in the cholinergic neurotransmission remains to be clarified. Incubation of embryonic primary hippocampal cultures with amyloidogenic peptides will allow for the investigation of possible links connecting β -amyloid accumulation, τ -hyperphosphorylation and nicotinic receptor expression. $A\beta_{1-42}$, being the β -amyloid form with the highest fibrillogenic potential, will be used for the experimental approach in this study. Additionally, the shorter synthetic peptide propionyl-IIGL, analogue of the region 31-34 of $A\beta$, will be employed in order to investigate its possible protective action against the impact of $A\beta_{1-42}$, as previously reported by studying $A\beta$ -induced calcium metabolism changes in cultured astrocytes (Laskay et al., 1997) and $A\beta$ -induced increase in the concentration of extracellular glutamate and aspartate in the magnocellular nucleus basalis of the rat (Harkany et al., 1999). During this work, it will be referred to this peptide as $A\beta_{31-34}$.

The following questions will be addressed in this study :

1. Cytoskeletal structure and τ -phosphorylation state

- a) Does the incubation with amyloidogenic peptides influence the neuron morphology and the neuronal cytoskeletal structure?
- b) Is there an increase in the level of τ -phosphorylation at different phosphorylation sites after treatment and how is the abnormal phosphorylated τ -protein distributed?

2. nAChR

- a) Are the expression and compartmentalization of the single nAChR subunits altered by the presence of the two different $A\beta$ fragments?
- b) Are nAChR subunits affected by τ -hyperphosphorylation?

2. MATERIALS AND METHODS

2.1 Antibodies

2.1.1 Primary antibodies

a) to the cytoskeletal proteins

		<u>source</u>	<u>manufacturer / reference</u>
• monoclonal:	AT8	mouse	Immunogenetics
	Tau-1	mouse	Roche
	AD2	mouse	Dr. Delacourte, University of Lille, France (Buée-Scherrer et al., 1996)
	AT180	mouse	Immunogenetics
	12E8	mouse	Dr. Seubert, Elan Pharmaceutical Inc. San Francisco, USA (Seubert et al., 1995)
	MAP2 (clone HM2)	mouse	Sigma

b) to the nAChR subunits

		<u>source</u>	<u>manufacturer / reference</u>
• monoclonal :	α 7-nAChR (mAb306)	mouse	Dr. Lindstrom, University of Pennsylvania, USA (Dominguez del Toro et al., 1994)
	• polyclonal:	α 7-nAChR (H-302)	rabbit
	β 2-nAChR	rabbit	Dr. Schütz, University of Cologne (Schütz, 1999)
	α 4-nAChR	guinea pig	Chemicon

c) used as neuronal markers for:

		<u>source</u>	<u>manufacturer / reference</u>
-pyramidal cells			
• monoclonal :	SMI32	mouse	Sternberger
-glutamatergic cells			
• polyclonal :	VGLUT1	guinea pig	Chemicon

2.1.2 Secondary antibodies and markers

	<u>source</u>	<u>manufacturer</u>
Anti-mouse IgG	goat	Dako
Anti-rabbit IgG	goat	Dako
Anti-guinea pig IgG	rabbit	Vector
Anti-mouse IgG Cy2-conjugated	goat	Jackson
Anti-rabbit IgG Cy3-conjugated	goat	Jackson
Streptavidin Cy-3		Amersham
Streptavidin-biotinylated horseradish peroxidase complex		Amersham

2.2 Media and buffers

2.2.1 Cell culture

-PBS (10X) pH 7.4

1.5 mM KH_2PO_4
 1.5 M NaCl
 2.7 M Na_2HPO_4
 in distilled water

-TBS pH 7.5

50 mM Tris
 150 mM NaCl
 in distilled water

-Isolation medium

20 mM HEPES (2% v/v HEPES 1M)
 in Dulbecco's modified Eagle Medium
 (with sodium pyruvate, 4.5 g/l glucose, pyridoxine)

Gibco™, Invitrogen Corporation
 Gibco™, Invitrogen Corporation

-Culture medium

1% Glutamate
 1% Penicillin/Streptomycin
 0.5 mM Glutamine (0.25% v/v Glutamine 200mM)
 2% B27 Supplement
 in Neurobasal Medium (without L-glutamine)

Sigma
 Gibco BRL, Life Technologies
 Gibco BRL, Life Technologies
 Gibco BRL, Life Technologies
 Gibco™, Invitrogen Corporation

2.2.2 Electrophoresis and Western blot

-Electrophoresis buffer

25 mM Tris
2.5 M Glycine
0.1% SDS
in distilled water

-Transfer buffer

25 mM Tris
150 mM Glycine
20 % Methanol
in distilled water

-Sample buffer

- SDS-mix solution : 1 ml Tris 1M pH 6.8
 4 ml SDS 10%
 5mg Bromophenol Blue
 2 ml Glycerol
 1 ml distilled water

- DTT 1M

Sample buffer was prepared before use mixing DTT and SDS-mix (1:4)

-Coomassie Blue

0,1 g Coomassie Blue
100 ml Methanol
33 ml Acetic acid
distilled water to 200 ml

2.3 Radioactive material

(3-[¹²⁵I]iodotyrosyl)α-Bungarotoxin
Specific activity: 5.5 TBq / mmol

Amersham

Chemical compounds were purchased from the companies Sigma, Merck, Promega, Pierce, Amersham and Serva.

2.4 Technical equipment

2.4.1 Microscope

To examine the immunocytochemical staining the Olympus Vanox AHB3 photo-microscope was used. The filter sets employed were “41007a filterblock for Cy2” and “41007a filterblock for Cy3” (AF-analysentechnik). The microscope is equipped with a DVC-1300 C RGB Color camera. Photos were taken using 40 x 2.5 magnification.

2.4.2 C.A.S.T.-Grid system

The **C**omputer **A**ssisted **S**tereological **T**oolbox (C.A.S.T.) is composed of a PC with installed stereology software (Olympus, Denmark), a SVHS video camera, a microscope equipped with a motorized specimen stage for automatic sampling, a multi-control unit for the control of the joystick movement (x- and y-axis) and of the focus (z-axis).

2.5 Cell culture

2.5.1 Dissection of the hippocampus

Brains of E18 to E19 Wistar fetal rats (local breeding) were collected in isolation buffer on ice (procedure conducted in accordance with the law for the prevention of cruelty to animals). Hippocampi were mechanically dissected from the brains (Fig.5) as described previously (Banker and Cowan, 1977; Goslin et al., 1998).

2.5.2 Preparation of the cell suspension

Hippocampi were collected in a 50 ml centrifuge tube containing isolation medium and maintained on ice. The medium was then poured off and the hippocampi treated with 5 ml 0.05% trypsin-0.02% EDTA (Gibco™, Invitrogen Corporation) for 15 min at 37°C under slight agitation and rotation (60 strokes/min) to allow the dissociation of the tissue. Trypsin was then discarded and the hippocampi washed three times with isolation medium. The resulting suspension (about 4 ml) was homogenized by gentle up-and-down pipetting using a long Pasteur pipette and its volume then filled to 35 ml with isolation medium.

Centrifugation at 1200 rpm for 8 min followed. The pellet was rinsed three times with isolation medium and re-homogenized as previously described. After filtration a 3 to 5 ml cell suspension was obtained.

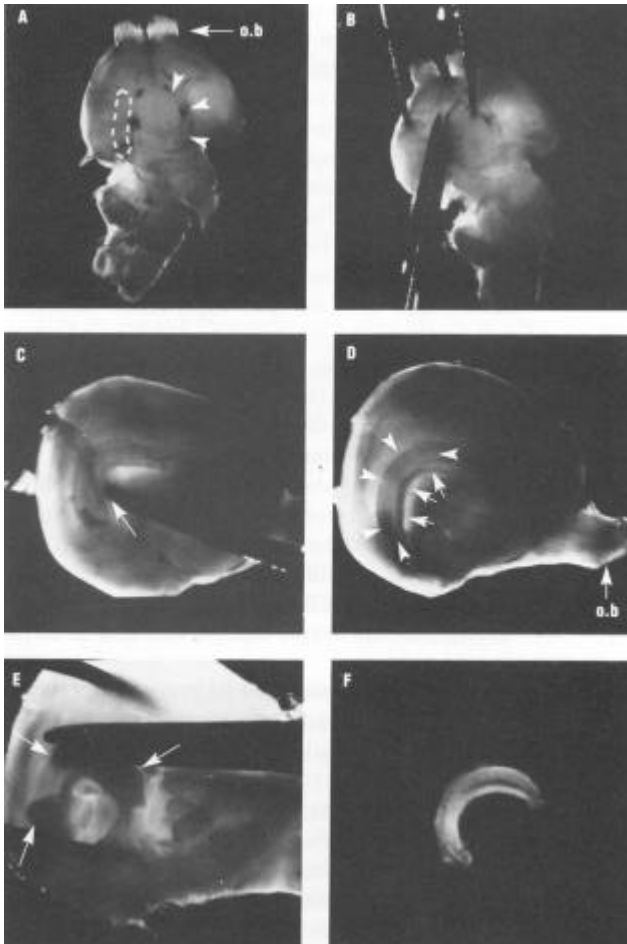


Fig.5: Dissection of the hippocampus. (A) Ventral view of the embryonic rat brain, with olfactory bulbs at the top. The dotted line indicates the approximate projection of the right hippocampus onto the surface. Arrowheads demarcate the junction between diencephalon and cerebral hemisphere, along which the first cut is made (B) to separate the two parts. (C) Meninges are removed and in (D) the two edges of the hippocampal structure are clearly recognizable. Using fine scissors it is possible to cut around the margin (E) and remove completely the hippocampus (F). (Goslin et al., 1998)

2.5.3 Cell plating

The concentration of viable cells in the suspension was approximately determined by trypan blue exclusion. For this measurement, 50 μ l of the suspension were incubated with 50 μ l of trypan blue (Sigma) for 5 min and cells were counted in a hemocytometer (Neubauer). The cell suspension was then diluted with an appropriate volume of culture medium before being plated on poly-L-lysine (Sigma, 10 μ g/ml) precoated coverslips (for immunocytochemistry) or precoated culture dishes, in order to obtain a final density of approximately 4.75×10^4 cells / cm^2 . Each of the culture dishes (\varnothing 60 mm), where the coverslips were placed, contained 5 ml of suspension. Cells were grown in the incubator at 37°C.

2.5.4 Medium change

After three days, 50% of the culture medium was replaced with fresh medium lacking glutamate. Three days later a 100% medium change was performed.

2.5.5 Incubation

One day after the 100% medium change (culture day 7), hippocampal neurons were incubated with vehicle or with aqueous solutions of $A\beta_{1-42}$ (Bachem) and $A\beta_{31-34}$ (Dr. Penke, University of Szeged, Hungary) at a final concentration of 0.5 μM and 0.125 μM , respectively. Aliquots of $A\beta_{1-42}$ (350 μM) were pre-aged at 37°C for 4 days to allow the formation of fibrils (Fig.6), as previously described (Lorenzo and Yankner, 1994). $A\beta_{31-34}$ was not pre-aggregated (Laskay et al., 1997).

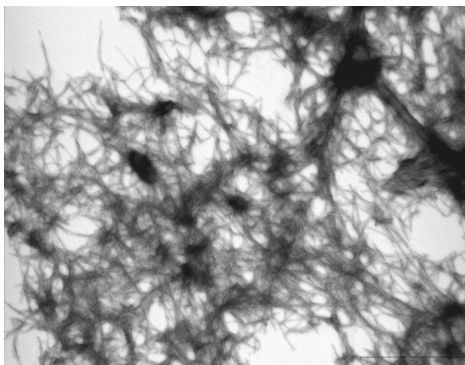


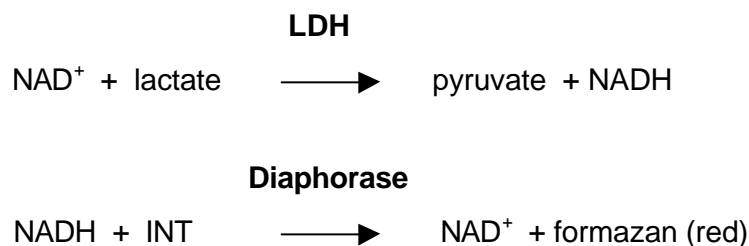
Fig.6: Formation of $A\beta_{1-42}$ fibrils after pre-aging was confirmed by electron microscopy (negative staining) using a Zeiss EM 902. Magnification x20000.

2.5.6 Fixation

After three days of treatment (culture day 10) the supernatant was removed (and collected for the cytotoxicity assay) and cells were washed 3 times with phosphate buffered saline (PBS), 37°C, pH 7.4. They were then fixed with 4% paraformaldehyde - 4% sucrose in PBS, pH 7.4, for 15 min at 37°C. A 3-times washing with PBS followed. Cells were stored in a moist chamber at 4°C.

2.6 Cytotoxicity assay

The measurement was performed employing the CytoTox® non-radioactive assay (Promega), a colorimetric quantitative determination of lactate dehydrogenase (LDH), in the cell culture supernatant. According to the manufacturer's protocol, 12 ml of room temperature assay buffer were added to one bottle of substrate mix. In a 96-well assay plate, 50 µl of the tetrazolium salt (INT) containing reconstituted substrate mix were added in each well to 50 µl of supernatant, collected from differently treated cultures. Every sample (Aβ₁₋₄₂ 0.5 µM, Aβ₃₁₋₃₄ 0.125 µM, Aβ₁₋₄₂ + Aβ₃₁₋₃₄ and vehicle), as well as the LDH positive control, were measured in quadruplicate. Culture medium was taken as blank for the absorbance values. After 30 min at room temperature the reaction converting tetrazolium into a red formazan product was stopped by 50 µl of stop solution (acetic acid 1M) and the absorbance read at 490 nm in a ELISA reader within 1h. The amount of color formed is proportional to the number of lysed cells.



Additionally, further vehicle-treated probes were incubated with lysis solution (Promega) for 45 min before the supernatant was collected, in order to determine the maximum of absorbance (all cells are lysed) and correlate it to the values measured for the samples.

2.7 Immunocytochemistry

2.7.1 Immunoperoxidase staining

Immunocytochemistry was performed by means of the avidin-biotin-peroxidase complex (ABC) method. Cells were permeabilized using 0.2% Triton X100 in PBS (20 min, RT) and subsequently incubated - with washes in PBS (3x5 min each) after each step - for 15 min in a 2% hydrogen peroxide solution in PBS. Cells were blocked for 1h in 10% normal rat serum in 1% BSA/PBS and the primary monoclonal antibody MAP2 (1:1000 in 1%

BSA/PBS) applied overnight at 4°C. After reblocking with 5% normal goat serum solution in 1% BSA/PBS for 1h, cultures were incubated in biotinylated secondary antibody goat anti-mouse IgG (1:200) in 1% BSA/PBS. Finally, a 40 min streptavidin-peroxidase complex (1:200 in 1% BSA/PBS) (Amersham) treatment followed. The final staining was achieved by using diaminobenzidine tetrahydrochloride (DAB) fortified with a glucose oxidase-nickel sulfate peroxidase substrate (5-10 min). Controls performed by omission of the primary antibody during the corresponding incubation gave negative results. All coverslips were mounted on glass slides using Entellan® (Merck).

2.7.2 Immunofluorescence

Following fixation, cells were washed 3 times with PBS and membranes permeabilized with 0.2% Triton X-100 in PBS for 20 min at RT. In the case of the β 2-nAChR subunit this step was omitted, because the epitope recognized by the β 2-nAChR antibody is known to be extracellular (Schütz, 1999). Washing with PBS (3x5 min each) followed each step of the procedure. After blocking with 10% BSA/PBS for 1h, cells were incubated with primary polyclonal antibodies directed to the α 7-nAChR subunit (H-302, 1:250), β 2-nAChR subunit (1:200), α 4-nAChR subunit (1:400) or VGLUT1 (1:5000) in 1% BSA/PBS overnight at 4°C. Blocking with 5% normal goat serum in 1% BSA/PBS for 30 min followed and Cy3-conjugated goat anti-rabbit IgG (1:1000 in 1% BSA/PBS) or biotinylated goat anti-guinea pig IgG (1:400) plus Streptavidin-Cy3 (1:500) were used as fluorescent secondary antibodies (40 min). Cells were then blocked again with 5% BSA/PBS for 1h and incubated with one of the primary mouse monoclonal antibodies (mAb) MAP2 (1:500), SMI32 (1:800), α 7-nAChR 306 (1:350), or with the τ -protein phosphorylation sites specific antibodies AT8 (Ser202) (1:1000), AD2 (Ser396 / Ser404) (1:10000), AT180 (Thr231 / Ser235) (1:400) and 12E8 (Ser262) (1:100) in 1% BSA/PBS overnight at 4°C. Blocking with 5% normal goat serum solution in 1% BSA/PBS for 1h and treatment with the secondary antibody Cy2-conjugated goat anti-mouse IgG (1:500) followed (40 min). Coverslips were mounted on glass slides using Entellan® (Merck).

2.7.3 Assessment of neuron numbers

The unbiased stereology-based estimation of total neuron numbers was performed using the 2D fractionator (Gundersen, 1986; Gundersen et al., 1988) in conjunction with the C.A.S.T.-Grid system, which allows systematic uniform random sampling using a soft-

ware-controllable microscope stage. At least three specimens were evaluated for each of the incubation conditions ($A\beta_{1-42}$ 0.5 μM , $A\beta_{31-34}$ 0.125 μM , $A\beta_{1-42}$ + $A\beta_{31-34}$ and vehicle). Means of the individual counting results were used for further statistical evaluation. The sampling area ($113.3 \pm 2.0 \text{ mm}^2$) was delineated manually at 1.25x magnification using a mouse-driven cursor, the margin of the coverslip representing the boundary.

The distance between the counting frames (frame area: $6344 \mu\text{m}^2$, corrected for magnification) was 800 μm in both the x and the y directions. The number of counting frames was calculated by a sub-routine in the C.A.S.T system and automatically superimposed on the video overlay. The 2D unbiased counting frame was displayed on the computer screen taking up 25% of the screen area. Counting of the neurons (40x oil immersion objective) was initiated at a random position, continued by moving the computer-controlled microscope stage holder stepwise in a meandering pattern over the entire section. All immunolabeled and morphologically intact-appearing neurons sampled were counted. The total number of neurons on the coverslip was obtained using the following formula (Ventimiglia et al., 1995):

$$\begin{aligned} N &= \sum Q_N * (dx * dy / A_{\text{FRAME}}) \\ &= \sum Q_N * (800 \mu\text{m} * 800 \mu\text{m} / 6344 \mu\text{m}^2) \end{aligned}$$

where $\sum Q_N$ is the sum of the neurons counted, dx and dy are the sampling steps (μm) in the x or y direction, respectively, and A_{FRAME} is the area of the counting frame corrected for magnification (μm^2) (Schröder et al., 2004).

2.7.4 Immunoreactive area measurement

This measurement was also performed using the C.A.S.T.-Grid system. The set-up was the same described in 2.7.3. A system-connected software allowed the estimation of the total stained surface appearing on the screen for every randomly-selected frame inside the delineated sample area. Five specimens were evaluated for each of the incubation conditions ($A\beta_{1-42}$ 0.5 μM , $A\beta_{31-34}$ 0.125 μM , $A\beta_{1-42}$ + $A\beta_{31-34}$ and vehicle). Means of the individual measurement results were used for further statistical evaluation. The immunoreactive area was expressed as percent of the total analyzed area on the coverslip using the following formula:

$$\% \text{ immunoreactive area} = \left(\frac{\sum A_s}{\sum A_{TOT}} \right) \times 100$$

where $\sum A_s$ is the total stained area measured and $\sum A_{TOT}$ is the total analyzed area.

2.8 Cell extract

After having undergone one of the various treatments described above, cells were washed in PBS (pH 7.4) and harvested from the culture dish scraping them directly in lysis buffer (1% Triton X-100 in PBS, 0.1 mM PMSF, 1% v/v protease inhibitors cocktail P 2714 stock solution [Sigma]) and the resulting suspension stirred at 4°C for 30 min. After a short sonication, the suspension was centrifuged at 10000 rpm for 10 min and an aliquot of the supernatant was used to determine the total protein concentration. The supernatant was then mixed 1:3 with electrophoresis sample buffer, boiled for 5 min and used for Western blot analysis.

2.9 Protein estimation

For the estimation of the total protein concentration in the samples the bicinchoninic acid method (BCA kit, Pierce) was applied. This colorimetric assay, in which Cu^{2+} ions are reduced to Cu^+ and form a violet-colored complex with bicinchoninic acid (Wiechelman et al., 1988), was chosen for its resistance against detergents like Triton X-100. The use of such detergents in the lysis buffer was in fact necessary for the extraction of membrane proteins (Rehm, 2000). Concentrations of 0.2, 0.5, 1.0, 1.5, 2.0, 2.5 and 3.0 mg/ml of BSA in lysis buffer were used to obtain the standard curve. 200 μl of a 1:50 solution of reagent A and B (BioRad) were added to 25 μl of each probe or standard solution pro well. 25 μl of buffer were used for the blank. The probes were then kept at 37°C for 30 min and subsequently 10 min at RT. The measurement of the protein concentration was performed using an ELISA reader at 570 nm.

2.10 Electrophoresis

Identical amounts (15-150 μ g) of differently treated samples were loaded on each lane and run on SDS-page (10% or 4-15%) at constant voltage (100v) in a Mini-PROTEAN® 3 Cell system (BioRad). Pre-stained protein molecular mass standards (Bio-Rad) were included in the same gel.

2.11 Western blot

Gels and membranes were equilibrated for 15 min in transfer buffer and proteins subsequently transferred onto the nitrocellulose membranes using a tank blotting system (BioRad). Gels were then treated with Coomassie Blue and decolorized with 8% methanol and 7% acetic acid to examine the quality of the electrophoretic separation. Membranes were stained with Ponceau S (Sigma) to verify the protein transfer and blocked with TTBS (0.1% Tween 20 in TBS) containing 5% milk powder for 1h. Incubation with antibodies against the τ -phosphorylation sites AT8 (1:2000), AT180 (1:2000), Tau-1 (1:4000), AD2 (1:5000), 12E8 (1:2000) and antibodies against the α 7- (306, 1:500) and α 4-subunit (1:1000) of the nAChR in TTBS containing 1%-5% milk powder overnight at 4°C followed. The biotinylated secondary antibodies anti-mouse IgG (1:5000) and anti-guinea pig (for the α 4-nAChR subunit) in 1%-5% milk powder/TTBS were used. After streptavidin-peroxidase treatment (1:5000-1:10000 in 5% milk powder/TTBS), immunodetection was performed using chemiluminescence reagents (Pierce). Immunoreactive bands were quantified with the Kodak Image Station 440.

2.12 Receptor binding assay

The binding capability of the homomeric α 7-nAChRs was measured using [¹²⁵I] α -bungarotoxin ([¹²⁵I] α -Bgt). Cultures were incubated with (for non-specific binding) or without (for total binding) 100 nM cold α -Bgt (Sigma) in 500 μ l culture buffer at 37°C for 30 min. Probes were then treated with different concentrations of the radioligand (0.039-39 nmol/l) for 1 h at RT. Three samples were incubated with each concentration. After treatment, coverslips were washed twice with cold PBS, dried, and the radioactivity measured using an Isomed 200 counter. The values obtained were then referred to the

average amount of protein present on the coverslip under each incubation condition, determined on separate culture samples.

2.13 Data bank search

The search for proteins containing the tetrapeptidic sequence of A β ₃₁₋₃₄ (IIIGL) was performed using the BLAST program (Basic Local Alignment Search Tool) from Expasy (www.expasy.org) and restricted to human proteins.

2.14 Statistical evaluation

For neuron number assessment, total MAP2-stained area measurement, cytotoxicity assay, Western blot analysis and binding assay, the determination of the statistical significance was performed employing the two-tailed paired Student's T-test. In the Western blot analysis and binding assay, the mean of three independent measurements of each sample was used for further statistical analysis.

3. RESULTS

3.1 Neuron labeling in cell culture

In order to investigate the general cell morphology in the hippocampal primary cultures - used as a model system in this study - neurons were immunostained with a MAP2 monoclonal antibody. This is an antibody directed against a group of microtubule-associated proteins (MAPs) and represents a specific marker for neurons. MAP2 proteins are in fact the neuronal MAPs, present only in trace amounts in non-neuronal cells. MAP2 proteins are preferentially localized in the dendrites of mature neurons (Dotti et al., 1988) and they are fundamental for microtubule polymerization (for review see Buée et al., 2000). The prevalent localization of MAP2 proteins in the somatodendritic compartment of hippocampal pyramidal cells is found not only in brain tissue sections, but also in hippocampal neurons which develop in culture, even if they grow at very low density without contacting neighboring cells (Caceres et al., 1984). MAP2 immunocytochemistry intensely stains the dendritic processes, including their finest branches, thus providing an overview of the dendritic tree in its full extension. The MAP2 staining can therefore give information about dendritic development, dendritic morphology in culture and possible changes in the cytoskeletal structure of neurons (Caceres et al., 1984; Busciglio et al., 1992). As expected, MAP2-positive cells in our cultures were labeled in the somatodendritic compartment and along the dendrites (Fig.7a). As reported in chapter 1.5, the “pyramidal-like” neurons in the culture should represent 85% to 90% of the total neuronal population (Goslin et al., 1998). In order to characterize these neurons, cultures were incubated with SMI32, an antibody against neurofilament proteins, which was shown to label a subset of pyramidal neurons in human and monkey neocortex (Campbell and Morrison, 1989) (Fig.7b). The immunolabeling obtained did not allow to differentiate between cells, as all of them were stained. Another attempt was made by using an antibody against the vesicular glutamate transporter 1 (VGLUT1). Glutamate is considered to be the main neurotransmitter of neocortical and hippocampal neurons (Francis et al., 2003) and VGLUT1 was found to be present in a subgroup of glutamatergic neurons (Bellocchio et al., 2000). Also in this case all cells were labeled (Fig.7c) (non-neuronal cultures were also used to check for unspecific binding and no staining was obtained with the two antibodies, data not shown). Under these culture conditions it seems therefore not possible to characterize neurons on the basis of their SMI32 or VGLUT1 immunoreactivity.

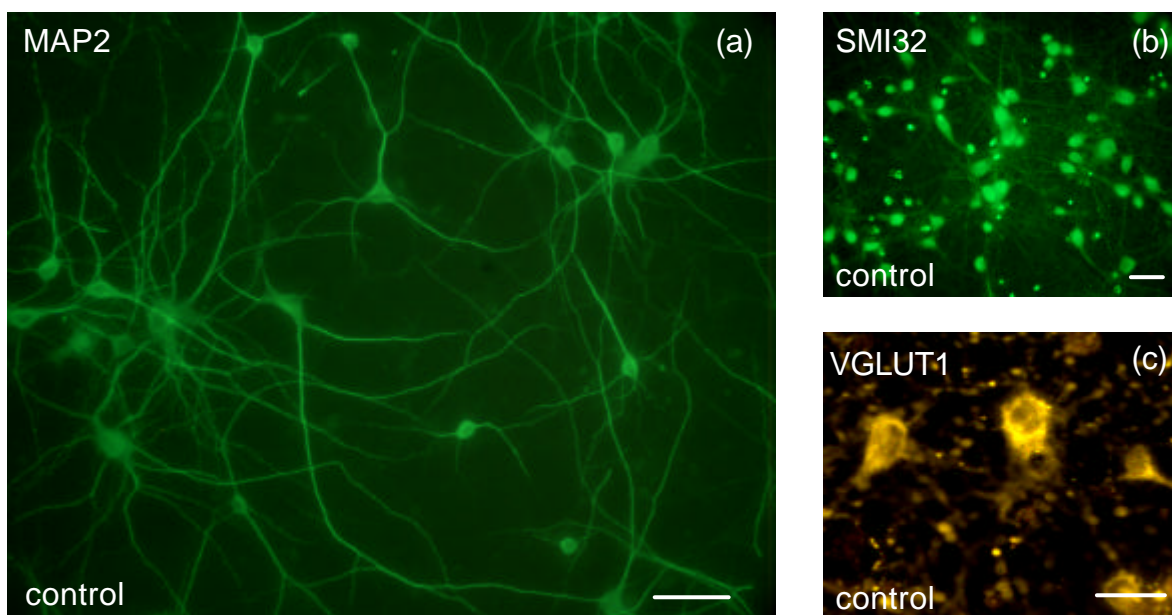


Fig.7: MAP2 staining in untreated cultures (a). Cell bodies and dendrites were intensely immunoreactive. When labeled with the antibodies SMI32 (b) or VGLUT1 (c), all neurons resulted to be stained. Bars: 50 μ m [(a) and (b)]; 20 μ m (c).

3.2 α 7- and β 2-nAChR subunit immunoreactivity in cultured neurons

All MAP2-positive neurons displayed α 7-nAChR immunoreactivity, indicating that this subunit is expressed by all neurons in our cultures (Fig.8a,8b). β 2-nAChR subunit immunoreactivity was also present in most neurons, but it seemed to be located in different cell compartments when compared to the α 7-nAChR subunit labeling. The latter was more homogeneously distributed on the cell surface, while the β 2-nAChR subunit exhibited an intermittent immunostaining in the perikarya and along the dendrites (Fig.8d). The peculiar pattern of the β 2-nAChR subunit labeling did not allow to make precise considerations about the neuron morphology. In the present study, a neuron was considered “healthy” when the cell body was completely stained and it had multiple dendrites. In the case of the β 2-nAChR subunit it would be impossible to determine if a given cell is only partially stained because it is damaged or because of the characteristic staining. For this reason it was decided not to proceed with further investigations of the β 2-nAChR subunit.

Immunochemical staining was performed also for the α 4-nAChR subunit, but the Western blot analysis raised some doubts about the specificity of the antibody used (see Results: appendix).

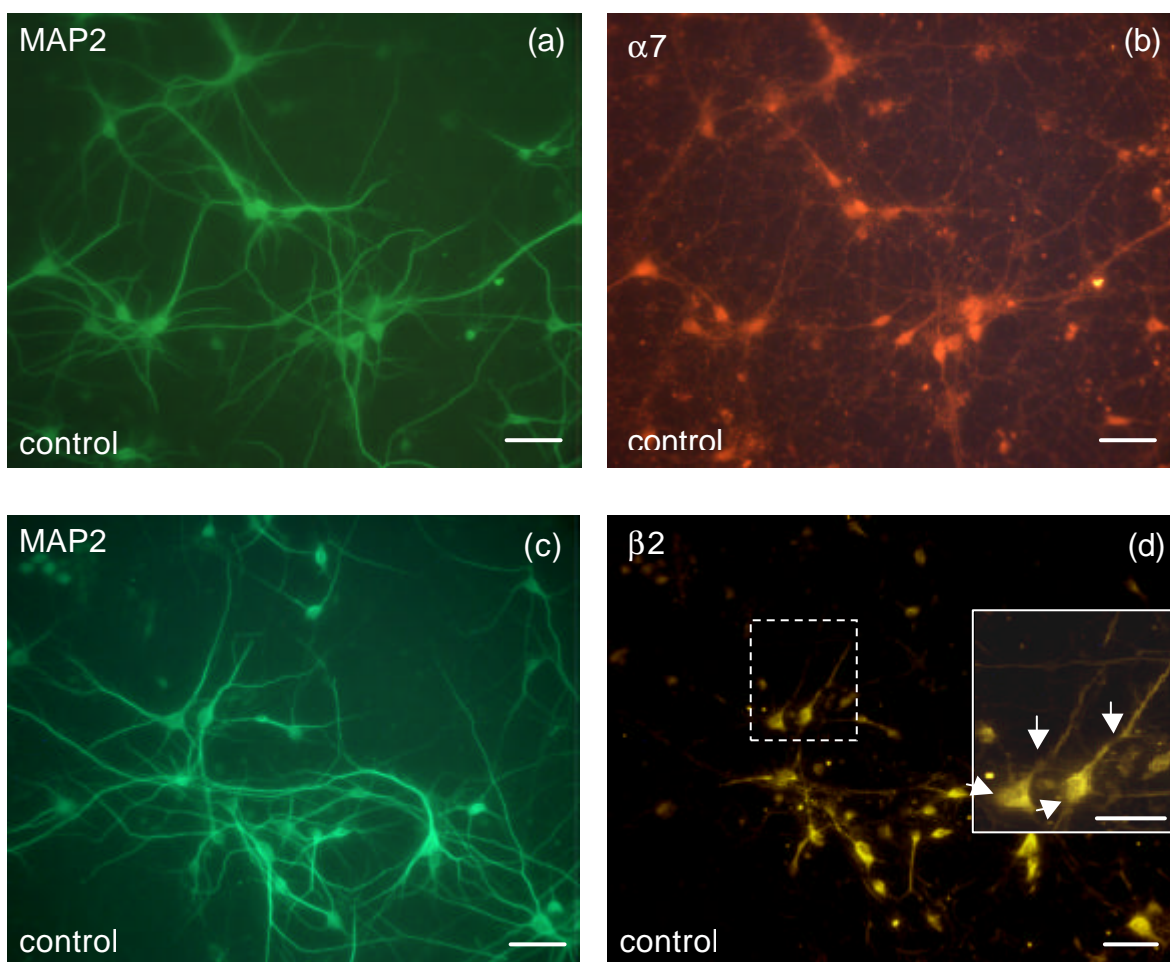


Fig.8: nAChR subunit labeling in rat hippocampal primary cultures. The $\alpha 7$ -nAChR staining (b) was homogeneously distributed on the cell surface, while only parts of the perikarya and of the dendrites were intensely labeled in neurons stained for the $\beta 2$ -nAChR subunit (d). For both subunits, the correspondent MAP2 staining is shown on the left-hand side (a,c). In (d), the inset is the enlargement of the area inside the dotted frame. Arrows indicate the intermittent labeling. Bars: 50 μm [(a), (b), (c) and (d)]; 20 μm [inset (d)].

3.3 Effect of Ab_{1-42} on cultured neurons

3.3.1 Neuron morphology and number

As can be seen in Fig.9, incubation with a 0.5 μM aqueous solution of pre-aged $\text{A}\beta_{1-42}$ resulted in retraction of the dendrites and shrinkage of the cell bodies in MAP2-immunoreactive (MAP2-ir) neurons. Morphologically altered neurons did not lose their MAP2 immunoreactivity: cell counting showed that the number of MAP2-positive neurons per coverslip was not significantly different when comparing treated cells with controls (Fig.10), immunoperoxidase staining and immunofluorescence yielding the same results.

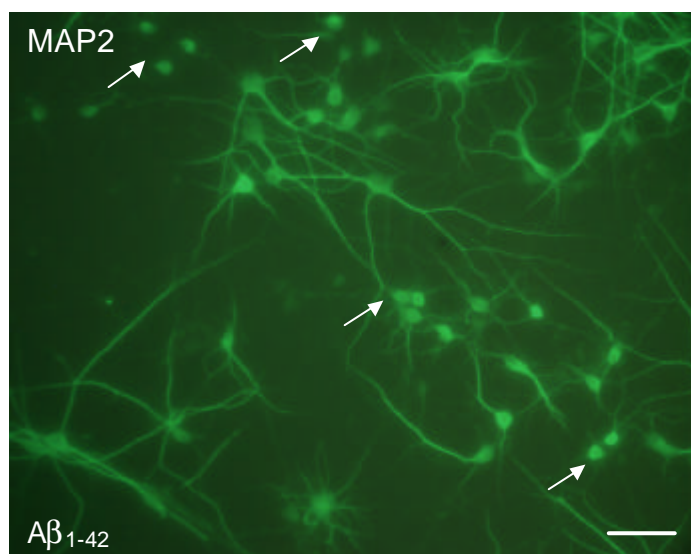


Fig.9: MAP2 immunoreactivity in Ab_{1-42} -treated cells. Many neurons were shrunken and had shorter or no dendrites (arrows). $[Ab_{1-42}] = 0.5 \text{ mM}$. Bar: 50 μm .

Sample	MAP2-positive cells per coverslip
Control	21508 \pm 904
Ab_{1-42}	21448 \pm 1062

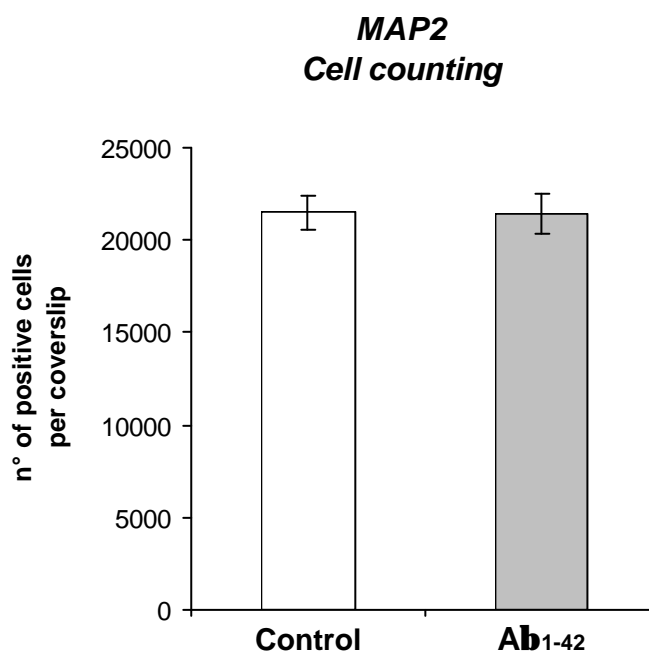


Fig.10: Total number of MAP2-positive cells in controls (\square) and Ab_{1-42} -treated cultures (\blacksquare) ($n=5$; results are expressed as mean \pm SEM; $P>0.05$). $[Ab_{1-42}] = 0.5 \text{ mM}$.

3.3.2 LDH determination

To get information about neuron viability the LDH release in the culture supernatant was measured, as it is proportional to the number of lysed cells. This technique allows fast and simple cytotoxicity measurements (Korzeniewski and Callewaert, 1983). The results obtained in controls were not significantly different from those obtained in incubated cultures (Fig.11). The presently used concentration of $A\beta_{1-42}$ seems therefore to cause cellular damage, as shown by MAP2 immunoreactivity, without affecting the neuron viability.

Sample	Absorbance (490 nm)
Control	0.15 \pm 0.03
$A\beta_{1-42}$	0.19 \pm 0.06

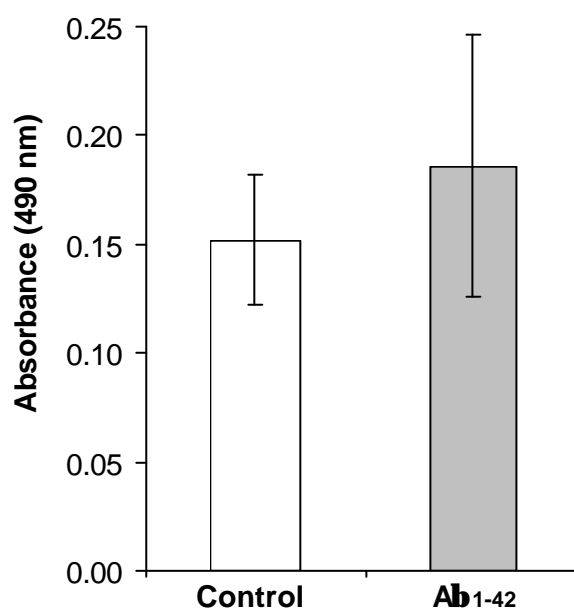
Cytotoxicity assay (LDH)

Fig.11: Cytotoxicity measurement in controls (\square) and $A\beta_{1-42}$ -treated cultures (\blacksquare), reported as formazan absorbance (n=4; results are expressed as mean \pm SEM; $P>0.05$). [$A\beta_{1-42}$] = 0.5 mM.

In order to determine the percentage of lysed cells normally present in the samples, vehicle treated cultures were incubated with a lysis solution (Promega). Under this treatment all cells should be lysed and the LDH release therefore correspond to the maximum LDH release. Comparing this value with the LDH release of vehicle-treated cultures not incubated with lysis solution, it turned out that the lysed cells in the samples represent about 13.12 ± 1.16 % of the total population (n=3; result expressed as mean \pm SEM).

3.3.3 Morphological measurements

The A β -induced morphological changes observed with immunocytochemistry (dendrite retraction and cell body shrinkage) were quantified measuring the total MAP2-stained area on the coverslip with and without A β_{1-42} treatment. As can be seen in Fig.12, there was a statistically significant difference in the MAP2-ir area between controls and A β_{1-42} -treated cultures. This finding is in accordance with the morphological alterations described in 3.3.1. As the total number of MAP2-positive cells was not affected after incubation, it can be assumed that a decrease in the total MAP2-labeled area only depends on the observed retraction of the dendrites and shrinkage of the cell bodies. For this determination immunoperoxidase labeling was used, because it allows a more precise staining of the processes and because the contrast can be better appreciated by the computer system.

3.3.4 Quantitative determination of MAP2 isoforms

The term MAP2 refers to three different proteins which are derived from a single gene and have a similar amino acid sequence. MAP2a and MAP2b are the high molecular weight isoforms (280 kD and 270 kD, respectively), while MAP2c represents a shorter form (70kD). MAP2b, which is composed of 1830 amino acids, is the only isoform expressed throughout life in rat brain and it is involved in neurite outgrowth, during which its level remains fairly constant. MAP2c, which is made up of 467 amino acids, lacks the projection domain that stabilizes microtubules and it is believed to maintain the cytoskeleton in a more flexible state during development (for review see Shafit-Zagardo and Kalcheva, 1998). MAP2c can be found in many brain areas only before P10, while MAP2a appears after P10 and seems to replace MAP2c in mature neurons. This developmental switch occurs during maturation of neuronal processes and it is thought to be related to the

growth of dendrites and their increasing thickness in this phase (for reviews see Goedert et al., 1991; Shafit-Zagardo and Kalcheva, 1998). Compared to vehicle-incubated cultures - the values of which were scaled to 100% - incubation with $A\beta_{1-42}$ led to a significantly decreased amount of MAP2b, while the amount of MAP2c (fetal form) was not altered (Fig.13).

Sample	Percent of MAP2-ir area
Control	12.7 \pm 0.6
$A\beta_{1-42}$	9.7 \pm 1.1

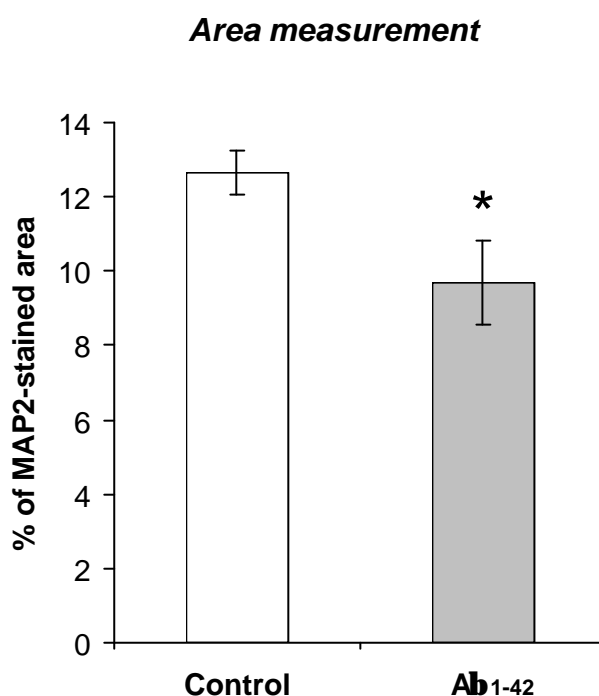
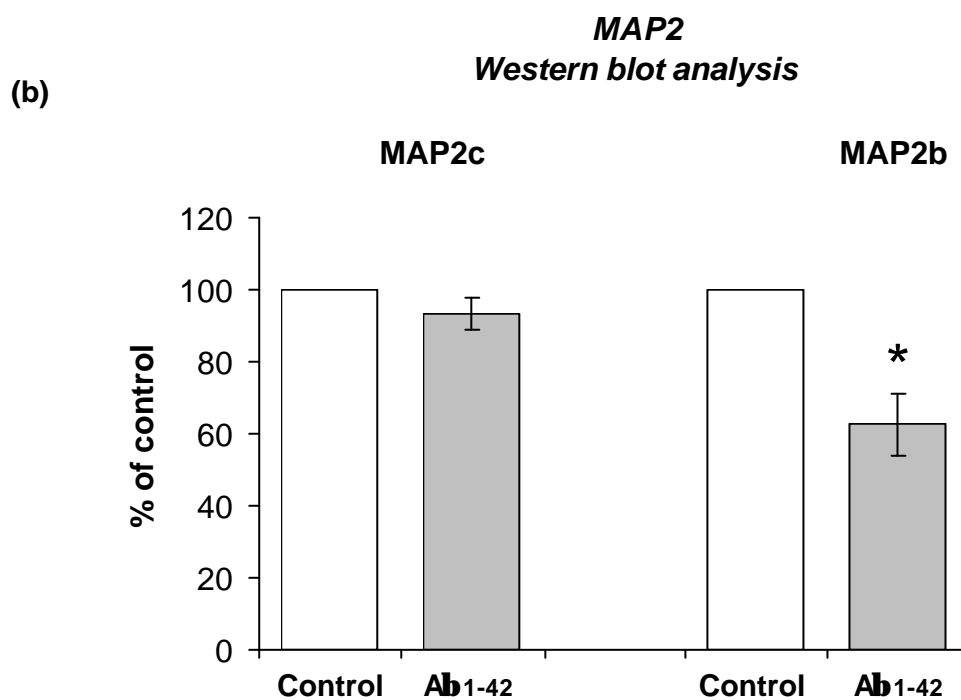
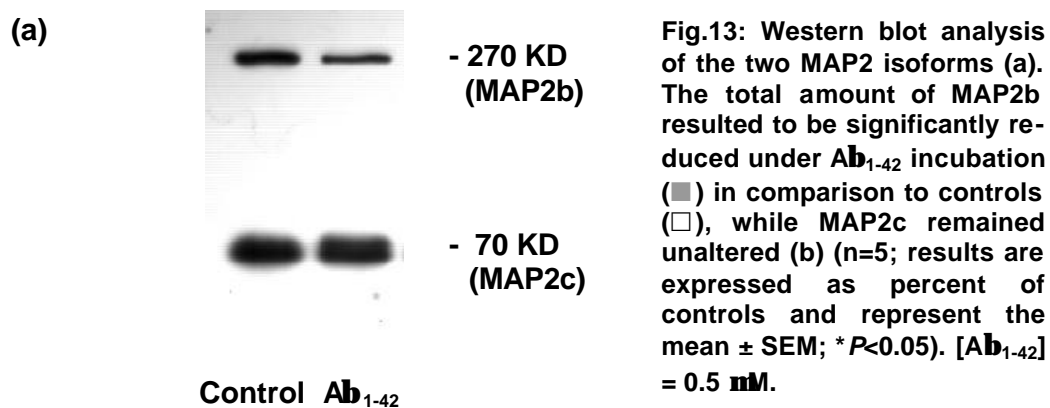


Fig.12: The MAP2-stained area was measured as percent of the total area on the coverslip in controls (□) and Ab_{1-42} -treated cultures (■) (n=5; results are expressed as mean \pm SEM; * P <0.05). [Ab_{1-42}] = 0.5 mM.

Sample	MAP2c	MAP2b
Control	100	100
A β ₁₋₄₂	93.3 \pm 4.3	63.7 \pm 8.7



3.4 Effect of Ab₁₋₄₂ on the phosphorylation state of the τ -protein

Among the different phosphorylation sites of the τ -protein, attention was focused on four of them, situated in different functional domains of the structure. The antibodies AT8 (Ser202), AT180 (Thr231 / Ser235), 12E8 (Ser262) and AD2 (Ser396 / Ser404) were used in this study. AT8 is the most commonly used antibody to detect τ -hyperphosphorylation in AD brains (Braak and Braak, 1995). AD2 detects τ -phosphorylation in the protein segment probably involved in the formation of paired helical filaments (PHFs) and is therefore highly interesting (Buée-Scherrer et al., 1996). AT180 sites are located in the proline-rich region flanking the microtubule binding domain, while the 12E8 site is located within the microtubule binding domain and its phosphorylation might lead to the dissociation of the τ -protein from the whole microtubule structure (for review see Mandelkow and Mandelkow, 1998).

3.4.1 Immunocytochemistry

The immunoreactivity pattern obtained with the antibodies directed to the different τ -protein phosphorylation sites did not show any difference after incubation. A β ₁₋₄₂- and vehicle-treated cells seemed to display the same level of immunoreactivity when labeled with AT8 (Fig.14), AD2 and 12E8 (Fig.15), while the signal obtained with AT180 was weak in both cases and it was hardly possible to distinguish the immunoreactivity from the background (Fig.15). In order to check these observations quantitatively, numbers of AT8-, AD2- and 12E8-ir neurons were assessed. No significant differences between vehicle- and A β ₁₋₄₂-treated cultures were found (Fig.16).

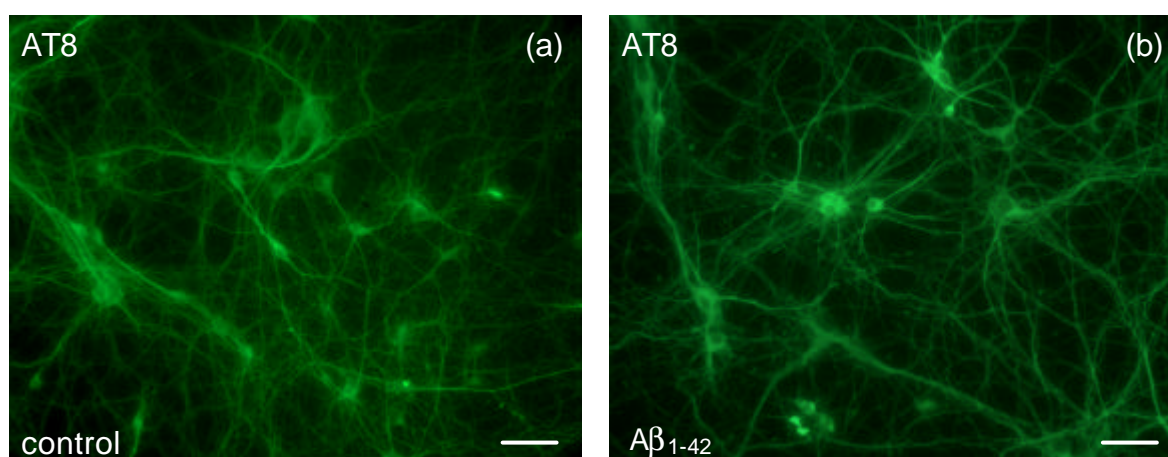


Fig.14: Immunostaining of phosphorylated τ -protein using AT8 antibody in controls (a) and A β ₁₋₄₂-treated cultures (b). [A β ₁₋₄₂] = 0.5 μ M. Bar: 50 μ m.

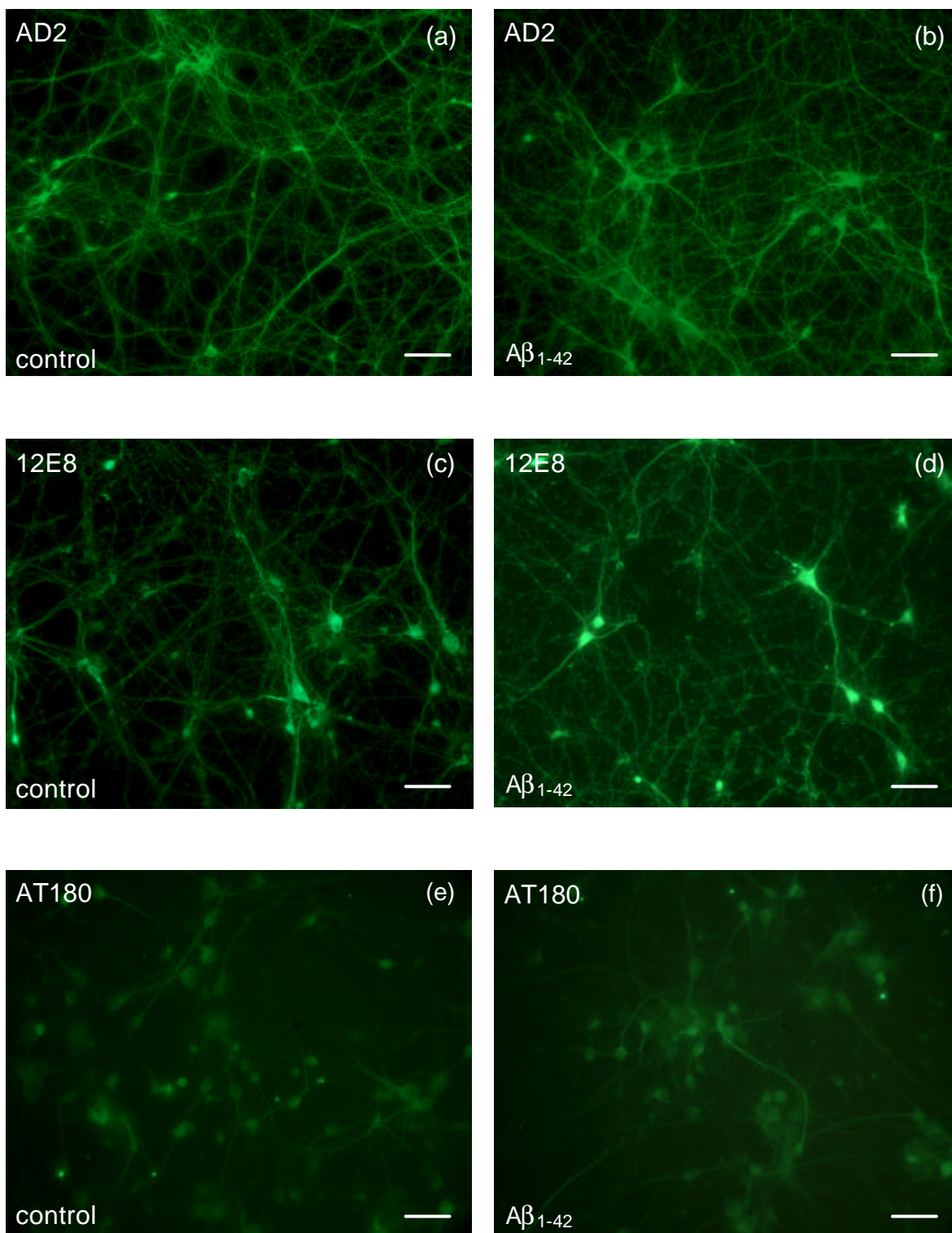
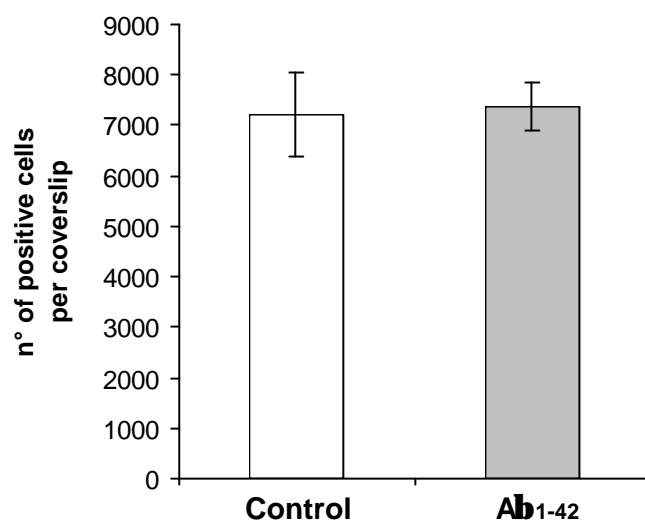


Fig.15: Immunofluorescence labeling of different τ -phosphorylation sites was performed using AD2 (a,b), 12E8 (c,d) and AT180 (e,f) antibodies in controls (left-hand side) and Ab_{1-42} -treated cultures (right-hand side). $[Ab_{1-42}] = 0.5 \text{ mM}$. Bar: 50 μm .

(a)

Sample	AT8-positive cells per coverslip
Control	7230 ± 828
A β ₁₋₄₂	7364 ± 477

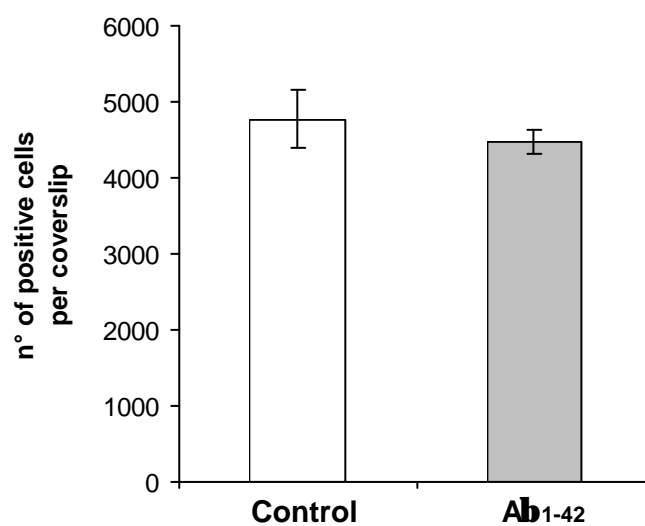
**AT8
Cell counting**



(b)

Sample	AD2-positive cells per coverslip
Control	4775 ± 338
A β ₁₋₄₂	4473 ± 168

**AD2
Cell counting**



(c)

Sample	12E8-positive cells per coverslip
Control	7314 ± 700
A β ₁₋₄₂	6456 ± 1071

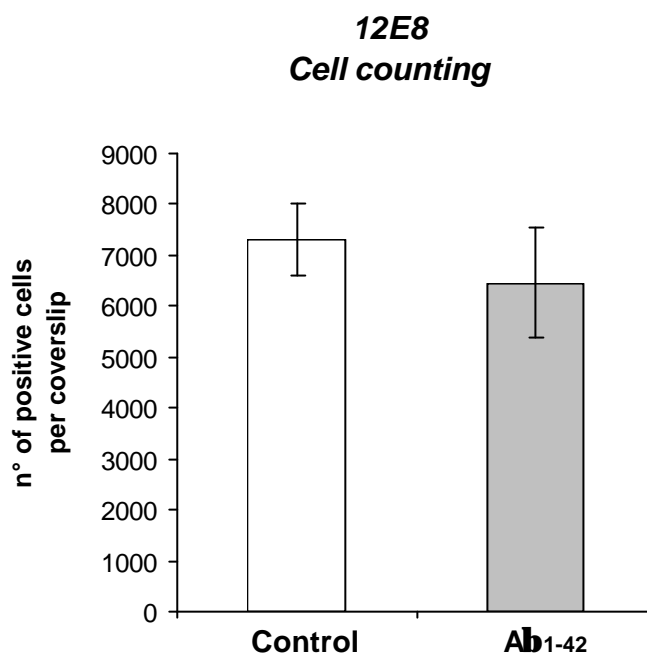


Fig.16: Total number of AT8- (a), AD2- (b) and 12E8-ir neurons (c) in controls (□) and Ab₁₋₄₂-treated cultures (■) (n=3; results are expressed as mean ± SEM; $P>0.05$). [Ab₁₋₄₂] = 0.5 mM.

The detection of phosphorylated τ -protein in untreated cells was not surprising, as the fetal form of the protein normally exhibits higher levels of phosphorylation in comparison to the adult forms (Goedert et al., 1993; Watanabe et al., 1993).

3.4.2 Western blot analysis

In order to complete the data obtained with cell counting, quantitative measurements of the total amount of phosphorylated τ -protein at the considered sites were performed. Also in this case, a certain level of phosphorylation, typical of the fetal τ -protein, was detected in untreated samples. No significant increase of phosphorylated τ -protein at AT8 sites occurred after $A\beta_{1-42}$ incubation (Fig.17). Membranes were also incubated with the antibody tau-1, directed against τ -protein dephosphorylated at Ser199 / Ser202 (AT8 site). As expected, there was no significant reduction in the concentration of this protein, confirming that the considered epitopes are not hyperphosphorylated under these incubation conditions (Fig.18).

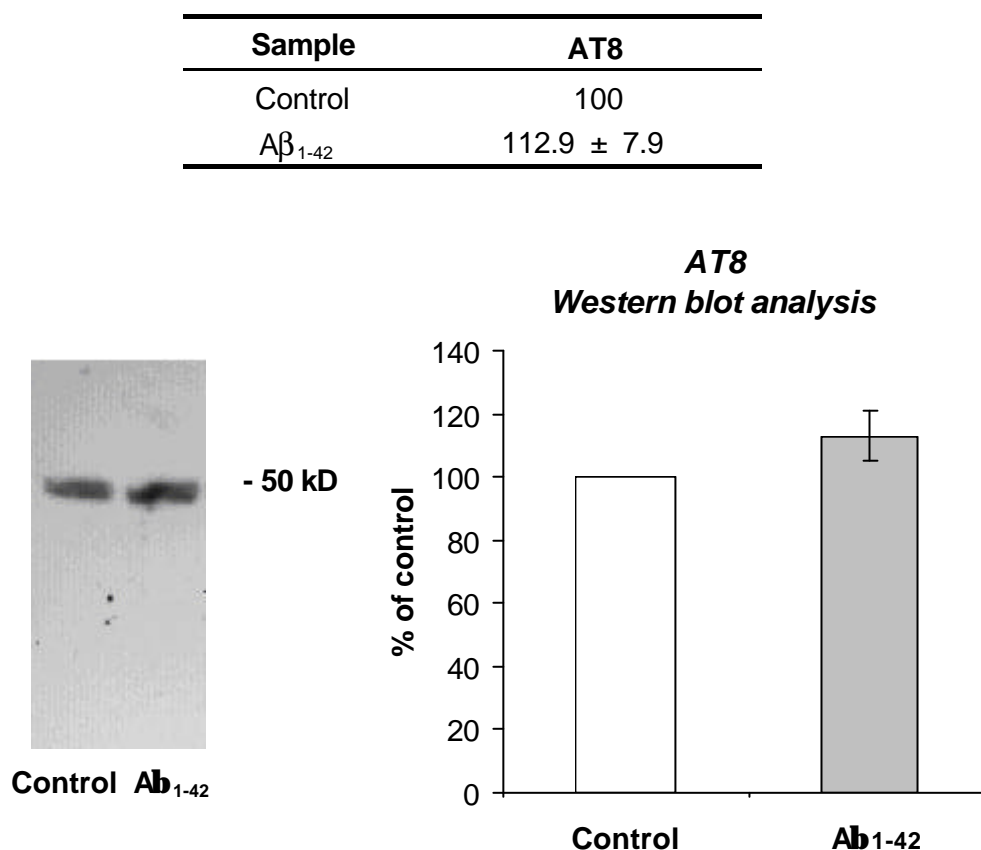


Fig.17: Total amount of τ -protein phosphorylated at AT8 epitopes. The bands obtained by Western blot analysis from controls (\square) and Ab_{1-42} -treated cultures (\blacksquare) were quantified using a densitometer ($n=5$; results are expressed as percent of controls and represent the mean \pm SEM; $P>0.05$). [Ab_{1-42}] = 0.5 mM.

Sample	Tau-1
Control	100
A β ₁₋₄₂	91.1 \pm 3.3

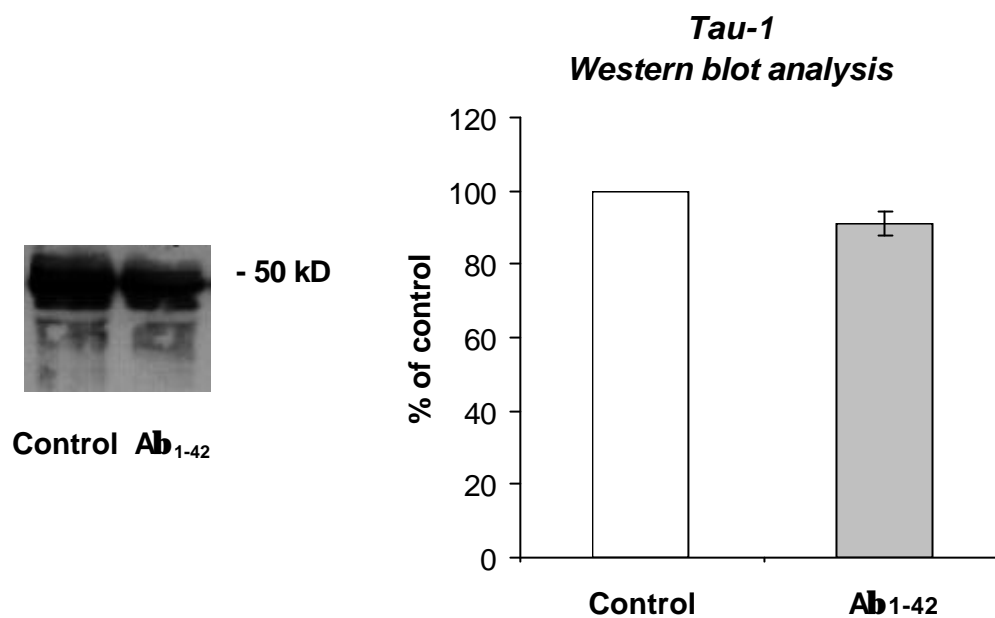


Fig.18: Densitometric analysis of the total amount of τ -protein dephosphorylated at tau-1 epitopes revealed no statistically significant alteration in the expression of the protein in Ab₁₋₄₂-treated cultures (■) in comparison to controls (□) (n=6; results are expressed as percent of controls and represent the mean \pm SEM; $P > 0.05$). [Ab₁₋₄₂] = 0.5 μ M.

The results obtained using AT180 (Fig.19), AD2 and 12E8 antibodies (Fig.20) pointed in the same direction, suggesting that $A\beta_{1-42}$ does not play a role as a τ -hyperphosphorylating agent at the concentrations currently used.

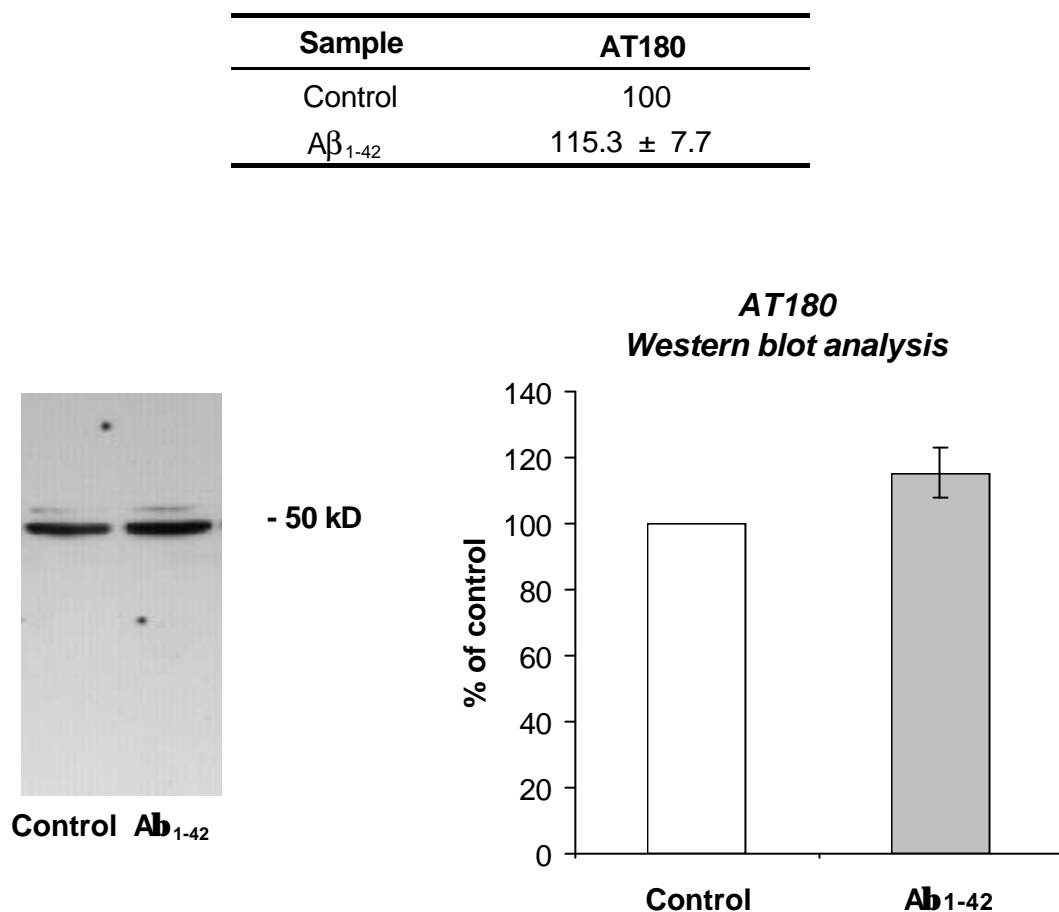


Fig.19: Western blot analysis of τ -protein phosphorylated at AT180 epitopes. In controls (□) and Ab_{1-42} -treated cultures (■) the amount of phosphorylated protein was not significantly different, as shown by quantitative measurements (n=5; results are expressed as percent of controls and represent the mean \pm SEM; $P>0.05$). [Ab_{1-42}] = 0.5 μ M.

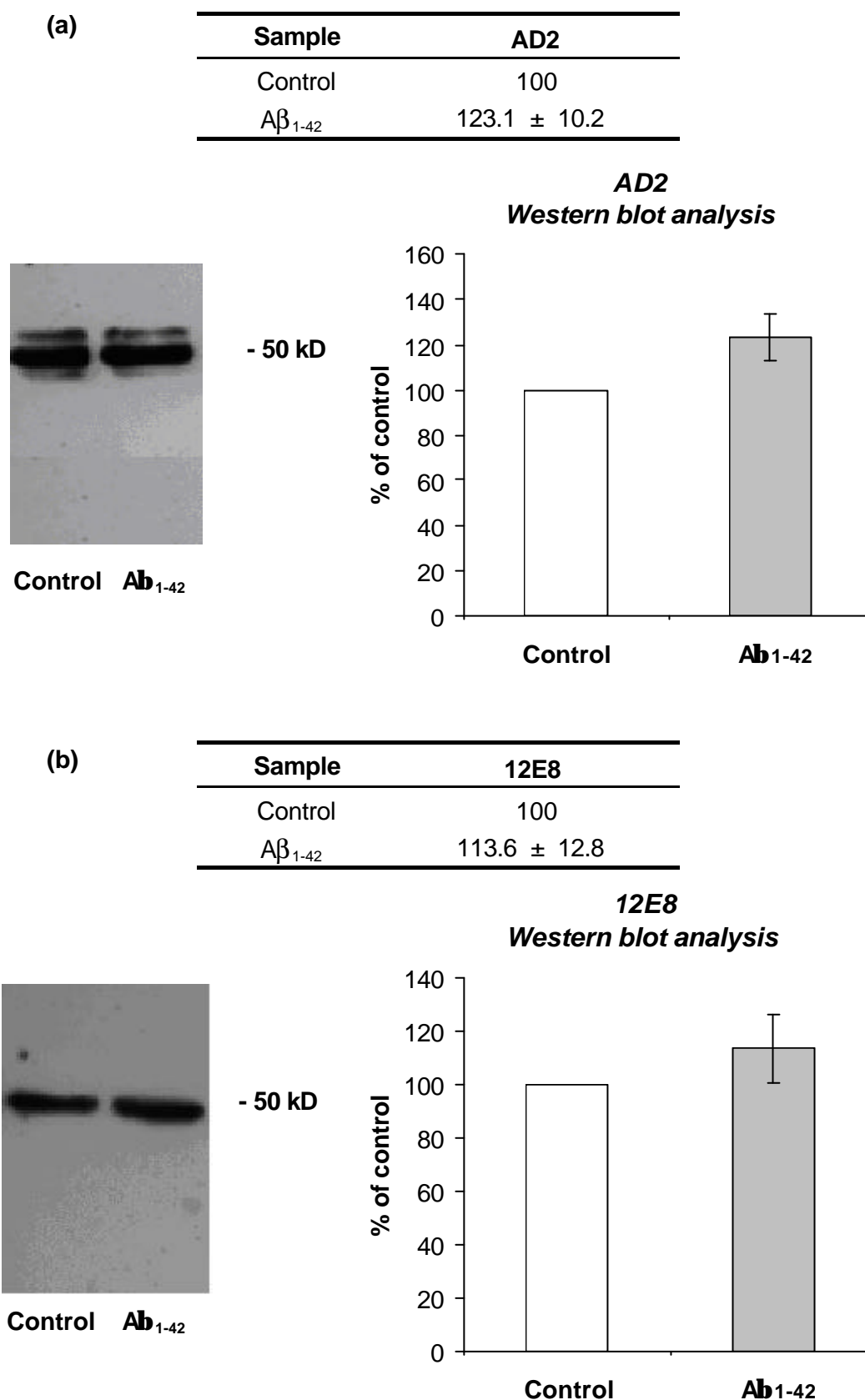


Fig.20: Western blot analysis of τ -protein phosphorylated at AD2 (a) and 12E8 epitopes (b). In Ab₁₋₄₂-treated cultures (■) the amount of phosphorylated protein was not significantly changed in comparison to controls (□) (n=3; results are expressed as percent of controls and represent the mean \pm SEM; $P > 0.05$). [Ab₁₋₄₂] = 0.5 mM.

3.5 Effect of $A\beta_{1-42}$ on the expression of the $\alpha 7$ -nAChR subunit

3.5.1 Immunocytochemical findings

Upon $A\beta_{1-42}$ treatment, most of the $\alpha 7$ -nAChR-ir neurons appeared shrunken and their dendrites were devoid of immunofluorescence (Fig.21). Some larger positive neurons displaying weak and diffuse immunostaining were seen. Their borders were difficult to define and they had a tendency to form blebs, as if they were about to dissolve (white arrows).

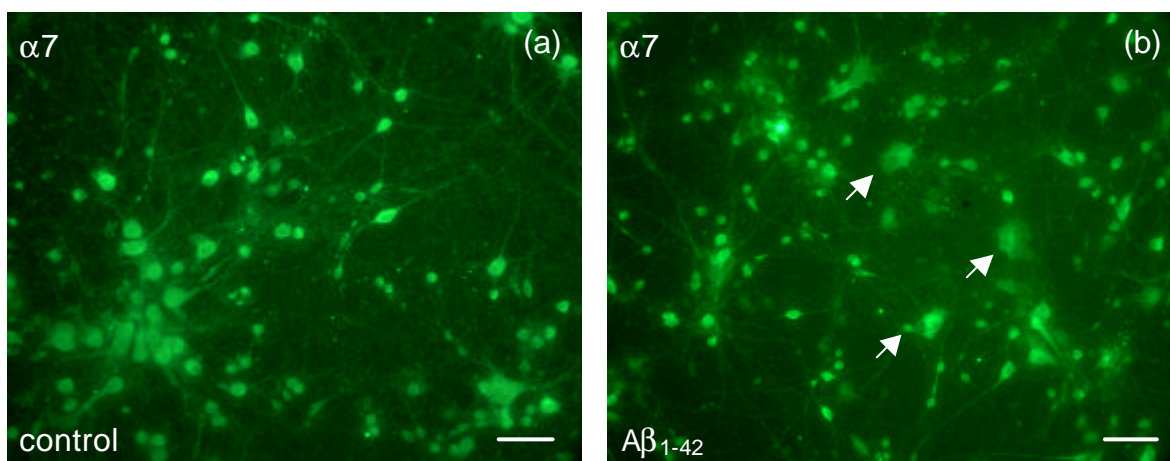


Fig.21: $\alpha 7$ -nAChR subunit immunoreactivity in controls (a) and $A\beta_{1-42}$ -treated cultures (b). [$A\beta_{1-42}$] = 0.5 mM. Bar: 50 μ m.

$\alpha 7$ -nAChR immunoreactivity was expressed in all MAP2-positive cells after $A\beta_{1-42}$ treatment. The total number of $\alpha 7$ -nAChR-bearing neurons appeared to be unaffected by $A\beta_{1-42}$. The larger “blebbing” neurons observed after treatment were also counted and were found to represent 8.45 ± 1.16 % of the total cell population (results are expressed as mean \pm SEM).

3.5.2 Quantitative determination

Following incubation with $A\beta_{1-42}$, the amount of $\alpha 7$ -nAChR protein was not significantly altered compared to control conditions (Fig.22). Together with the unchanged number of $\alpha 7$ -nAChR-ir neurons after $A\beta_{1-42}$ treatment, this speaks in favor of unchanged concentrations of the receptor protein in individual neurons.

Sample	$\alpha 7$ -nAChR
Control	100
$A\beta_{1-42}$	94.2 \pm 5.9

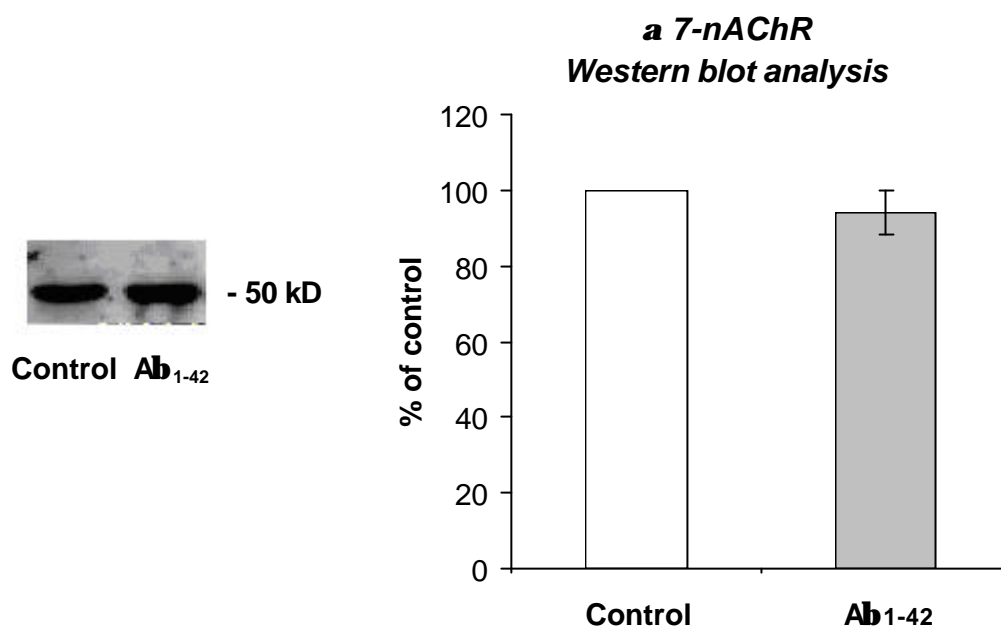


Fig.22: Western blot analysis of the $\alpha 7$ -nAChR protein. The total amount of protein was not significantly reduced after Ab_{1-42} incubation (■) in comparison to controls (□) (n=3; results are expressed as percent of controls and represent the mean \pm SEM; $P > 0.05$). [Ab_{1-42}] = 0.5 mM.

The presently used mAb 306, described by Dominguez del Toro et al. (1994), is currently undergoing specificity tests in our laboratory. Immunohistochemical assays recently performed by our group on brain sections of $\alpha 7$ -nAChR knock-out mice raised the possibility that mAb 306 could recognize unexpected epitopes in addition to the $\alpha 7$ -nAChR subunit. All the antibodies most commonly used against the $\alpha 7$ -nAChR subunit (mAb 319, Sigma; C-20 and H-302, Santa Cruz) were tested by immunochemistry, leading to similar results. The same observations were made by another group (Herbert et al., 2004). In Western blot analysis, the mAb 306 gave only one band at the expected MW. 2D-electrophoresis will now be performed to investigate further the nature of possibly cross-reacting proteins.

3.5.3 Receptor binding assay

It has recently been demonstrated that the neuronal nAChRs which bind α -bungarotoxin with high affinity (α -BgtRs) and are found throughout the nervous system (Castro and Albuquerque, 1995), appear to be composed solely of α 7 subunits in rat brain (Drisdell and Green, 2000). These receptors can assume two different conformations, which correspond to the active and to the inactive binding states, and only those receptors which are in the active conformation are able to interact with α -bungarotoxin (α -Bgt) and acetylcholine (Rakhilin et al., 1999). Using iodinated α -Bgt for binding assays it is therefore possible to implement the data obtained by Western blot analysis on the total amount of receptor protein with information about their functionality.

Cultures were therefore incubated with [125 I] α -Bgt and the receptor affinity and the total binding sites determined. The results obtained do not point to a statistically significant difference between the K_d values of treated and untreated cultures ($P > 0.05$), showing that the affinity of the homomeric α 7-nAChRs for [125 I] α -Bgt was unaffected by $A\beta_{1-42}$ incubation (Fig.23). The total number of binding sites (R_{TOT}) remained also unaltered ($P > 0.05$) (Figs.23,24).

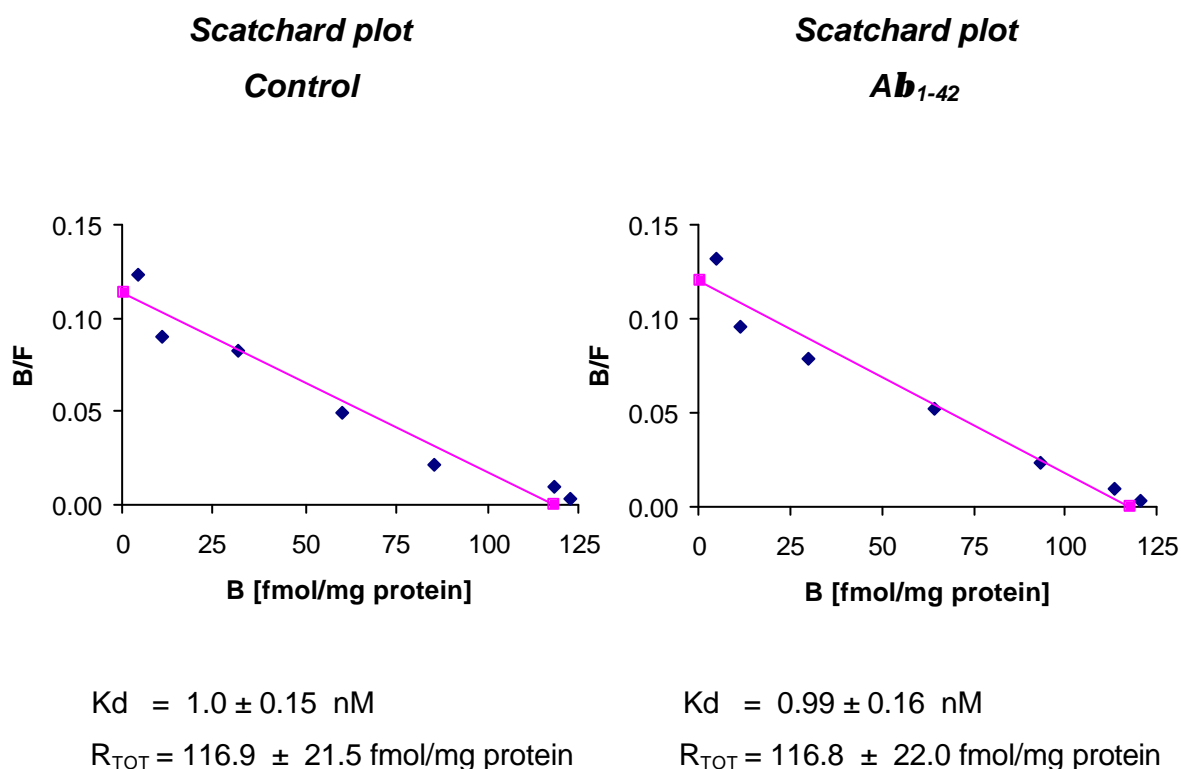


Fig.23: Scatchard plot of the data (results are expressed as mean \pm SEM). [Ab_{1-42}] = 0.5 mM.

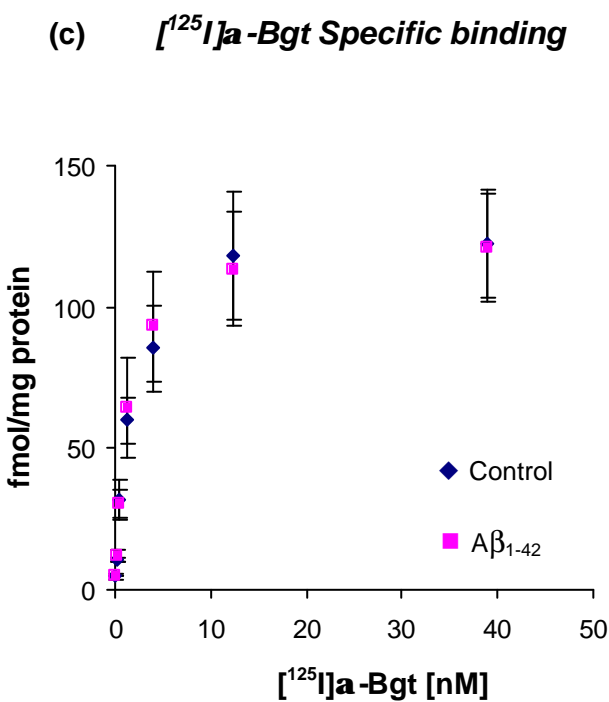
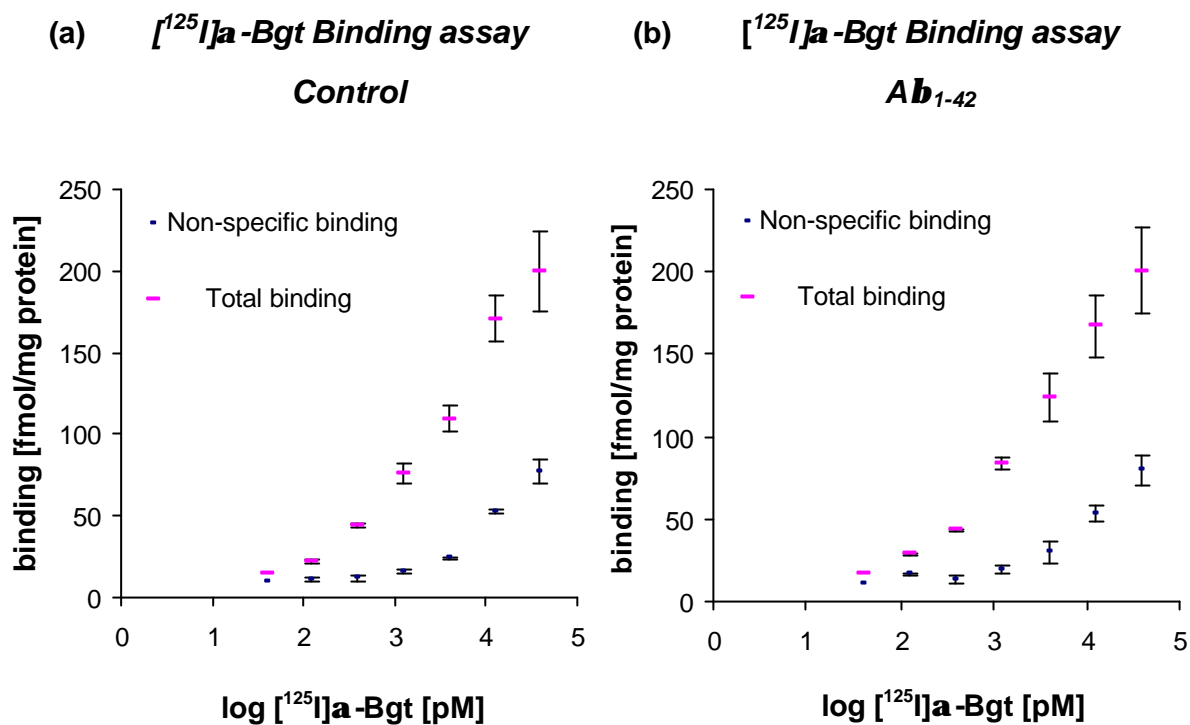


Fig.24: Total and non-specific binding are represented for controls (a) and Ab_{1-42} -treated cultures (b). In (c) the specific binding in controls and under incubation condition is reported (n=3; results are expressed as mean \pm SEM). $[\text{Ab}_{1-42}] = 0.5$ mM.

3.6 Effect of $A\beta_{31-34}$ on cultured neurons

The modification of $[Ca^{2+}]$ homeostasis is thought to be one of the various cytotoxic alterations caused by $A\beta_{1-42}$ at the cellular level (Mattson et al., 1993). Laskay et al. (1997) described the effect of different amyloidogenic peptides on the long-term elevation of intracellular $[Ca^{2+}]$ in primary rat astrocyte cultures. Comparative fluorimetric studies showed that $A\beta_{1-40}$, $A\beta_{1-42}$ and $A\beta_{25-35}$ induce similar effects on the intracellular $[Ca^{2+}]$, suggesting the region 25-35 to be the active center of the peptide. $A\beta_{31-34}$, on the other hand, was able to antagonize this effect, raising the possibility that the short peptide may be protective towards $A\beta_{1-42}$. In this study, the possible protective action of $A\beta_{31-34}$ against some $A\beta_{1-42}$ -induced alterations, like the retraction of the dendrites and the shrinkage of the cell bodies, was investigated. The impact of $A\beta_{31-34}$ on τ -protein phosphorylation state was also studied.

3.6.1 Neuron morphology and number

Upon $A\beta_{31-34}$ incubation, MAP2 immunoreactivity revealed alterations of the cytoskeletal structure which appeared to be different from those caused by $A\beta_{1-42}$. Many cells exhibited a swollen cell body in the region of the apical dendrite and the staining in these parts was often weaker (Fig.25a, white arrows). To test the possible protective action of $A\beta_{31-34}$ against $A\beta_{1-42}$, cultures were treated with both amyloidogenic peptides. As shown in Fig.25b, neurons exhibited damages typical for both $A\beta_{1-42}$ (white arrow-heads) and $A\beta_{31-34}$ (white arrows), showing the own toxic properties of the shorter peptide .

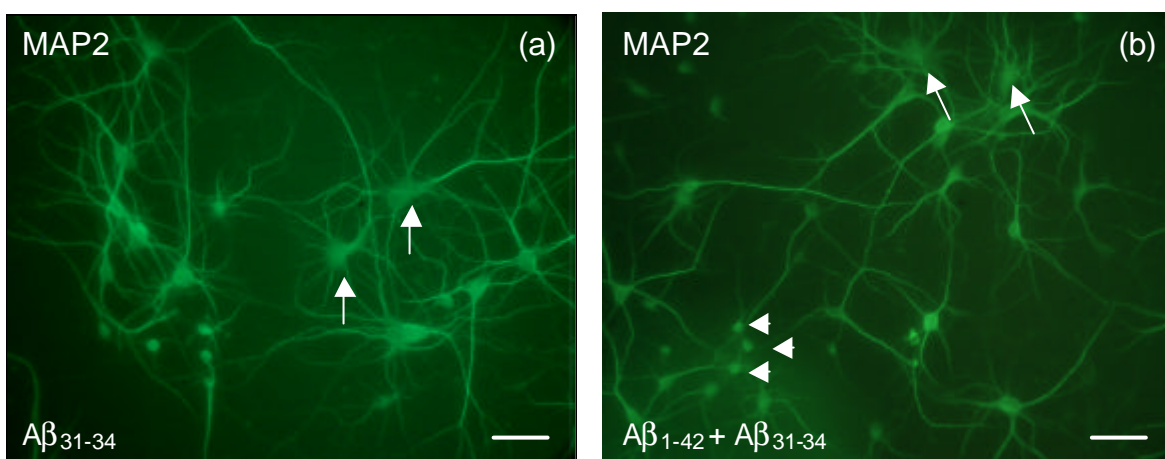


Fig.25: MAP2 immunoreactivity in $A\beta_{31-34}$ -treated cells (a). In (b), $A\beta_{31-34}$ and $A\beta_{1-42}$ were used simultaneously for the incubation. $[A\beta_{1-42}] = 0.5 \text{ mM}$; $[A\beta_{31-34}] = 0.125 \text{ mM}$. Bar: 50 μm .

In the presence of $A\beta_{31-34}$ or $A\beta_{31-34} + A\beta_{1-42}$ the total number of MAP2-positive neurons per coverslip was not altered in comparison to controls (Fig.26).

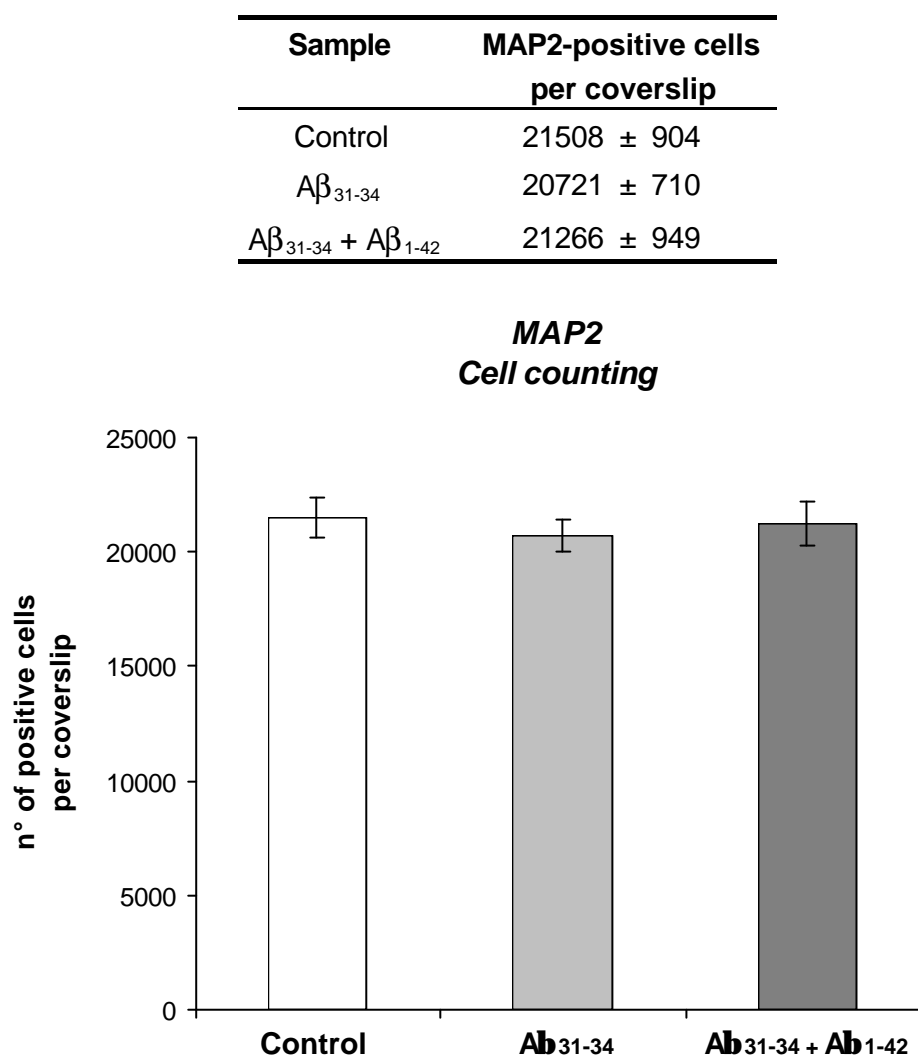


Fig.26: Assessment of the total number of MAP2-positive cells in controls (□), Ab_{31-34} (■) and $Ab_{31-34}+Ab_{1-42}$ -treated cultures (■) (n=5; results are expressed as mean ± SEM; $P>0.05$). $[Ab_{1-42}] = 0.5$ mM; $[Ab_{31-34}] = 0.125$ mM.

3.6.2 LDH determination

The cytotoxicity of $A\beta_{31-34}$ was tested measuring the LDH release in the cell supernatant after treatment. Upon $A\beta_{31-34}$ incubation, no significant difference in the LDH release was found (Fig.27) indicating that the cell viability remained unaltered. The same observation on cell viability was made when both peptides were used for the incubation (Fig.27).

Sample	Absorbance (490 nm)
Control	0.15 ± 0.03
A β ₃₁₋₃₄	0.19 ± 0.04
A β ₃₁₋₃₄ + A β ₁₋₄₂	0.17 ± 0.05

Cytotoxicity assay (LDH)

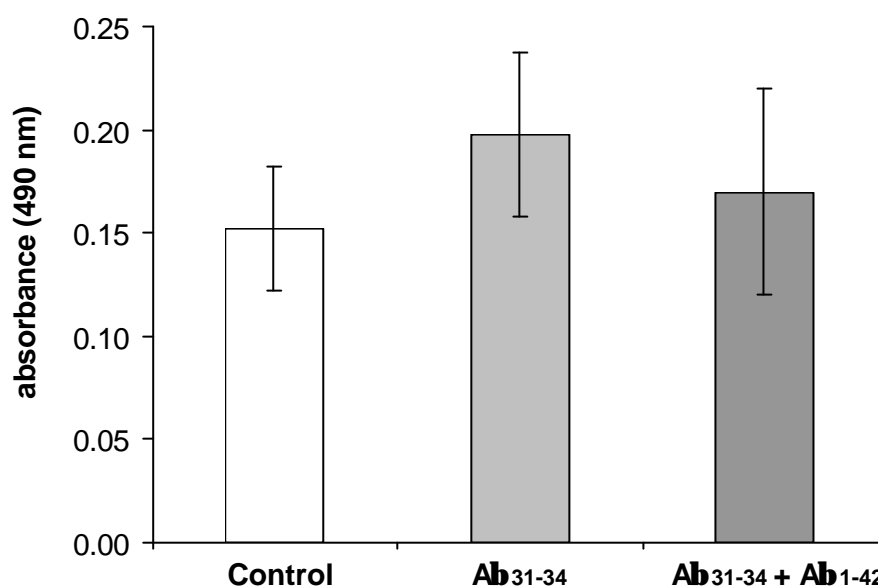


Fig.27: Cytotoxicity in controls (□), Ab₃₁₋₃₄- (■) and Ab₃₁₋₃₄+Ab₁₋₄₂-treated cultures (■), reported as formazan absorbance (n=4; results are expressed as mean ± SEM; $P>0.05$).

[Ab₁₋₄₂] = 0.5 mM; [Ab₃₁₋₃₄] = 0.125 mM.

3.6.3 Morphological measurements

The determination of the total MAP2-stained area in the presence of A β ₃₁₋₃₄ or A β ₃₁₋₃₄ + A β ₁₋₄₂ revealed no significant difference between controls and treated cultures. The decrease of the MAP2-ir area measured after A β ₁₋₄₂ incubation could not be observed under these incubation conditions (Fig.28).

Sample	Percent of MAP2-ir area
Control	12.7 ± 0.6
A β ₃₁₋₃₄	12.6 ± 0.4
A β ₃₁₋₃₄ + A β ₁₋₄₂	11.5 ± 0.6

Area measurement

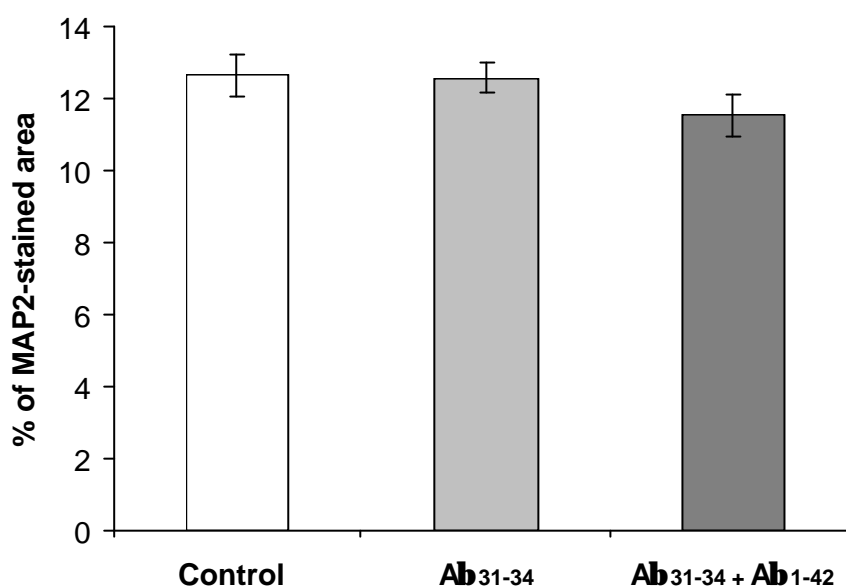
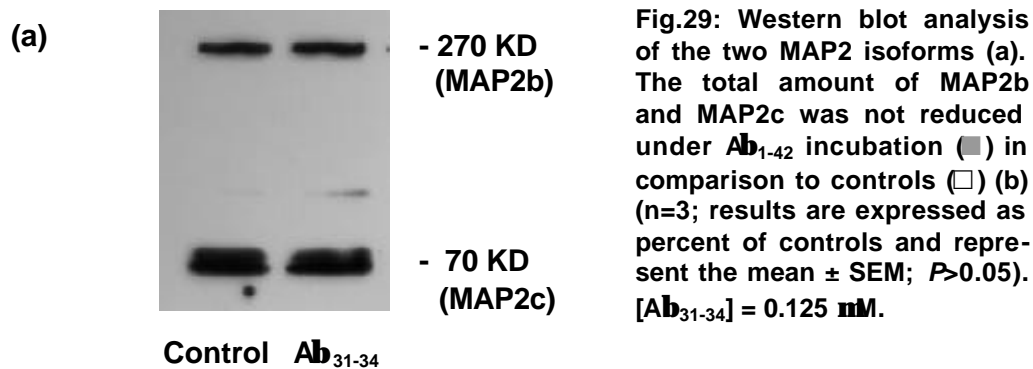


Fig.28: The MAP2-stained area was measured as percent of the total area on the coverslip in controls (□), Ab₃₁₋₃₄ (■) and Ab₃₁₋₃₄+Ab₁₋₄₂-treated cultures (■) (n=5; results are expressed as mean ± SEM; *P*>0.05). [Ab₁₋₄₂] = 0.5 mM; [Ab₃₁₋₃₄] = 0.125 mM.

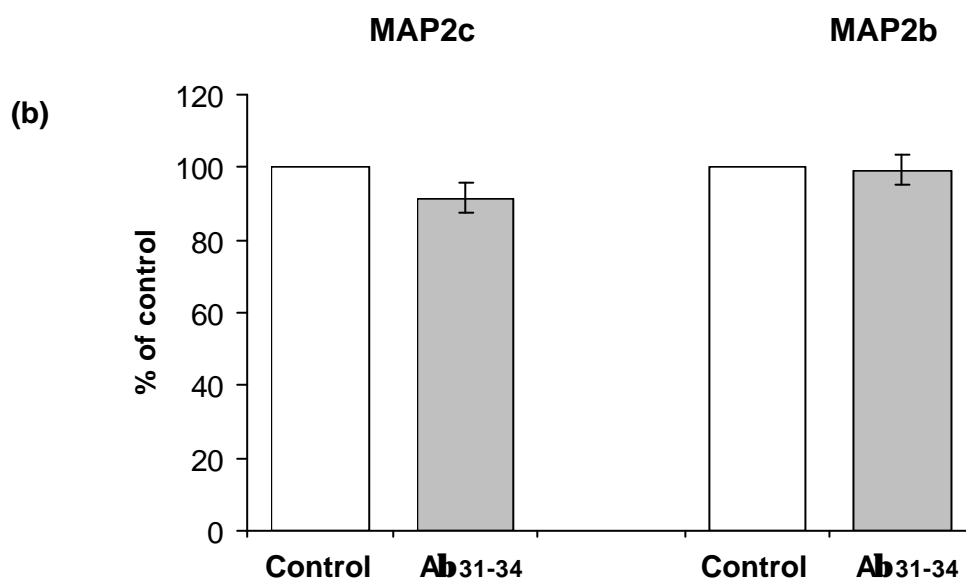
3.6.4 Quantitative determination of MAP2 isoforms

The effect of A β ₃₁₋₃₄ on the expression of the different MAP2 isoforms was investigated by means of Western blot. The total amount of MAP2c remained unaffected (Fig.29), as it was noticed with A β ₁₋₄₂. In contrast to the findings obtained upon A β ₁₋₄₂ treatment, no decrease in the total amount of MAP2b was seen under A β ₃₁₋₃₄ incubation (Fig.29), suggesting a different impact of the smaller peptide on the expression of cytoskeletal proteins in comparison to the longer A β form.

Sample	MAP2c	MAP2b
Control	100	100
A β ₃₁₋₃₄	92.2 \pm 4.2	99.2 \pm 4.1



MAP2
Western blot analysis



3.7 Effect of Ab₃₁₋₃₄ on the phosphorylation state of the τ -protein

Incubation with the antibodies AT8, AT180, 12E8 and AD2 was performed in order to investigate the impact of A β ₃₁₋₃₄ on the phosphorylation state of the τ -protein in the different functional domains.

3.7.1 Immunocytochemistry

In the presence of the short amyloid fragment $A\beta_{31-34}$, AT8 and AD2 immunoreactivity seemed to be increased when compared to controls (Fig.30). The positive staining appeared to be localized particularly in the cell body and in the apical dendrite, where cells were swollen. As already mentioned, τ -protein is distributed in axons under normal conditions (Binder et al., 1985). Its presence in the cell bodies and in the dendrites is a consequence of its abnormal phosphorylation state (for reviews see Mandelkow et al., 1995; Trojanowski and Lee, 1995). AT8, AD2 and 12E8 immunostaining revealed positivity in the apical dendrite, which was more intensely stained in comparison to untreated cultures, while AT180 labeling was too weak to distinguish the immunoreactivity from the background (Fig.30).

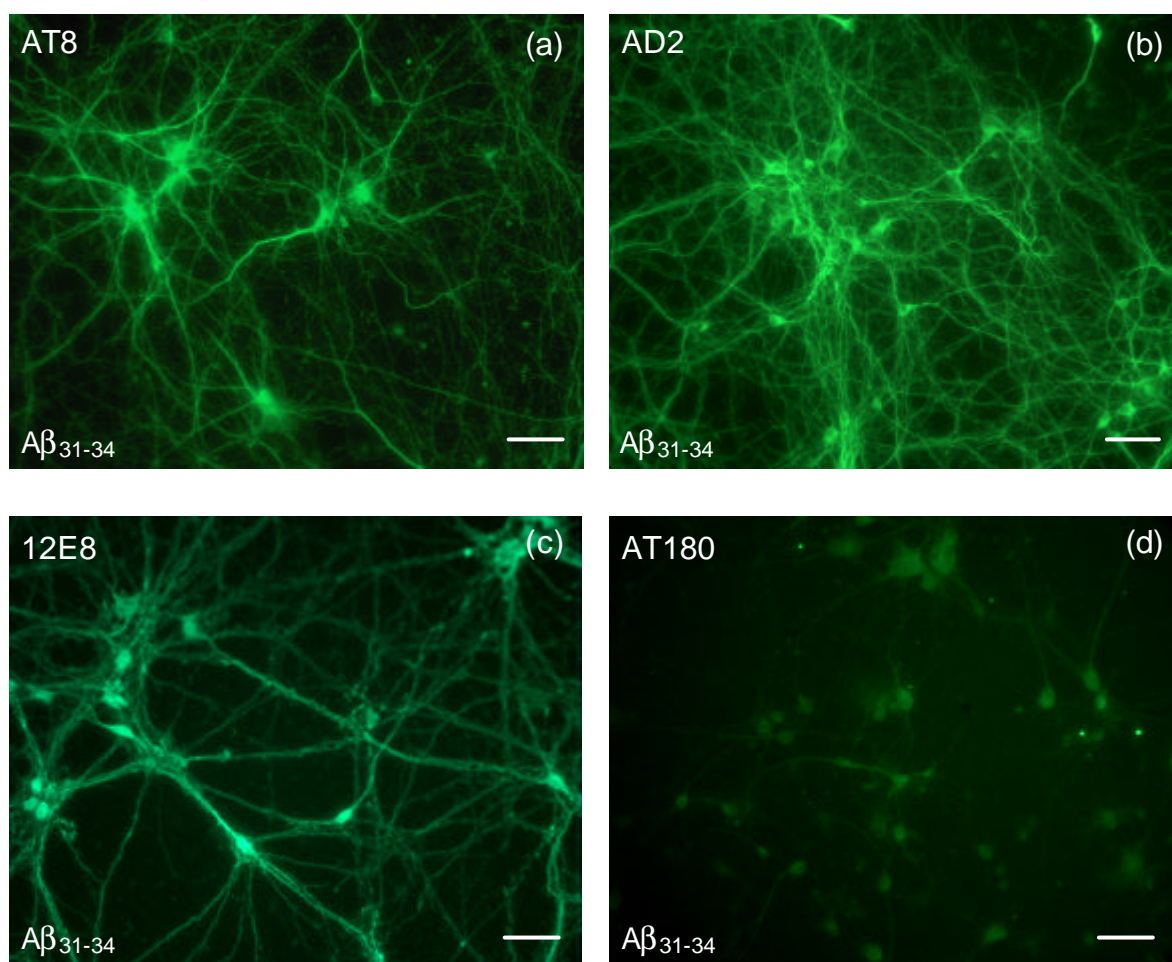


Fig.30: Immunofluorescence labeling of different τ -phosphorylation sites using AT8 (a), AD2 (b), 12E8 (c) and AT180 (d) antibodies in Ab_{31-34} -treated cultures. $[Ab_{31-34}] = 0.125 \text{ mM}$. Bar: 50 μm .

To extend the reported findings, AT8-, 12E8- and AD2-ir neurons were counted. Upon $A\beta_{31-34}$ incubation, a statistically significant increase in the number of AT8- and AD2-ir neurons was found in comparison to vehicle-treated cultures, while numbers of 12E8-ir cells remained unaltered (Fig.31).

(a)

Sample	AT8-positive cells per coverslip
Control	7230 \pm 828
$A\beta_{31-34}$	9146 \pm 728

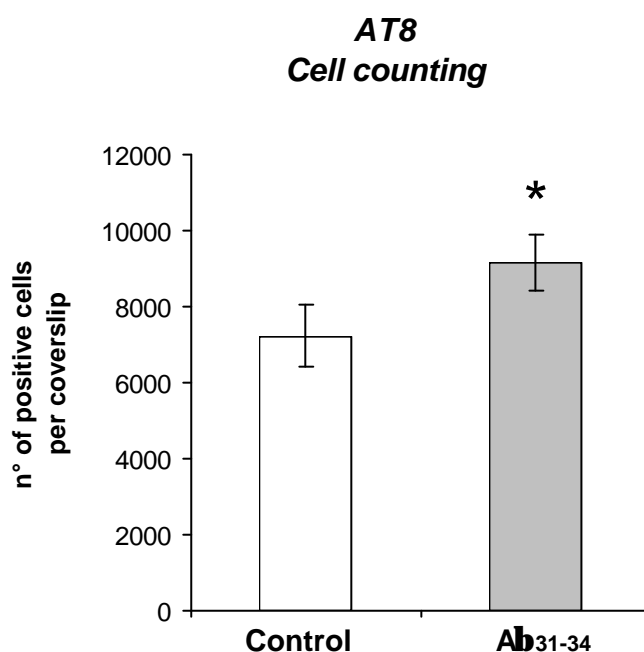
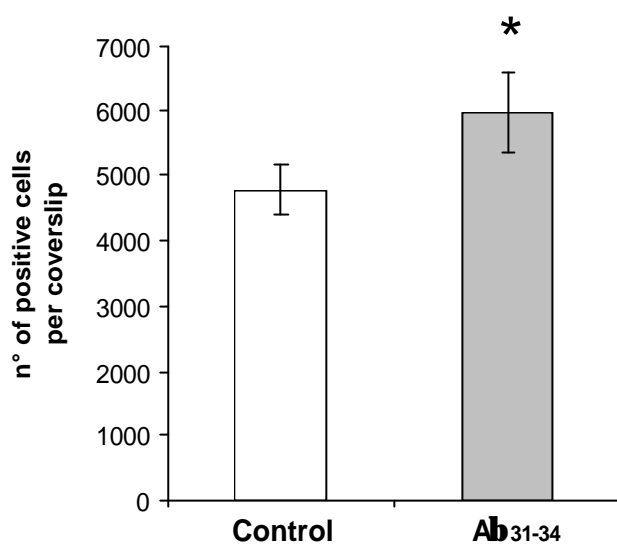


Fig.31: Total number of AT8- (a), AD2- (b, next page) and 12E8-positive cells (c, next page) in controls (\square) and Ab_{31-34} -treated cultures (\blacksquare) (n=3; results are expressed as mean \pm SEM; * $P < 0.05$). [Ab_{31-34}] = 0.125 mM.

(b)

Sample	AD2-positive cells per coverslip
Control	4775 ± 388
A β ₃₁₋₃₄	5952 ± 608

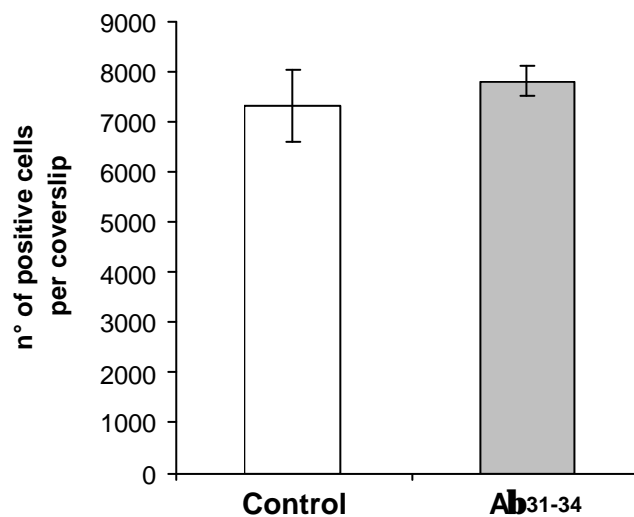
**AD2
Cell counting**



(c)

Sample	12E8-positive cells per coverslip
Control	7314 ± 700
A β ₃₁₋₃₄	7802 ± 299

**12E8
Cell counting**



3.7.2 Western blot analysis

Quantitative determination of τ -protein phosphorylated at the distinct epitopes supported the results obtained by immunocytochemistry. In contrast to the observations made after $A\beta_{1-42}$ -treatment, following incubation with $A\beta_{31-34}$ the level of phosphorylation of fetal τ -protein resulted to be significantly increased at AT8 sites (Fig.32).

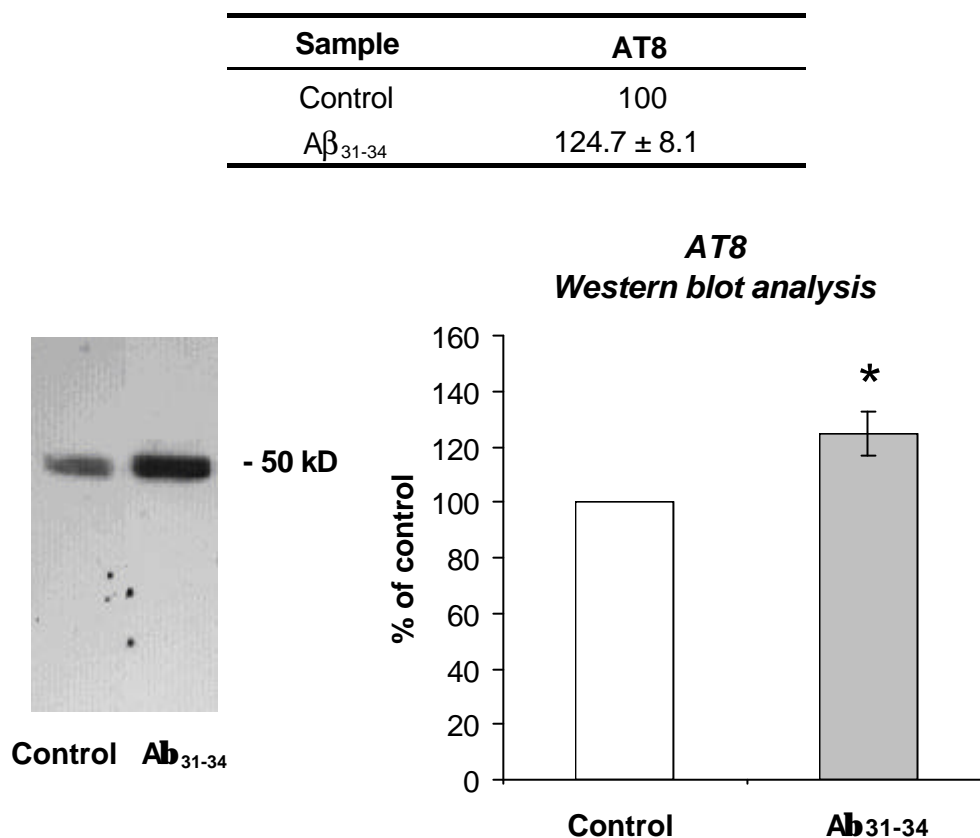


Fig.32: Total amount of τ -protein phosphorylated at AT8 epitopes. Compared to controls (□), Ab_{31-34} -treated cultures (■) contained a higher amount of phosphorylated τ -protein at these epitopes (n=5; results are expressed as percent of controls and represent the mean \pm SEM; * $P<0.05$). [Ab_{31-34}] = 0.125 mM.

In accordance with the increase of τ -protein phosphorylated at AT8 sites, the total amount of τ -protein dephosphorylated at Ser199 / Ser202, detected using the antibody tau-1, was significantly reduced under incubation conditions in comparison to vehicle-treated cells (Fig.33), in contrast to the $A\beta_{1-42}$ -incubation (see 3.4.2).

Sample	Tau-1
Control	100
A β ₃₁₋₃₄	79.4 \pm 6.9

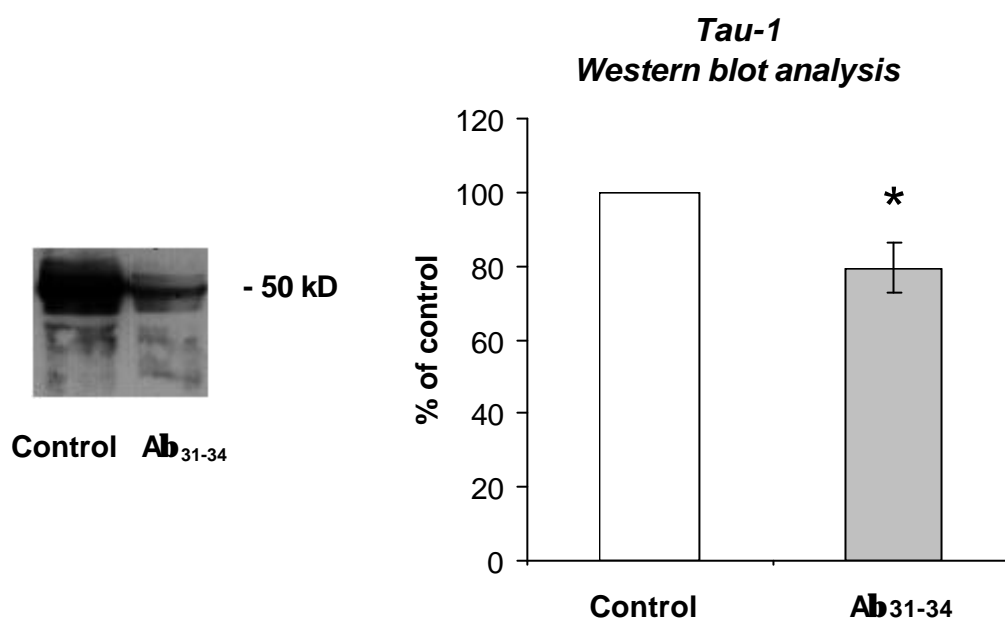


Fig.33: The total amount of τ -protein dephosphorylated at tau-1 epitopes was significantly decreased in Ab₃₁₋₃₄-treated cultures (■) in comparison to controls (□), as revealed by densitometric analysis of Western blot bands (n=5; results are expressed as percent of controls and represent the mean \pm SEM; * P <0.05). [Ab₃₁₋₃₄] = 0.125 mM.

Results obtained when the AD2 antibody was used to detect τ -phosphorylation at Ser396 and Ser404 also indicated an increase in the phosphorylation state. In the presence of the short A β fragment, the amount of phosphorylated τ -protein at these epitopes was significantly increased (Fig.34).

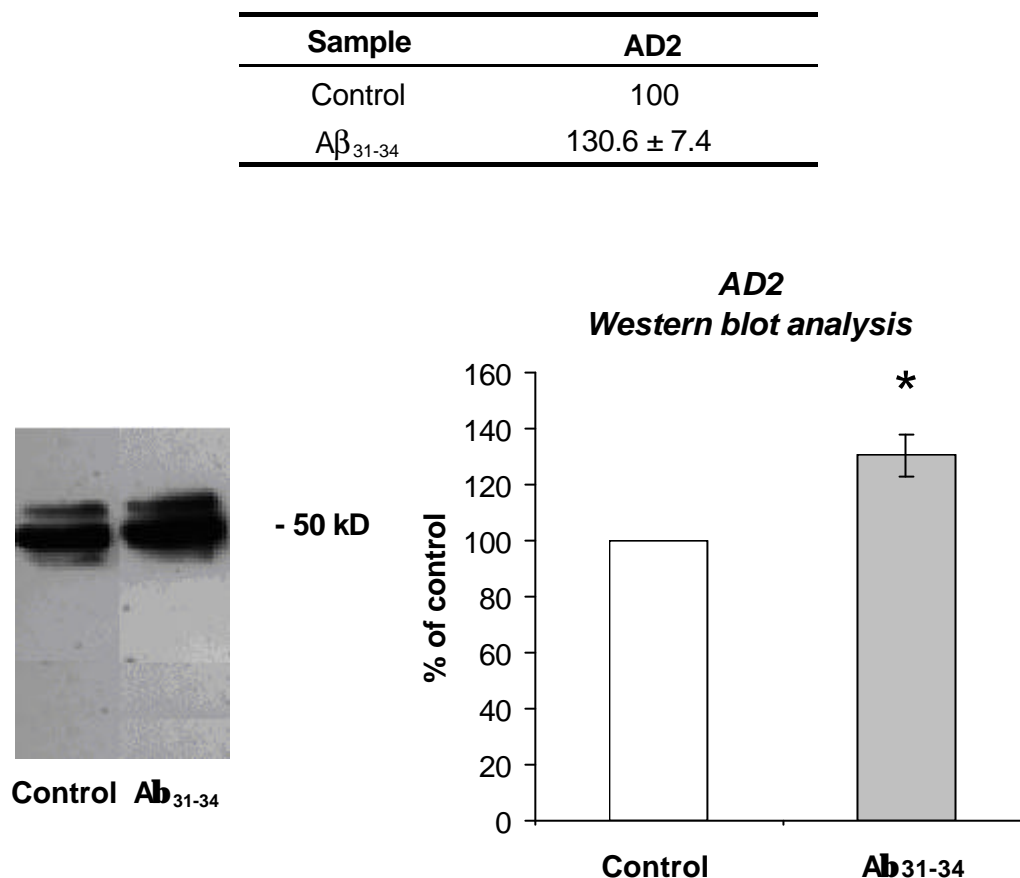


Fig.34: The total amount of τ -protein phosphorylated at AD2 epitopes was significantly higher in Ab₃₁₋₃₄-treated cultures (■) than in controls (□) (n=3; results are expressed as percent of controls and represent the mean \pm SEM; * P <0.05). [Ab₃₁₋₃₄] = 0.125 mM.

In contrast to the effect observed at AT8 and AD2 sites, no significant difference in the amount of phosphorylated τ -protein at AT180 (Fig.35) and 12E8 epitopes (Fig.36) was found between vehicle- and $A\beta_{31-34}$ -treated cells.

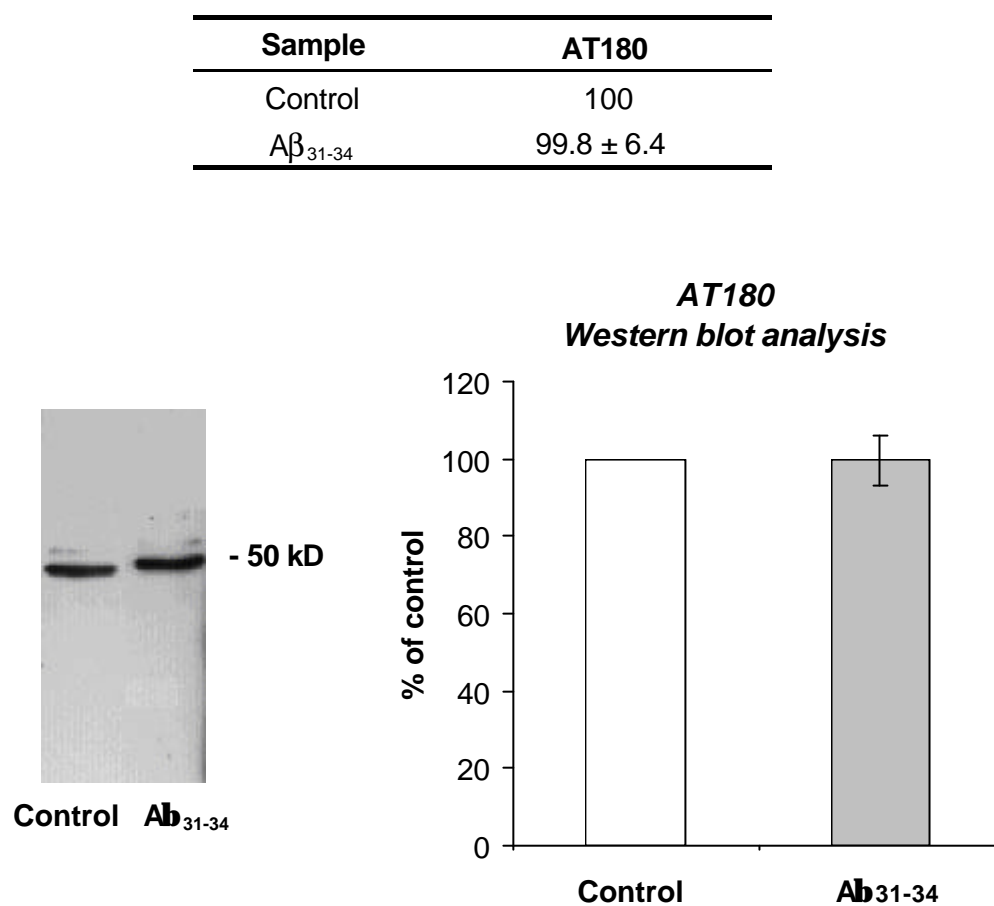


Fig.35: Western blot analysis of τ -protein phosphorylated at AT180 epitopes did not show any significant difference in the total amount of protein in controls (\square) and Ab_{31-34} -treated cultures (\blacksquare) (n=6; protein amounts are expressed as percent of controls and represent the mean \pm SEM; $P>0.05$). [Ab_{31-34}] = 0.125 mM.

Sample	12E8
Control	100
A β_{31-34}	128.2 \pm 14.5

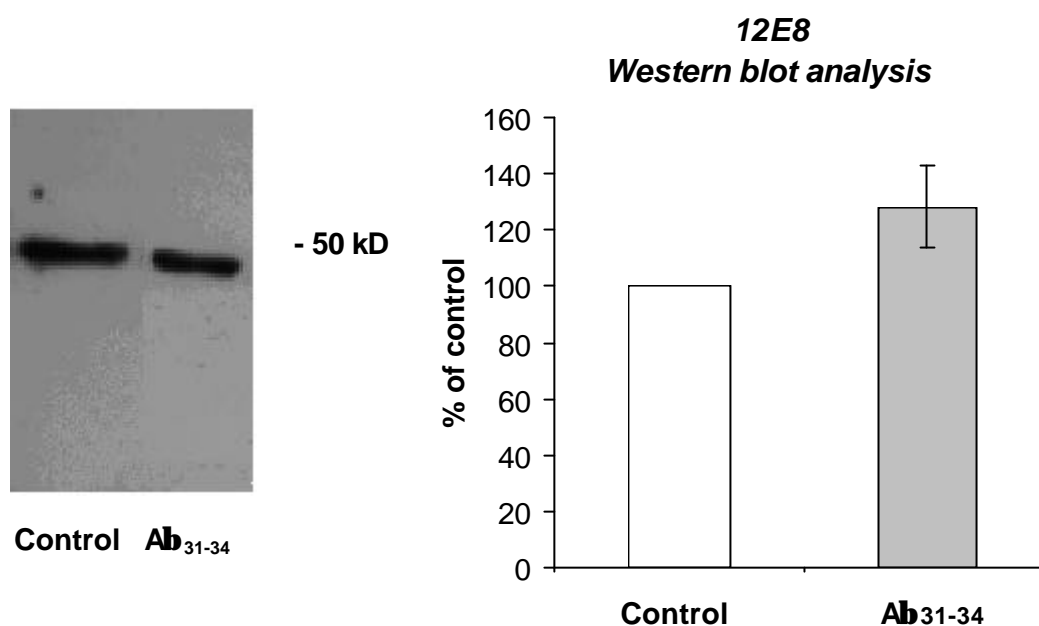


Fig.36: Western blot analysis of t-protein phosphorylated at 12E8 epitopes. No significant change in the total amount of protein in controls (□) and Ab₃₁₋₃₄-treated cultures (■) was found (n=3; protein amounts are expressed as percent of controls and represent the mean \pm SEM; $P>0.05$). [Ab₃₁₋₃₄] = 0.125 mM.

3.8 Effect of Ab₃₁₋₃₄ on the expression of the $\alpha 7$ -nAChR subunit

3.8.1 Immunocytochemical findings

$\alpha 7$ -nAChR immunostaining following A β_{31-34} treatment (Fig.37) showed a more conserved cell morphology in comparison to A β_{1-42} -treated cultures, indicating a probably minor effect of the shorter peptide on the $\alpha 7$ -nAChR subunit. As previously reported, all MAP2-positive neurons express the $\alpha 7$ -nAChR subunit, and their number, like the number of MAP2 cells, was therefore not affected by the presence of A β_{31-34} .

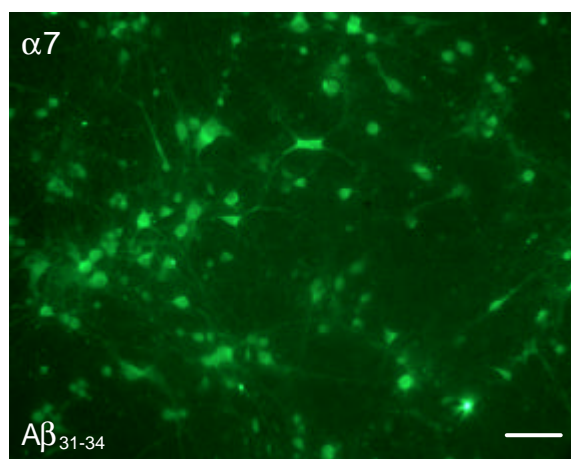


Fig.37: $\alpha 7$ -nAChR subunit immunoreactivity in Ab_{31-34} -treated cells. $[Ab_{31-34}] = 0.125$ mM. Bar: 50 μ m.

3.8.2 Quantitative determination

The total amount of $\alpha 7$ -nAChR protein did not change significantly under Ab_{31-34} incubation in comparison to vehicle-treated cultures (Fig.38).

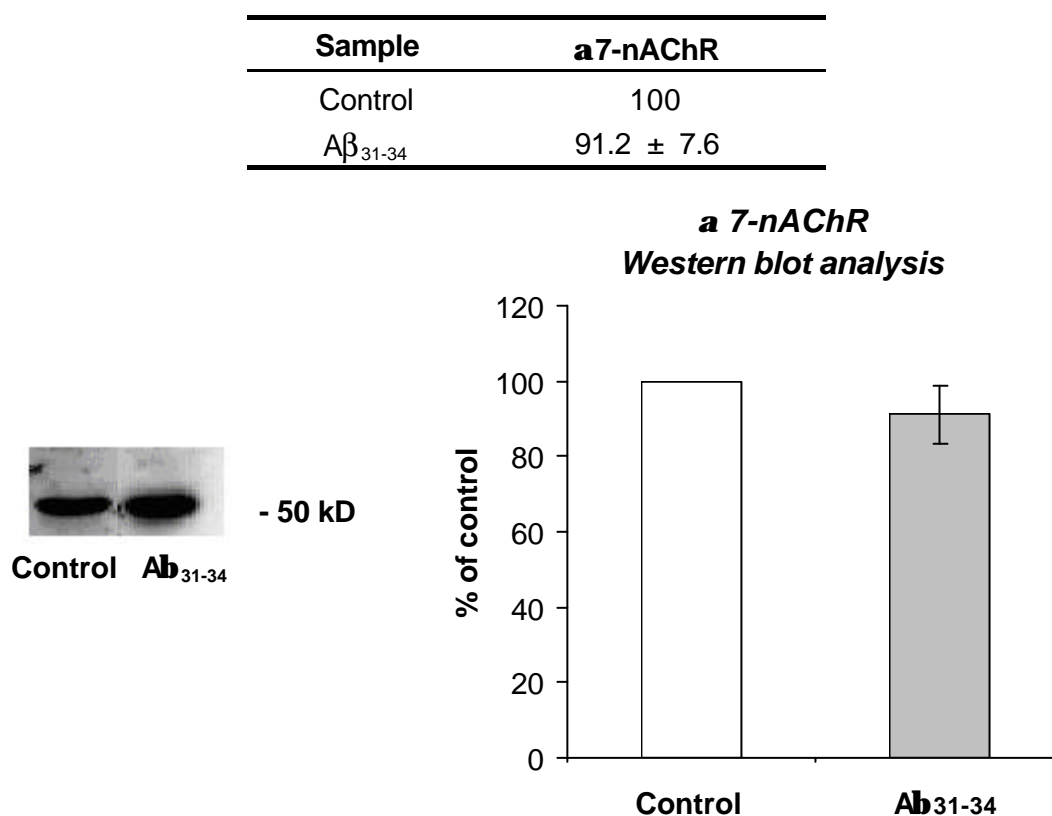


Fig.38: Western blot analysis of the $\alpha 7$ -nAChR protein. Its total amount was not significantly changed after Ab_{31-34} treatment (■) compared to controls (□) (n=3; results are expressed as percent of controls and represent the mean \pm SEM; $P > 0.05$). $[Ab_{31-34}] = 0.125$ mM.

3.8.3 Receptor binding assay

The binding assay performed after $A\beta_{31-34}$ treatment did not reveal any significant difference in the affinity of the homomeric $\alpha 7$ -nAChRs for $[^{125}I]\alpha$ -Bgt. The value of K_d (Fig.39a) remained in fact in the same range as measured in controls (see 3.5.3) and was not significantly different ($P > 0.05$). The total number of binding sites (R_{TOT}) was also not affected by the incubation ($P > 0.05$) (Fig.39).

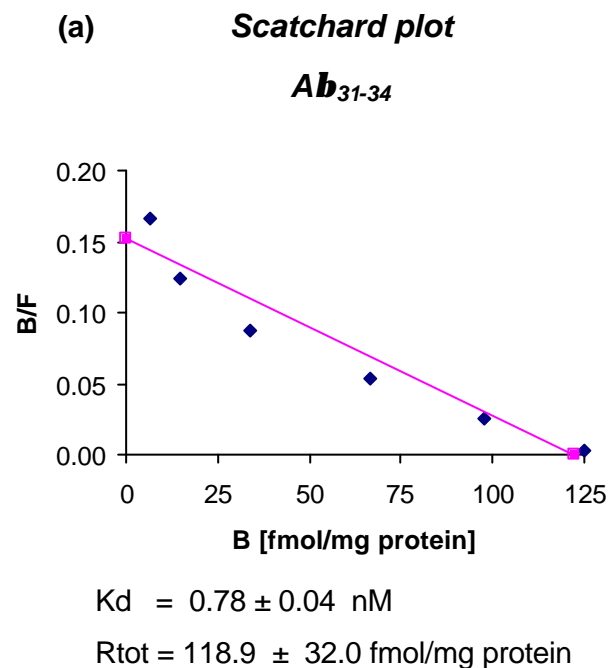
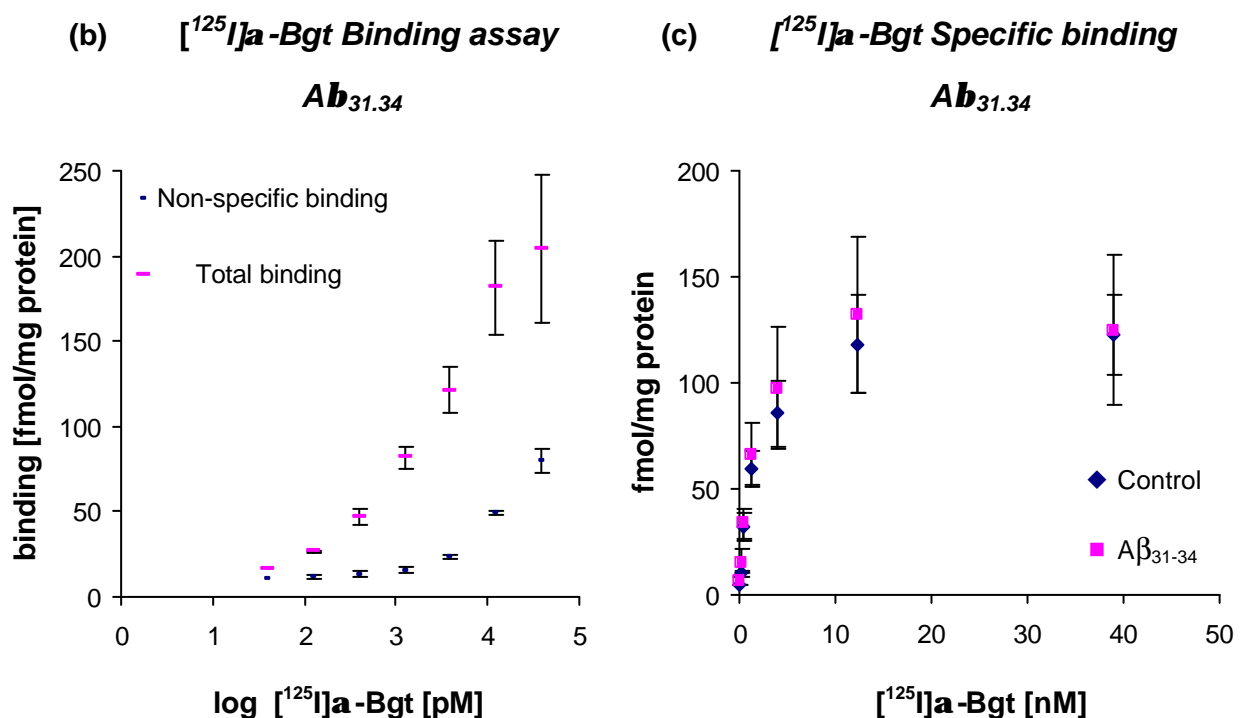


Fig.39: Scatchard plot of the data (a). Total and non specific binding are reported for Ab_{31-34} -treated cultures (b). In (c) the specific binding in controls and under incubation conditions is represented (n=3; results are expressed as mean \pm SEM). $[Ab_{31-34}] = 0.125$ mM.



3.9 Colocalization of the $\alpha 7$ -nAChR subunit with hyperphosphorylated τ -protein

Immunocytochemical assays were performed to check whether the localization of the $\alpha 7$ -nAChR subunit was influenced by the $A\beta_{31-34}$ -induced τ -hyperphosphorylation. $\alpha 7$ -nAChR subunit immunoreactivity was detected in all AT8- and AD2-positive neurons (Fig.40).

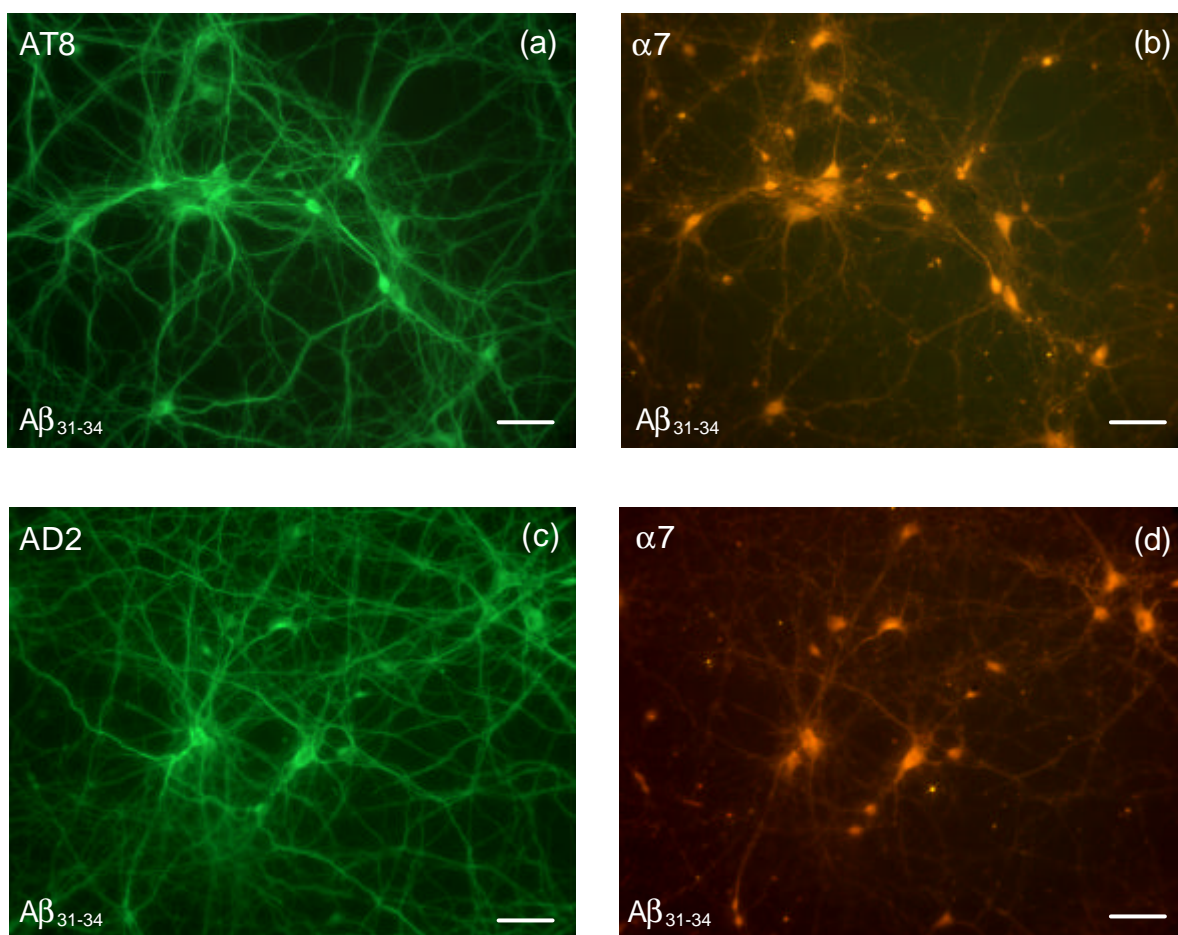


Fig.40: The immunolabeling of the $\alpha 7$ -nAChR subunit (b,d) was not influenced by the presence of τ -protein phosphorylated at AT8 (a) and AD2 epitopes (c). $[A\beta_{31-34}] = 0.125 \text{ mM}$. Bar: 50 μm .

3.10 Summary of results

The effects of the two peptides are schematically represented here.

		Ab ₁₋₄₂ (0.5 mM)	Ab ₃₁₋₃₄ (0.125 mM)
Cell viability	LDH release	unchanged	unchanged
MAP2 IR	MAP2-ir cells	unchanged	unchanged
	MAP2-ir area	decreased	unchanged
	MAP2 c WB	unchanged	unchanged
	MAP2 b WB	decreased	unchanged
t-hyperphosphorylation	AT8-ir cells	unchanged	increased
	AT8 WB	unchanged	increased
	Tau-1 WB	unchanged	decreased
	AD2-ir cells	unchanged	increased
	AD2 WB	unchanged	increased
	12E8-ir cells	unchanged	unchanged
	12E8 WB	unchanged	unchanged
	AT180 WB	unchanged	unchanged
α7-nAChR subunit	α7-nAChR-ir cells	unchanged	unchanged
	α7-nAChR WB	unchanged	unchanged
	Kd ([¹²⁵ I]α-Bgt binding)	unchanged	unchanged
	R0 (¹²⁵ I]α-Bgt binding)	unchanged	unchanged

Results: appendix

α 4-nAChR subunit

Immunocytochemical studies were performed using the anti- α 4-nAChR subunit antibody from Chemicon (Fig.41).

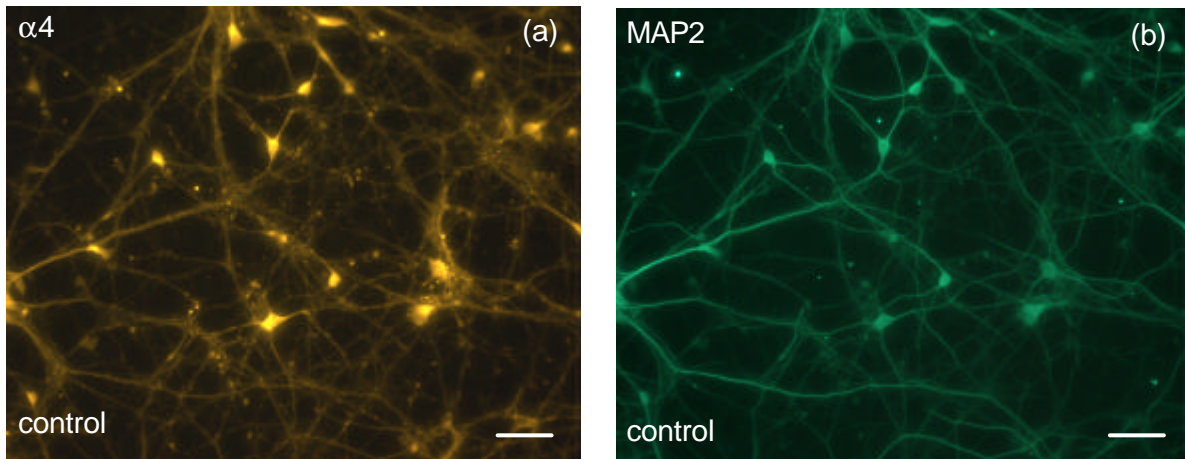
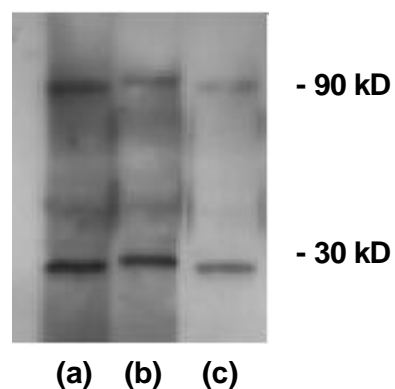


Fig.41: α 4-nAChR subunit immunoreactivity (a) and correspondent MAP2 staining (b) in untreated cultures. Bar: 50 μ m.

The α 4-nAChR subunit immunoreactivity appeared to be homogeneously distributed on the cell surface. It was present in all MAP2-positive cells, as revealed by neuron counting. However, the following Western blot analysis, for which the antibody has not been tested by the manufacturer, cast doubt on the specificity of the antibody. For the rat α 4-nAChR subunit, a 74 kD band was expected. Instead, two other bands at about 30 and 90 kD, respectively, were found (Fig.42).



**Fig.42: Western blot analysis of the α 4-nAChR subunit. Two main bands were obtained at 30 and 90 kD using different concentrations of antibody.
(a)=1:1000
(b)=1:2000
(c)=1:5000**

The investigation of the α 4-nAChR subunit was therefore not continued.

4. DISCUSSION

In Alzheimer's disease, the possible mechanisms linking A β deposition, cytoskeletal damage, τ -protein hyperphosphorylation and nAChR expression still need to be clarified. The aim of the present study was the evaluation of the neurotoxic effects of the A β fragment A β ₁₋₄₂ and the putatively protective fragment A β ₃₁₋₃₄ on the cytoskeletal proteins of cultured rat hippocampal neurons, more precisely on MAP2 expression and on the phosphorylation state of the τ -protein. A second point of interest was the attempt to determine expression and distribution of some nAChR subunits in the same model, and their possible alterations after treatment with the two amyloidogenic peptides.

4.1 Effects of A β ₁₋₄₂

Soon after the neurotoxic potency of amyloid peptides had been corroborated (Yankner et al., 1990; Pike et al., 1991a, 1991b) attempts have been made to elucidate the possible molecular mechanisms leading to neuronal dystrophy in A β -exposed cultured hippocampal neurons. In this vein, different A β fragments have been employed for the incubation. In this study, the first amyloidogenic peptide used for the treatment was fibrillar A β ₁₋₄₂. This A β fragment was chosen for the following reasons. (1) Together with A β ₁₋₄₀, A β ₁₋₄₂ in fact is one of the two products generated *in vivo* by the β - and γ -secretase APP-cleavage (for review see Mattson, 1997). (2) Methodological studies concerned with the physicochemical nature of A β peptides and their biological effects when used for *in vitro* approaches (Busciglio et al., 1992; Lorenzo and Yankner, 1994) showed that there is a correlation between the toxicity and the aggregation state of the peptide, and that the reported neurotoxic effects, like retraction of neurites, dystrophic changes and decreased density of the presynaptic terminals along the dendrites, can only be expected from incubation with fibrillar A β . The longer and more hydrophobic forms of A β aggregate more rapidly: self-association has in fact been reported to occur faster for A β ₁₋₄₂ than for the shorter form A β ₁₋₄₀ (Snyder et al., 1994). The usual technique to obtain amyloid fibrils is the pre-aging of an aqueous 350 μ M stock solution for at least 4 days at 37°C, from which the actual incubation solutions are prepared (Lorenzo and Yankner, 1994). This is exactly how we prepared our solutions (cf. 2.5.5). The formation of fibrils was confirmed by

electron microscopy. Although $A\beta_{1-42}$ toxicity is comparable in aqueous solution, acetonitrile and DMSO (Busciglio et al., 1992), an aqueous solution was preferred to exclude any possible toxic role of the solvent. (3) $A\beta_{1-42}$ is more abundant in AD brains in comparison to non-diseased ones and cell transfection experiments have shown that mutations of APP and presenilin, which can cause AD, and other risk factors (Apo E alleles) lead to $A\beta_{1-42}$ production and accumulation (Schmechel et al., 1993; Suzuki et al., 1994; Scheuner et al., 1996). (4) Relevant for the choice of $A\beta_{1-42}$ were also observations indicating strong similarities between neurite dystrophy in AD and $A\beta_{1-42}$ -induced neurite dystrophy in hippocampal neuronal cultures (Pike et al., 1992).

Cells were incubated after seven days in culture, as the neuronal differentiation normally occurs within five days (Busciglio et al., 1995). A three-day $A\beta_{1-42}$ treatment allowed the appreciation of morphological changes without leading to neuron death. The last point was taken into consideration also when deciding the appropriate concentration of $A\beta_{1-42}$, as concentrations higher than 2.5 μM have shown to cause cell death (Pike et al., 1991b). In the present study, a concentration of 0.5 μM was used. Gravina et al. (1995) have shown that $A\beta_{1-42}$, the major peptide fragment of amyloid plaques in full-blown Alzheimer's disease, is present in concentrations of about 3000 to 5000 pmol/g w.w. in Alzheimer brains. Similar ranges have been demonstrated in plaque-forming mouse strains like the Tg2576 mouse (Kawarabayashi et al., 2001). Wiebringhaus et al. (2000) reported concentrations of 2.3 pmol/g w.w. of $A\beta_{1-42}$ in the brains of APP SL x PS1mut mice. Taken together, these data suggest that concentrations of $A\beta_{1-42}$ in the end-stage of Alzheimer's disease amount to maximally 5 μM while those reflecting the development of amyloid plaque formation, e.g. in the APP SL x PS1mut mice, range from low initial values to maxima of 2 nM concentrations at the age of 16 months. The presently used concentration of 0.5 μM thus represents a concentration that ranges between the level that is probably necessary to induce plaque formation in mouse mutants and the ones seen in full-blown Alzheimer's disease.

4.1.1 Cell morphology

Looking at the impact of $A\beta_{1-42}$ on cell morphology, retraction of the dendrites and shrinkage of the cell bodies were evident after the current treatment, and the quantification of these alterations resulted to be significant, as shown by stereological

measurements of the total MAP2-positive area on the coverslip. These observations are consistent with previous studies on hippocampal primary cultures treated with fibrillary A β , which reported similar findings (Yankner et al., 1990; Pike et al., 1992; Lorenzo and Yankner, 1994). In contrast to those studies, where a 20 μ M concentration caused a massive cell death, the observed effect on cell morphology with A β ₁₋₄₂ in the currently used 0.5 μ M concentration was not accompanied by any significant impact either on the total number of neurons or on the number of lysed cells. The only alteration which occurred at the cytoskeletal level in the presence of A β ₁₋₄₂ was a reduction in the total amount of MAP2b. MAP2b is normally expressed pre- and postnatally in rat brain (for review see Goedert et al., 1991) and its level remains fairly constant during brain development. As it is generally accepted that MAP2b is required for neurite outgrowth (for review see Shafit-Zagardo and Kalcheva, 1998), a decrease in its expression may play a role in the observed retraction of dendrites.

4.1.2 Phosphorylation state of the τ -protein

Besides the investigation of A β effects on cell morphology, its potential impact on the hyperphosphorylation of the τ -protein became of particular interest. Takashima et al. (1993) were able to show an increase in the activity of τ -protein protein kinase / glycogen synthase kinase 3 (TPK1/GSK-3 β), one of the most important enzymes involved in τ -hyperphosphorylation, after a 24-hour incubation with 20 μ M A β ₁₋₄₃. They also detected immunoreactivity using the “Alz-50” antibody under incubation conditions. This antibody, although it is not specific for phosphorylated derivatives of the τ -protein, recognizes a τ -epitope associated with PHFs in AD brains (Wolozin et al., 1986). Busciglio et al. (1995), using rat and human cortical dissociation cultures, investigated the phosphorylation state of the τ -protein upon a seven-day exposure to 20 μ M A β ₁₋₄₀. They could show that this kind of treatment resulted in a distinct phosphorylation of the τ -protein at Ser-202 (antibody AT8) and at Ser-396 / Ser-404 (antibody PHF) which was reversible after induction of dephosphorylating conditions. Götz et al. (2001) reported that the injection of A β ₁₋₄₂ fibrils in the brain of P301L mutant human τ transgenic mice can significantly accelerate NFT formation in the cell bodies within the amygdala. However, neither the mutation nor A β ₁₋₄₂ injection alone were sufficient to generate high numbers of NFTs. In this study, a 0.5 μ M concentration of A β ₁₋₄₂ did not lead to a statistically significant

increase in τ -phosphorylation at Ser-202 (antibody AT8) or Ser-396 / Ser-404 (antibody AD2) after three days of exposure. The same result was obtained at the phospho-epitopes Thr-231 / Ser-235 (antibody AT180) and Ser-262 (antibody 12E8). These findings suggest that $A\beta_{1-42}$, at these concentrations, does not lead to τ -hyperphosphorylation, and that τ -hyperphosphorylation is consequently not involved in the morphological alterations observed after $A\beta_{1-42}$ incubation. The major $A\beta$ fragment used by Busciglio et al. (1995) was $A\beta_{1-40}$, but they also reported the use of $A\beta_{1-42}$. As mentioned above, previous studies had mostly used concentrations in the range of 15-25 μ M (Pike et al., 1991, 1992; Busciglio et al., 1995; Grace et al., 2003). These concentrations are far beyond the highest values assessed in human AD brain as well as in transgenic mice and have been applied for quite long incubation times. Moreover, we observed that a 0.5 μ M concentration of $A\beta_{1-42}$ was sufficient to induce morphological changes in treated neurons after a three-day incubation.

Assessment of phosphorylation sites was presently performed with standard immunochemical procedures: for the immunocytochemical demonstration well-established immunoperoxidase and immunofluorescent techniques were used. The same holds true for the Western blot techniques. The only relevant difference between the conditions used in this study and those employed by others (Takashima et al., 1993; Busciglio et al., 1995) appears therefore to be the amyloid peptide concentration. It may be that the massive effect on τ -protein phosphorylation sites described in those studies is related to the use of rather high concentrations of $A\beta$ which are unlikely to occur even in full-blown AD (cf. Gravina et al., 1995).

The present results do not exclude an interplay between amyloid and τ -hyperphosphorylation in AD, but suggest that the formation of more complex structures, like amyloid plaques, may be required. In the initial phases of the disease, with $A\beta_{1-42}$ levels still being low, the peptide most likely induces morphological alterations in exposed neurons which, however, seem to be connected with changes in MAP2 metabolism but not with the phosphorylation status of the τ -protein. Whether the currently observed alterations in MAP2 expression may be related to an impact on the τ -protein which is not accompanied by its hyperphosphorylation will have to be elucidated in the future.

4.1.3 $\alpha 7$ -nAChRs

Immunocytochemical staining of the cultures was performed with antibodies directed against the $\alpha 7$ -nAChR subunit. Following $A\beta_{1-42}$ treatment, nAChR-immunoreactive neurons exhibited an altered cell morphology in comparison with untreated cultures: neurons were shrunken and showed a tendency to form blebs to different extent or even displayed signs of dissolution.

No difference in the total number of $\alpha 7$ -nAChR-positive cells was found. To the best of our knowledge this is the first *in vitro* study concerned with the effects of $A\beta_{1-42}$ on nAChR expression in primary neuronal cell cultures. Previous studies on AChRs performed on human brains showed that $\alpha 7$ -immunoreactive neurons were detected in all cortical layers in non-diseased subjects, matching the pattern of their mRNA transcript distribution, which also holds true for the rat brain (Luetje et al., 1990). In AD patients, by contrast, a loss of immunoreactive neurons occurred, especially in the upper cortical layers, where most of them were only weakly stained (Wevers et al., 2000).

In the present study, quantitative determination of the $\alpha 7$ -nAChR subunit by means of Western blot revealed no change in its expression under incubation conditions in comparison to untreated cultures. In contrast to our findings, Guan et al. (2001) found a reduction in the $\alpha 7$ -nAChR subunit expression and in the correspondent mRNA transcript in PC12 cells after incubation with non-fibrillar $A\beta_{1-40}$. The incubation with a diverse peptide, its different aggregation state and the choice of a different cell model could explain the different results obtained. In AD patients, Guan et al. (2000) found the $\alpha 7$ -nAChR subunit expression not to be affected in the cerebral cortex, while Burghaus et al. (2000) reported a significant reduction in the same brain area. In the hippocampus, the total amount of $\alpha 7$ -nAChR protein was shown to be decreased (Guan et al., 2000). No difference either in the cortical distribution pattern of $\alpha 7$ -nAChR subunit mRNA-expressing neurons or in their density was found in the frontal cortex (Wevers et al., 2000). The reduction in the expression of receptor protein in AD brains could be region-specific and reflect the severity of the disease (for review see Bourin et al., 2003), and the conditions leading to the possible damage therefore difficult to reproduce in cell culture.

The binding assay performed with [125 I] α -Bgt to test the functional state of the homomeric $\alpha 7$ -nAChRs in our cultures resulted in no change in the total number of binding sites after $A\beta_{1-42}$ treatment. In PC12 cells, incubation with non-fibrillar $A\beta_{1-40}$ led to a decrease in the number of binding sites in comparison to untreated cultures (Guan et al., 2001). In

contrast to those findings, Dineley et al. (2002) reported that the incubation of $\alpha 7$ -nAChR subunit-transfected cells with non-fibrillar $A\beta_{1-42}$ leads to receptor activation. It seems that the outcome of the different experiments is strongly influenced by the individual model used and by the form of amyloid employed. In AD brains, some groups found no difference in the total amount of binding sites (Perry et al., 2000), while others detected a region-specific loss (Hellstrom-Lindahl et al., 1999), thus supporting the hypothesis of a possible relation between localization of the damage and severity of the pathology (for review see Bourin et al., 2003).

It has been recently demonstrated that $A\beta_{1-42}$ can bind the $\alpha 7$ -nAChR with very high affinity (Wang et al., 2000) and that it tends to accumulate in $\alpha 7$ -nAChR rich cells (Nagele et al., 2002). However, nothing is known about the underlying mechanism and the site of interaction. In the present study, no effect on the affinity of homomeric $\alpha 7$ -nAChRs for [125 I] α -Bgt was found after $A\beta_{1-42}$ incubation. Our results do not exclude that $A\beta_{1-42}$ could interact with the receptor, but suggest that possible interactions do not influence the α -Bgt binding site. It could be speculated that the capability of the homomeric $\alpha 7$ -nAChRs to bind ACh remains also unaffected, as it was demonstrated that the receptors which are able to bind α -Bgt are in the active conformation and can also bind ACh (Rakhilin et al., 1999).

4.2 Effects of $A\beta_{31-34}$

The second amyloidogenic peptide used in this study was the shorter fragment $A\beta_{31-34}$. Previous studies reported a protective action of this shorter form against $A\beta_{1-42}$ effects. $A\beta_{31-34}$ was shown to antagonize the $A\beta_{1-42}$ -induced elevation of intracellular [Ca^{2+}] in primary cultures of rat astrocytes (Laskay et al., 1997), and to abolish the elevation of extracellular glutamate and aspartate concentrations caused by $A\beta_{1-42}$ on cholinergic neurons of the rat basal nucleus of Meynert *in vivo* (Harkany et al., 1999). The shorter fragment could also attenuate the $A\beta_{1-42}$ -induced behavioral dysfunctions (markedly reduced horizontal motor activities) in rats. An updated search for sequence similarities revealed that the amino acid sequence Ile-Ile-Gly-Leu is present in about 250 human proteins. It appears, however, difficult to find a relation between the functions of these peptides and the effects caused by the tetrapeptide. Yankner et al. (1990) were able to show that the highly hydrophobic sequence Ile-Ile-Gly-Leu is contained in a number of

peptides belonging to the tachykinin family. It is noteworthy, however, that only the application of tachykinin antagonists and not of agonists led to neurotoxic effects comparable to those obtained with A β . A β ₃₁₋₃₄ was presently employed to investigate further its possible role as a neuroprotective agent.

In the above mentioned studies, A β ₃₁₋₃₄ and A β ₁₋₄₂ were used in equimolar concentrations. In this work, a concentration of 0.125 μ M was chosen for the A β ₃₁₋₃₄ incubation because it represented the highest concentration not affecting the cell viability. The LDH cytotoxicity assay revealed in fact no impact of 0.125 μ M A β ₃₁₋₃₄ on cell survival and on the total number of neurons. The other incubation conditions were the same as for A β ₁₋₄₂.

4.2.1 Cell morphology

As regards the morphological aspects, A β ₃₁₋₃₄ led to alterations in the region of the apical dendrite, which resulted to be swollen. These alterations apparently do not involve MAP2b or MAP2c expression, as their level remained unaffected. In the presence of both peptides, neurons exhibited the reported morphological changes caused by A β ₃₁₋₃₄, i.e the swollen cell body in the region of the apical dendrite, together with the A β ₁₋₄₂-induced retraction of dendrites. With both peptides, however, the total MAP2-stained area was not significantly decreased. Looking at these findings, it can be concluded that A β ₃₁₋₃₄ prevents to some extent the alterations caused by A β ₁₋₄₂, but it can not be considered protective for the cell morphology, as it showed own toxic effects.

4.2.2 Phosphorylation state of the τ -protein

In contrast to A β ₁₋₄₂, the shorter fragment A β ₃₁₋₃₄ was able to cause a massive hyperphosphorylation of the τ -protein at Ser-202 (AT8) and at Ser-396 / Ser-404 (AD2), while no increase in the phosphorylation levels at Ser-262 (12E8) and Ser-231 / Ser-235 (AT180) was found.

The observed hyperphosphorylation of the τ -protein at AD2 sites is of main importance, as it concerns epitopes possibly involved in the formation of paired helical filaments. The microtubule binding capability of the τ -protein is necessary for the maintenance of τ functions in the stabilization of microtubules. It has been reported that the detachment of

the protein from the microtubular structure occurs only when the hyperphosphorylation takes place at Ser-262 or Ser-214 (for review see Mandelkow and Mandelkow, 1998). τ -protein microtubule binding is therefore most likely not directly affected by the $A\beta_{31-34}$ -induced hyperphosphorylation. On the other hand, even if the hyperphosphorylation at Ser-262 dramatically reduces the affinity of τ -protein for microtubules, this alteration alone is not sufficient to provoke the loss of binding, which is strongly influenced by hyperphosphorylation at sites located outside the microtubule binding domain (for review see Buè et al., 2000). It can therefore not be excluded that the hyperphosphorylation at AD2 sites might play a role in the detachment of the τ -protein, which in AD could account for the microtubule disappearance, breakdown of the cellular trafficking and subsequent death of neurons (for review see Mandelkow and Mandelkow, 1998).

$A\beta_{31-34}$ is a synthetic peptide which does not occur *in vivo*. Its capability to induce τ -hyperphosphorylation at some epitopes could however be used to obtain an *in vitro* model in which different cellular aspects (e.g. protein expression or receptor functionality) can be studied under hyperphosphorylating conditions. This model would thus allow to investigate possible correlations between hyperphosphorylated τ -protein and alterations in cellular pathways of interest.

4.2.3 nAChRs

$A\beta_{31-34}$ did not produce any morphological alteration in cells stained with the anti- $\alpha 7$ -nAChR subunit antibody. As with $A\beta_{1-42}$, the number of $\alpha 7$ -nAChR subunit-expressing neurons was not altered and the level of $\alpha 7$ -nAChR subunit expression maintained when comparing vehicle-treated cultures with those exposed to the tetrapeptide $A\beta_{31-34}$. The treatment did not affect either the affinity of the homomeric $\alpha 7$ -nAChRs for [125 I] α -Bgt or their total number.

4.2.4 Possible mechanisms of action of $A\beta_{31-34}$.

Studies concerned with the design of potential anti- $A\beta$ drugs suggest that synthetic amyloidogenic peptides could antagonize the recognition and surface binding of $A\beta$ (Cowburn et al., 1997). Another line of evidence attributes to the synthetic short

amyloidogenic peptides the capability of acting as β -sheet breakers and avoiding in this way the formation of amyloid fibrils (Soto et al., 1998, 2000). Looking at the results obtained in this study, it appears difficult, however, even to speculate about the mechanism of action of $A\beta_{31-34}$.

4.3 Colocalization of the $\alpha 7$ -nAChR subunit with hyperphosphorylated τ -protein

Colocalization studies showed that the $\alpha 7$ -nAChR subunit was not affected by the presence of hyperphosphorylated τ -protein at AT8 and AD2 epitopes. Upon $A\beta_{31-34}$ incubation, which has been demonstrated to increase the level of phosphorylation at these sites, the expression pattern of the $\alpha 7$ -nAChR subunit remained unaltered.

When looking for the colocalization of nAChR neurons with NFT-bearing neurons in autopsy samples, it turned out that almost none of these neurons simultaneously displayed nAChR- and NFT-immunoreactivity (Wevers et al., 1999). This led us to the idea that hyperphosphorylated τ -protein or NFTs may interfere with nAChR expression *in vivo*. Given the only slight, although significant, decrease of total $\alpha 7$ -nAChR amount in AD patients, this finding may appear of minor relevance at first sight. It has to be kept in mind, however, that the loss of receptors can be region specific (Hellstrom-Lindahl et al., 1999) and that strategically important neurons - e.g. in the entorhinal cortex - are prone to develop NFTs and lose their receptor equipment (Wevers et al., 1999).

As shown presently, however, the $A\beta_{31-34}$ -induced τ -phosphorylation is not a sufficient prerequisite for a reduced nAChR expression. The latter may rather be a function of NFT formation. So far, no *in vitro* model is available in which tangle-like structures could be elicited by hyperphosphorylation. Tackling this problem will probably require the *in vitro* use of neurons derived from transgenic tangle-forming mice.

4.4 Conclusions

It could be presently shown that $A\beta_{1-42}$, in concentrations most likely occurring during the development of amyloid plaques in AD (cf. data on human AD brain and transgenic mice as reported in 4.1) does not lead to an increase in τ -phosphorylation at the AD relevant sites Ser-202 and Ser-396 / Ser-404 in cultured hippocampal neurons. This finding is

accompanied by a lack of changes in the expression of the $\alpha 7$ -nAChR subunit, in the affinity of the homomeric $\alpha 7$ -nAChRs for [125 I] α -Bgt and in their total number.

Data obtained from transgenic mice do not provide an unequivocal answer to the problem of τ -hyperphosphorylation. On one hand, plaque-forming strains have never been shown to develop NFTs. On the other hand, the P301L mouse (Götz et al., 2001) is known to develop a high number of NFTs in the amygdala upon $A\beta$ injection into the ipsilateral hippocampus.

$A\beta_{31-34}$, by contrast, induces a massive increase in τ -phosphorylation at Ser-202 or Ser-396 / Ser-404. However, there was no change in the expression of the $\alpha 7$ -nAChR subunit, which was still present in neurons that expressed AT8 and AD2 immunoreactivity upon $A\beta_{31-34}$ treatment. This is in contrast with the finding that in human AD brains a colocalization of nAChRs and NFT is hardly ever encountered (Wevers et al., 1999; Wevers et al., 2001). Experiments performed over defined time courses in humans as well as in the mouse mutants will be helpful to get more insight into these phenomena.

The “amyloid cascade” hypothesis, proposed for the first time about a decade ago (Hardy and Higgins, 1992), remains a central point in the investigation of the AD neurodegeneration. The recent generation of various transgenic mice carrying single or double APP, PS and τ -protein mutations represents a useful tool for the elucidation of possible mechanisms linking $A\beta$, τ -hyperphosphorylation and cognitive deficit (for review see Sommer, 2002), as shown by different studies (Götz et al., 2001; Lewis et al., 2001). It is, however, tempting to speculate that the formation of NFTs and the reduced expression of nAChRs in AD brain may be the endpoint of a rather long development starting with the induction of τ -hyperphosphorylation. The present findings do not exclude an active involvement of $A\beta$ in these long-lasting processes, but raise some doubts about the role of $A\beta_{1-42}$ fibrils as a direct trigger of τ -hyperphosphorylation.

5. ZUSAMMENFASSUNG

Kennzeichen der Alzheimerschen Erkrankung sind die abnormale Ablagerung von Proteinen wie β -Amyloid und hyperphosphoryliertem τ -Protein, Veränderungen des Zytoskeletts und Störungen der cholinergen Transmission. Mögliche Zusammenhänge zwischen β -Amyloid-Ablagerung, τ -Hyperphosphorylierung und Expression der nicotinischen Acetylcholinrezeptoren wurden durch Inkubation neuronaler Dissoziationskulturen aus den Hippocampi embryonaler Ratten mit amyloidogenen Peptiden untersucht. Für die Inkubation wurden das β -Amyloid-Fragment mit der höchsten Tendenz zu Fibrillenbildung, $A\beta_{1-42}$, und das kürzere, putativ protektive Fragment, $A\beta_{31-34}$, eingesetzt. $A\beta_{1-42}$ verursachte eine Retraktion der Dendriten und das Schrumpfen der Zellkörper. Weder die Zahl der Neuronen noch die Gesamtzahl lysierter Zellen wurde beeinflusst. Eine reduzierte Expression von MAP2b war die einzig beobachtete Veränderung. Es wurde keine statistisch signifikante Erhöhung der Phosphorylierungsrate der Epitope Ser-202 (Antikörper AT8), Thr-231 / Ser-235 (Antikörper AT180), Ser-262 (Antikörper 12E8) oder Ser-396 / Ser-404 (Antikörper AD2) des τ -Proteins beobachtet. Die Gesamtzahl der $\alpha 7$ -homomeren Rezeptoren und ihre Affinität für [125 I] α -Bgt blieben unverändert.

Die Inkubation mit $A\beta_{31-34}$ führte hingegen zu anderen morphologischen Veränderungen, wie dem Anschwellen des apikalen Dendriten. Die von $A\beta_{31-34}$ hervorgerufenen Veränderungen betrafen nicht MAP2, die Expression aller MAP2-Proteinkomponenten blieb unbeeinflusst. Im Gegensatz zu $A\beta_{1-42}$ verursachte das kürzere Fragment eine massive Hyperphosphorylierung des τ -Proteins an den Aminosäuren Ser-202 (AT8) und Ser-396 / Ser-404 (AD2), jedoch konnte keine Erhöhung der Phosphorylierung an Thr-231 / Ser-235 (AT180) oder Ser-262 (12E8) festgestellt werden. Weiterhin beeinflusste $A\beta_{31-34}$ weder die Anzahl der $\alpha 7$ -nAChR-exprimierenden Neurone noch die Expression des Proteins der Untereinheit selbst. Es konnte kein Unterschied in der Anzahl der $\alpha 7$ -homomeren Rezeptoren und in ihrer Affinität für [125 I] α -Bgt bestimmt werden. Die $\alpha 7$ -nAChR-Untereinheit zeigte Kollokalisierung mit dem hyperphosphorylierten τ -Protein in allen AT8- und AD2-positiven Neuronen.

Zusammengefasst zeigen die vorliegenden Ergebnisse toxische Einflüsse von $A\beta_{1-42}$ auf das Zytoskelett bei Konzentrationen, die üblicherweise in Gehirnen von Alzheimer-

patienten zu finden sind. Gleichzeitig bestehen aber noch einige Zweifel über die Rolle der $A\beta_{1-42}$ -Fibrillen als direkte Auslöser der τ -Hyperphosphorylierung. Was $A\beta_{31-34}$ betrifft, so kann es in Bezug auf die Zellmorphologie trotz seiner offensichtlich positiven Wirkung auf die $A\beta_{1-42}$ -induzierte Dendritenretraktion nicht als protektiv angesehen werden, da es eigene toxische Eigenschaften besitzt.

6. REFERENCES

Albuquerque E.X., Alkondon M., Pereira E.F., Castro N.G., Schratzenholz A., Barbosa C.T. (1997). Properties of neuronal acetylcholine receptors: pharmacological characterization and modulation of synaptic function. *J. Pharmacol. Exp. Ther.* 280, 1117-1136.

Arriagada P.V., Growdon J.H., Hedley-Whyte E.T., Hyman B.T. (1992). Neurofibrillary tangles but not senile plaques parallel duration and severity of Alzheimer's disease. *Neurology* 42, 631-639.

Banker G.A., Cowan W.M. (1977). Rat hippocampal neurons in dispersed cell culture. *Brain Res.* 126, 397-425.

Bellocchio E.E., Reimer R.J., Fremeau R.T.Jr., Edwards R.H. (2000). Uptake of glutamate into synaptic vesicles by an inorganic phosphate transporter. *Science* 289, 957-960.

Bennecib M., Gong C.X., Grunke-Iqbal I., Iqbal K. (2001). Inhibition of PP-2A upregulates CaMKII in rat forebrain and induces hyperphosphorylation of tau at Ser 262 / 356. *FEBS Lett.* 490, 15-22.

Binder L.I., Frankfurter A., Rebhun L.I. (1985). The distribution of tau in the mammalian central nervous system. *J. Cell Biol.* 101, 1371-1378.

Blondel A., Sanger D.J., Moser P.C. (2000). Characterization of the effect of nicotine in the five-choice serial reaction time task in rats: antagonist studies. *Psychopharmacol.* 149, 293-305.

Bourin M., Ripoli N., Dailly E. (2003). Nicotinic receptors and Alzheimer's disease. *Curr. Med. Res. Opin.* 19, 169-177.

Braak H., Braak E., Mandelkow E.-M. (1994). A sequence of cytoskeletal changes related to the formation of neurofibrillary tangles and neuropil threads. *Acta Neuropathol.* 87, 554-567.

- Braak H., Braak E. (1995). Staging of Alzheimer's disease-related neurofibrillary tangles. *Neurobiol. Aging* 16, 271-284.
- Brandt R., Leger J., Lee G. (1995). Interaction of tau with the neural plasma membrane mediated by tau's amino-terminal projection domain. *J. Cell Biol.* 131, 1327-1340.
- Brusés J.L., Chauvet N., Rutishauser U. (2001). Membrane lipid rafts are necessary for the maintenance of the $\alpha 7$ nicotinic acetylcholine receptor in somatic spines of ciliary neurons. *J. Neurosci.* 21, 504-512.
- Buée L., Bussièrè T., Buée-Scherrer V., Delacourte A., Hof P.R. (2000). Tau protein isoforms, phosphorylation and role in neurodegenerative disorders. *Brain Res.* 33, 95-130.
- Buée-Scherrer V., Condamines O., Mourton-Gilles C., Jakes R., Goedert M., Pau B., Delacourte A. (1996). AD2, a phosphorylation-dependent monoclonal antibody directed against tau proteins found in Alzheimer's disease. *Mol. Brain Res.* 39, 79-88.
- Burghaus L., Schütz U., Krempel U., de Vos R.A.I., Jansen Steur E.N.H., Wevers A., Lindstrom J., Schröder H. (2000). Quantitative assessment of nicotine acetylcholine receptor proteins in the cortex of Alzheimer patients. *Brain Res. Mol. Brain Res.* 76, 385-388.
- Busciglio J., Lorenzo A., Yankner B.A. (1992). Methodological variables in the assessment of beta amyloid neurotoxicity. *Neurobiol. Aging* 13, 609-612.
- Busciglio J., Lorenzo A., Yeh J., Yankner B.A. (1995). β -amyloid fibrils induce tau phosphorylation and loss of microtubule binding. *Neuron* 14, 879-888.
- Caceres A., Banker G., Steward O., Binder L., Payne M. (1984). MAP2 is localized to the dendrites of hippocampal neurons which develop in culture. *Brain Res.* 13, 314-418.
- Campbell M.J., Morrison J.H. (1989). Monoclonal antibody to neurofilament protein (SMI32) labels a subpopulation of pyramidal neurons in the human and monkey neocortex. *J. Comp. Neurol.* 282, 191-205.

- Carter J., Lippa C.F. (2001). β -Amyloid, neuronal death and Alzheimer's disease. *Curr. Mol. Med.* 1, 733-737.
- Castro N.G., Albuquerque E.X. (1995). alpha-Bungarotoxin-sensitive hippocampal nicotinic receptor channel has a high calcium permeability. *Biophys. J.* 68, 516-524.
- Cowburn R.F., Wiehager B., Trief E., Li-Li M., Sundstrom E. (1997). Effects of beta-amyloid-(25-35) peptides on radioligand binding to excitatory amino acid receptors and voltage-dependent calcium channels: evidence for a selective affinity for the glutamate and glycine recognition sites of the NMDA receptor. *Neurochem. Res.* 22, 1437-1442.
- Dani J.A. (2001). Overview of nicotinic receptors and their role in the central nervous system. *Biol. Psychiatry* 49, 166-174.
- De Strooper B., Saftig P., Craessaerts K., Vanderstichele H., Guhde G., Annaert W., Von Figura K., Van Leuven F. (1998). Deficiency of presenilin-1 inhibits the normal cleavage of amyloid precursor protein. *Nature* 22, 387-390.
- Dineley K.T., Bell K.A., Bui D., Sweatt J.D. (2002). β -amyloid peptide activates $\alpha 7$ nicotinic acetylcholine receptors expressed in *Xenopus* oocytes. *J. Biol. Chem.* 277, 25056-25061.
- Dominguez del Toro E.D., Juiz J.M., Peng X., Lindstrom J., Criado M. (1994). Immunocytochemical localization of the $\alpha 7$ subunit of the nicotinic acetylcholine receptor in the rat central nervous system. *J. Comp. Neurol.* 349, 325-342.
- Dotti C.G., Sullivan C.A., Banker G.A. (1988). The establishment of polarity by hippocampal neurons in culture. *J. Neurosci.* 8, 1454-1468.
- Drewes G., Ebner A., Mandelkow E.-M. (1998). MAPs, MARKs and microtubule dynamics. *TIBS* 23, 307-311.
- Drisdel R.C., Green W.N. (2000). Neuronal α -bungarotoxin receptors are $\alpha 7$ homomers. *J. Neurosci.* 20, 133-139.

Drouet B., Pincon-Raymond M., Chambaz J., Pillot T. (2000). Molecular basis of Alzheimer's disease. *Cell. Mol. Life Sci.* 57, 705-715.

Ebneth A., Godemann K., Illeberger S., Trinczek B., Mandelkow E.-M., Mandelkow E. (1998). Overexpression of tau protein inhibits kinesin-dependent trafficking of vesicles, mitochondria, and endoplasmic reticulum : implications for Alzheimer's disease. *J. Cell Biol.* 143, 774-794.

Francis P.T. (2003). Glutamatergic system in Alzheimer's disease. *Int. J. Geriatr. Psychiatry* 18, S15-S21.

Friedhoff P., von Bergen M., Mandelkow E.-M., Mandelkow E. (2000). Structure of tau protein and assembly into paired helical filaments. *Biochim. Biophys. Acta* 1502, 122-132.

Giacobini E. (2000). Cholinesterase inhibitor therapy stabilizes symptoms of Alzheimer's disease. *Alzheimer Dis. Assoc. Disord.* 14, S3-S10.

Goedert M., Crowther R.A., Garner C.C. (1991). Molecular characterization of microtubule-associated proteins tau and MAP2. *Trends Neurosci.* 14, 193-199.

Goedert M., Jakes R., Crowther R.A., Six J., Lübke U., Vandermeeren M., Cras P., Trojanowski J.Q., Lee V.M.-Y. (1993). The abnormal phosphorylation of tau protein at Ser-202 in Alzheimer's disease recapitulates phosphorylation during development. *Proc. Natl. Acad. Sci. USA* 90, 5066-5070.

Goslin K., Asmussen H., Banker G. Rat hippocampal neurons in low density culture. In: *Culturing nerve cells*, 2nd edition. Banker G., Goslin K., editors. Cambridge, MA: The MIT Press, 1998.

Götz J., Chen F., van Dorpe J., Nitsch R.M. (2001). Formation of neurofibrillary tangles in P301L tau transgenic mice induced by A β 42 fibrils. *Science* 293, 1491-1495.

Gouras G.K., Tsaiu J., Naslund J., Vincent B., Edgar M., Checler F., Greenfield J.P., Haroutunian V., Buxbaum J.D., Xu H., Greencard P., Relkin N.R. (2000). Intraneuronal A β 42 accumulation in human brain. *Am. J. Pathol.* 156, 15-20.

Grace E.A., Busciglio J. (2003). Aberrant activation of focal adhesion proteins mediates fibrillary amyloid β -induced neuronal dystrophy. *J. Neurosci.* 23, 493-502.

Gravina S.A., Ho L., Eckman C.B., Long K.E., Otvos L.Jr., Younkin L.H., Suzuki N., Younkin S.G. (1995). Amyloid β protein ($A\beta$) in Alzheimer's disease brain. Biochemical and immunocytochemical analysis with antibodies specific for forms ending at $A\beta$ 40 or $A\beta$ 42(43). *J. Biol. Chem.* 270, 7013-7016.

Gray R., Rajan A.S., Radcliffe K.A., Yakehiro M., Dani J.A. (1996). Hippocampal synaptic transmission enhanced by low concentration of nicotine. *Nature* 383, 713-716.

Grottick A.J., Higgins G.A. (2000). Effect of subtype selective nicotinic compounds on attention as assessed by the five-choice serial reaction time task. *Behav. Brain Res.* 117, 197-208.

Grundke-Iqbal I., Iqbal K., Tung Y.-C., Quinlan M., Wisniewsky H.M., Binder L.I. (1986). Abnormal phosphorylation of the microtubule-associated protein tau in Alzheimer cytoskeletal pathology. *Proc. Natl. Acad. Sci. USA* 83, 4913-4917.

Guan Z.Z., Zhang X., Ravid R., Nordberg A. (2000). Decreased protein levels of nicotinic receptor subunits in the hippocampus and temporal cortex of patients with Alzheimer's disease. *J. Neurochem.* 74, 237-243.

Guan Z.Z., Zhang X., Mousavi M., Tian J.Y., Ungar C., Nordberg A. (2001). Suppressed expression of nicotinic acetylcholine receptors by nanomolar β -amyloid peptides in PC12 cells. *J. Neural Transm.* 108, 1417-1433.

Gundersen H.J. (1986). Stereology of arbitrary particles. A review of unbiased number and size estimators and the presentation of some new ones, in memory of William R. Thompson. *J. Microsc.* 143, 3-45.

Gundersen H.J., Bagger P., Bendtsen T.F., Evans S.M., Korbo L., Marcussen N., Moller A., Nielsen K., Nyengaard J.R., Pakkenberg B., Sørensen F.B., Vesterby A., West M.J. (1988). The new stereological tools: disector, fractionator, nucleator and point sampled intercepts and their use in pathological research and diagnosis. *Apmis* 96, 857-881.

- Hardy J.A., Higgins G.A. (1992). Alzheimer's disease: the amyloid cascade hypothesis. *Science* 256, 184-185.
- Harkany T., Abraham I., Laskay G., Timmerman W., Jost K., Zarandi M., Penke B., Nyakas C., Luiten P.G. (1999). Propionyl-IIGL tetrapeptide antagonizes β -amyloid excitotoxicity in rat nucleus basalis. *Neuroreport* 10, 1693-1698.
- Hellstrom-Lindahl E., Mousavi M., Zhang X., Ravid R., Nordberg A. (1999). Regional distribution of nicotinic receptor subunit mRNAs in human brain: comparison between Alzheimer and normal brain. *Brain Res. Mol. Brain Res.* 66, 94-103.
- Herbert D.L., Severance E.G., Cuevas J., Morgan D., Gordon M.N. (2004). Nonspecific binding of $\alpha 7$ nAChR antibodies in murine models of Alzheimer's disease and neuroinflammation. Submitted.
- Hirokawa N., Shiomura Y., Okabe S. (1988). Tau-proteins: the molecular structure and mode of binding on microtubules. *J. Cell Biol.* 107, 1449-1459.
- Kang J., Lemaire H.G., Unterbeck A., Salbaum J.M., Masters C.L., Grzeschik K.H., Multhaup G., Beyreuther K., Mueller-Hill B. (1987). The precursor of Alzheimer's disease amyloid A4 protein resembles a cell-surface receptor. *Nature* 325, 733-736.
- Kawarabayashi T., Younkin L.H., Saido T.C., Shoji M., Hsiao Ashe K., Younkin S.G. (2001). Age dependent changes in brain, CSF, and plasma amyloid β protein in the Tg2576 transgenic mouse model of Alzheimer's disease. *J. Neurosci.* 21, 372-381.
- Kasa P. (1986). The cholinergic systems in brain and spinal cord. *Prog. Neurobiol.* 26, 211-272.
- Koh J., Yang L.L., Cotman C.W. (1990). β -Amyloid protein increases the vulnerability of cultured cortical neurons to excitatory damage. *Brain Res.* 533, 315-320.
- Korzeniewski C., Callewaert D.M. (1983). An enzyme-release assay for natural cytotoxicity. *J. Immunol. Meth.* 64, 313-320.

- Laskay G., Zarandi M., Varga J., Jost K., Fobagy A., Torday C., Latzkovits L., Penke B. (1997). A putative tetrapeptide antagonist prevents β -amyloid-induced long-term elevation of $[Ca^{2+}]_i$ in rat astrocytes. *Biochem. Biophys. Res. Comm.* 235, 479-481.
- Levin E.D. (1992). Nicotinic system and cognitive function. *Psychopharmacology* 108, 417-431.
- Lewis J., Dickson D.W., Lin W.L., Chisholm L., Corral A., Jones J., Yen S.H., Sahara N., Skipper L., Yager D., Eckman C., Hardy J., Hutton M., McGowan E. (2001). Enhanced neurofibrillary degeneration in transgenic mice expressing mutant tau and APP. *Science* 293, 1487-1491.
- Li X., Rainnie D.G., McCarley R.W., Greene R.W. (1998). Presynaptic nicotinic receptors facilitate monoaminergic transmission. *J. Neurosci.* 18, 1904-1912.
- Li Y., Black M.M. (1996). Microtubule assembly and turnover in growing axons. *J. Neurosci.* 16, 531-544.
- Lindstrom J., Anand R., Peng X., Gerzanich V., Wang F., Li Y. (1995). Neuronal nicotinic receptor subtypes. *Ann. Acad. Sci. NY* 757, 100-116.
- Lloyd G.K., Menzaghi F., Bontempi B., Suto C., Siegel R., Akong M., Stauderman K., Valicelebi G., Johnson E., Harpold M.M., Rao T.S., Sacaan A.I., Chavez-Noriega L.E., Washburn M.S., Vernier J.M., Casford N.D., McDonald L.A. (1998). The potential of subtype-selective neuronal nicotinic acetylcholine receptor agonists as therapeutic agents. *Life Sci.* 62, 1601-1606.
- Lorenzo A., Yankner B.A. (1994). β -amyloid neurotoxicity requires fibril formation and is inhibited by Congo red. *Proc. Natl. Acad. Sci. USA* 91, 12243-12247.
- Lorenzo A., Yuan M., Zhang Z., Paganetti P.A., Sturchler-Pierrat C., Staufenbil M., Mautino J., Sol Vigo F., Sommer B., Yankner B.A. (2000). Amyloid β interacts with the amyloid precursor protein: A potential toxic mechanism in Alzheimer's disease. *Nat. Neurosci.* 3, 460-464.

Luetje C.W., Patrick J., Séguéla P. (1990). Nicotinic receptors in the mammalian brain. *FASEB* 4, 2753-2760.

Lukas R.J., Changeux J.-P., Le Novère N., Albuquerque E.X., Balfour D.J.K., Berg D.K., Bertrand D., Chiappinelli V.A., Clarke P.B.S., Collins A.C., Dani J.A., Grady S.R., Kellar K.J., Lindstrom J.M., Marks M.J., Quik M., Taylor P.W., Wonnacott S. (1999). International union pharmacology. XX. Current status of the nomenclature for nicotinic acetylcholine receptors and their subunits. *Pharmacol. Rev.* 51, 397-401.

Lustig L.R., Peng H., Hiel H., Yamamoto T., Fuchs P.A. (2001). Molecular cloning of the human nicotinic acetylcholine receptor $\alpha 10$ (CHRNA10). *Genomics* 73, 272-283.

Mandelkow E.-M., Biernat J., Drewes G., Gustke G., Trinczek B., Mandelkow E. (1995). Tau domains, phosphorylation, and interactions with microtubules. *Neurobiol. Aging* 16, 335-362.

Mandelkow E.-M., Mandelkow E. (1998). Tau in Alzheimer's disease. *Trends Cell Biol.* 8, 425-427.

Mandell J.W., Banker J. (1996). A spatial gradient of tau protein phosphorylation in nascent axons. *J. Neurosci.* 16, 5727-5740.

Mattson M.P. (1997). Cellular actions of β -amyloid precursor protein and its soluble and fibrillogenic derivatives. *Pharmacol. Rev.* 77, 1081-1132.

Mattson M.P., Tomaselli K.J., Rydel R.E. (1993). Calcium-destabilizing and neurodegenerative effects of aggregated β -amyloid peptide are attenuated by basic FGF. *Brain Res.* 621, 35-49.

McGehee D.S., Heath M.J., Gelber S., Devay P., Role L.W. (1995). Nicotine enhancement of fast excitatory synaptic transmission in CNS by presynaptic receptors. *Science* 269, 1692-1696.

Miyazawa A., Fujiyoshi Y., Unwin N. (2003). Structure and gating mechanisms of the acetylcholine receptor pore. *Nature* 423, 949-955.

- Nagele R.G., D'Andrea M.R., Anderson W.J., Wang H.-Y. (2002). Intracellular accumulation of β -amyloid₁₋₄₂ in neurons is facilitated by the α 7 nicotinic acetylcholine receptor in Alzheimer's disease. *Neurosci.* 110, 199-211.
- Newhouse P.A., Potter A., Levin E.D. (1997). Nicotinic system involvement in Alzheimer's and Parkinson's diseases. Implication for therapeutics. *Drugs Aging* 11, 206-228.
- Nordberg A., Svensson A.L. (1998). Cholinesterase inhibitors in the treatment of Alzheimer's disease: A comparison of tolerance and pharmacology. *Drug Saf.* 19, 465-480.
- Nordberg A., Winblad B. (1986). Reduced number of [³H]nicotine and [³H]acetylcholine binding sites in the frontal cortex of Alzheimer brains. *Neurosci. Lett.* 72, 115-119.
- Pei J.J., Grunke-Iqbal I., Iqbal K., Bogdanovic N., Winblad B., Cowburn R.F. (1998). Accumulation of cyclin-dependent kinase 5 (cdk5) in neurons with early stages of Alzheimer's disease neurofibrillary degeneration. *Brain Res.* 797, 267-277.
- Perry E.K., Court J.A., Johnson M., Smith C.J., James W., Cheng A., Kerwin J.M., Morris C.M., Piggott M.A., Edwardson J.A., Birdsall N.J.M., Turner J.T., and Perry R.H. (1993). Autoradiographic comparison of cholinergic and other transmitter receptors in the normal human hippocampus. *Hippocampus* 3, 307-315.
- Perry E., Martin-Ruiz C., Lee M., Griffiths M., Johnson M., Piggott M., Haroutunian V., Buxbaum J.D., Nasland J., Davis K., Gotti C., Clementi F., Tzartos S., Cohen O., Soreq H., Jaros E., Perry R., Ballard C., McKeith I., Court J. (2000). Nicotinic receptor subtypes in human brain ageing, Alzheimer and Lewi body diseases. *Eur. J. Pharmacol.* 30, 215-222.
- Pike C.J., Walencewicz A.J., Glabe G.C., Cotman C.W. (1991a). Aggregation-related toxicity of synthetic A β -amyloid protein in hippocampal cultures. *Eur. J. Pharmacol.* 207, 367-368.
- Pike C.J., Walencewicz A.J., Glabe G.C., Cotman C.W. (1991b). In vitro aging of β -amyloid protein causes peptide aggregation and neurotoxicity. *Brain Res.* 563, 311-314.

Pike C.J., Cummings B.J., Cotman C.W. (1992). β -amyloid induces neuritic dystrophy in vitro: similarities with Alzheimer pathology. *Neuroreport* 3, 769-772.

Radcliffe K.A., Fisher J., Gray R., Dani J.A. (1999). Nicotine potentiates glutamate and GABA synaptic transmission. *NY Acad. Sci.* 868, 591-610.

Rakhilin S., Drisdell R.C., Sagher D., Mc Gehee D.S., Vallejo Y., Green W.N. (1999). α -bungarotoxin receptors contain $\alpha 7$ subunits in two different disulfide-bonded conformations. *J. Biol. Chem.* 146, 203-218.

Rehm H. Membranproteine solubilisieren. In: Der Experimentator: Proteinbiochemie / Proteomics. 3. Auflage. Spektrum Akademischer Verlag, Heidelberg-Berlin, 2000.

Role L.W. (1992). Diversity in primary structure and function of neuronal nicotinic acetylcholine receptor channels. *Curr. Opin. Neurobiol.* 2, 254,262.

Rosser M.N., Svendsen C., Hunt S.P., Mounjoy C.Q., Roth M., Iversen L.L. (1982). The substantia innominata in Alzheimer's disease: A histochemical and biochemical study of cholinergic marker enzymes. *Neurosci. Lett.* 28, 217-222.

Sargent P.B. (1993). The diversity of neuronal acetylcholine receptors. *Annu. Rev. Neurosci.* 16, 403-443.

Scheuner D., Eckman C., Jensen M., Song X., Citron M., Suzuki N., Bird T.D., Hardy J., Hutton M., Kukull W., Larson E., Levy-Lahad E., Viitanen M., Peskind E., Poorkaj P., Schnellemberg G., Tanzi R., Wasco W., Lannfelt L., Selkoe D., Younkin S. (1996). Secreted amyloid β -protein similar to that in the senile plaques of Alzheimer's disease is increased in vivo by the presenilin 1 and 2 and APP mutations linked to familial Alzheimer's disease. *Nat. Med.* 2, 864-870.

Schlessinger A.R., Cowan W.M., Swanson L.W. (1978). The time of origin of neurons in Ammon's horn and the associated retrohippocampal fields. *Anat. Embryol. (Berl.)* 154, 153-173.

Schmechel D.E., Saunders A.M., Strittmatter W.J., Crain B.J., Hulette C.M., Joo S.H., Pericak-Vamce M.A., Goldgaber D., Roses A.D. (1993). Increased amyloid β -peptide exposition in cerebral cortex as a consequence of apolipoprotein E genotype in late-onset Alzheimer's disease. *Proc. Natl. Acad. Sci. USA* 90, 9649-9653.

Schröder H., Nyengaard R., Selberis W., Lain E., Keller A., Köhler C., Witter B. Unbiased morphometrical techniques for the quantitative assessment of cells in primary dissociation cultures. In: Quantitative methods in neuroscience - a neuroanatomical approach. Evans, Janson & Nyengaard, editors. Oxford University Press, 2004.

Schütz U. (1999). Klonierung der β 2-Untereinheit des neuronalen nicotinischen Acetylcholin-rezeptors und deren Colokalisation mit der α 7-Untereinheit im Zentralnervensystem der Maus. Thesis, Medical Faculty, University of Cologne.

Seubert P., Mawal-Denwan M., Barbour R., Jakes R., Goedert M., Johnson G.V.W., Liew J.M., Schenk D., Lieberburg I., Trojanowski J.Q., Lee V.M.-Y. (1995). Detection of phosphorylated Ser262 in fetal tau, adult tau, and paired helical filament tau. *J. Biol. Chem.* 270, 18917-18922.

Shafit-Zagardo B., Kalcheva N. (1998). Making sense of the multiple MAP-2 transcripts and their role in neuron. *Mol. Neurobiol.* 16, 149-162.

Shimohama S., Kihara T. (2001). Nicotinic receptor-mediated protection against β -amyloid neurotoxicity. *Biol. Psychiatry* 49, 233-239.

Simons K., Ikonen E. (1997). Functional rafts in cell membranes. *Nature* 387, 569-572.

Sine S.M. (2002). The nicotinic receptor binding domain. *J. Neurobiol.* 53, 431-446.

Small D.H., McLean C.A. (1999). Alzheimer's disease and the amyloid β protein: what is the role of amyloid? *J. Neurochem.* 73, 443-448.

Snyder S.W., Ladror U.S., Wade W.S., Wang G.T., Barret L.W., Matayoshi E.D., Huffaker H.J., Krafft G.A., Holzman T.F. (1994). Amyloid- β aggregation: selective inhibition of aggregation in mixtures of amyloid with different chain lengths. *Biophys. J.* 67, 1216-1228.

- Sommer B. (2002). Alzheimer's disease and the amyloid cascade hypothesis: ten years on. *Curr. Opin. Pharmacol.* 2, 87-92.
- Soto C., Sigurdsson E.M., Morelli L., Kumar R.A., Castano E.M., Frangione B. (1998). β -sheet breaker peptides inhibit fibrillogenesis in a rat brain model of amyloidosis: implications for Alzheimer's therapy. *Nat. Med.* 4, 822-826.
- Soto C., Saborio G.P., Permanne B. (2000). Inhibiting the conversion of soluble amyloid- β peptide into abnormally folded amyloidogenic intermediates: relevance for Alzheimer's disease therapy. *Acta Neurol. Scand.* 176, 90-95.
- Stamer K., Vogel R., Mandelkow E., Mandelkow E.-M. (2002). Tau blocks traffic of organelles, neurofilaments and APP vesicles in neurons and enhances oxidative stress. *J. Cell Biol.* 156, 1051-1063.
- Suzuki N., Cheung T.T., Cai X.D., Odaka A., Otvos L.Jr., Eckman C., Golde T.E., Younkin S.G. (1994). An increased percentage of long amyloid beta-protein secreted by familial amyloid β -protein precursor (beta APP717) mutants. *Science* 264, 1336-1340.
- Takashima A., Noguchi K., Sato K., Hoshino T., Imahori K. (1993). Tau protein kinase I is essential for amyloid β -protein induced neurotoxicity. *Proc. Natl. Acad. Sci. USA* 90, 7789-7793.
- Trinczek B., Ebner A., Mandelkow E.-M., Mandelkow E. (1999). Tau regulates the attachment / detachment but not the speed of motors in microtubule-dependent transport of single vesicles and organelles. *J. Cell Sci.* 112, 2355-2367.
- Trojanowski J.Q., Lee V.M.-Y. (1995). Phosphorylation of paired helical filament tau in Alzheimer's neurofibrillary lesions: focusing on phosphatases. *FASEB J.* 9, 1570-1576.
- Van den Berg C.M., Kazmi Y., Jann M.W. (2000). Cholinesterase inhibitors for the treatment of Alzheimer's disease in the elderly. *Drugs Aging* 16, 123-138.

Ventimiglia R., Jones B.E., Moller A. (1995). A quantitative method for morphometric analysis in neuronal cell culture: unbiased estimation of neuron area and number of branch points. *J. Neurosci. Methods* 57, 63-66

Wang H.-Y., Lee D.H.S., Davis C.B., Shank R.P. (2000). Amyloid peptide A β ₁₋₄₂ binds selectively with picomolar affinity to α 7 nicotinic acetylcholine receptors. *J. Neurochem.* 75, 1155-1161.

Watanabe A., Hasegawa M., Suzuki M., Takio K., Morishima-Kawashima M., Titani K., Arai T., Kosik K.S., Ihara Y. (1993). In vivo phosphorylation sites in fetal and adult tau. *J. Biol. Chem.* 268, 25712-25717.

Wesnes K., Warburton D. (1983). Smoking, nicotine and human performance. *Pharmacol. Ther.* 21, 189-208.

Wevers A., Schröder H. (1999). Nicotinic acetylcholine receptors in Alzheimer's disease. *J. Alzheimers Dis.* 1, 207-219.

Wevers A., Monteggia L., Nowacki S., Bloch W., Schütz U., Lindstrom J., Pereira E.F.R., Eisenberg H., Giacobini E., de Vos R.A.I., Jansen Steur E.N.H., Maelicke A., Albuquerque E.X., Schröder H. (1999). Expression of nicotinic acetylcholine receptor subunits in Alzheimer's disease: histotopographical correlation with amyloid plaques and hyperphosphorylated tau-protein. *Eur. J. Neurosci.* 11, 2551-2565.

Wevers A., Burghaus L., Moser N., Witter B., Steinlein O.K., Schütz U., Achnitz B., Krempel U., Nowacki S., Pilz K., Stoodt J., Lindstrom J., de Vos R.A.I., Jansen Steur E.N.H., Schröder H. (2000). Expression of nicotinic acetylcholine receptors in Alzheimer's disease: postmortem investigations and experimental approaches. *Behav. Brain Res.* 113, 207-215.

Wevers A., Tima W., Nonn M., de Vos R., Jansen Steur E., Lindstrom J., Schröder H. (2001). Colocalization of nicotine receptor proteins with plaques and tangles in Alzheimer's disease. *Soc. Neurosci. Abstr.* 27 No. 487.4.

Whitehouse P.J., Price D.L., Clark A.W., Coyle T.T., DeLong M. (1981). Alzheimer's disease: evidence for a selective loss of cholinergic neurons in the nucleus basalis. *Ann. Neurol.* 10, 122-126.

Whitehouse P.J., Martino A.M., Wagster M.V., Price D.L., Mayeux R., Atack J.R., Kellar K.J. (1988). Reductions in [³H]nicotinic acetylcholine binding in Alzheimer's disease and Parkinson's disease: an autoradiographic study. *Neurology* 38, 720-723.

Wiebringhaus T., Wirak D., Altman R., Cahill K., Duff K., Ruhland M., Boess F., König G., Baumann K. (2000). The effect of presenilin on β -amyloid in knock-in mice carrying the human amyloid precursor protein with Swedish and/or London mutation. *Neurobiol. Aging* 21, S224, 1018.

Wiechelmann K.J., Braun R.D., Fitzpatrick J.D. (1988). Investigation of the bicinchoninic acid protein assay: identification of the groups responsible for the color formation. *Anal. Biochem.* 175, 231-233.

Wolozin B.L., Pruchnicki A., Dickinson D.W., Davies P. (1986). A neuronal antigen in the brains of Alzheimer patients. *Science* 232, 648-650.

Wonnacott S. (1997). Presynaptic nicotinic ACh receptors. *Trends Neurosci.* 20, 92-98.

Wolf N.J. (1991). Cholinergic systems in mammalian brain and spinal cord. *Prog. Neurobiol.* 37, 475-524.

Yankner B.A., Duffy L.K., Kirschner D.A. (1990). Neurotrophic and neurotoxic effects of amyloid β protein: reversal by tachykinin neuropeptides. *Science* 250, 279-282.

Zarei M.M., Radcliffe K.A., Chen D., Patrick J.W., Dani J.A. (1999). Distributions of nicotinic acetylcholine receptor $\alpha 7$ and $\beta 2$ subunits on cultured hippocampal neurons. *Neurosci.* 88, 755-764.

ACKNOWLEDGEMENTS

The present work was done at the Institute II of Anatomy, Neuroanatomy, of the University of Cologne and supported by the Deutsche Forschungsgemeinschaft (Sch 283/18-3,18-4) and Frau Maria Pesch Stiftung.

I would like to thank Prof. Dr. H. Schröder for giving me the possibility of working on this project and for his supervision, Dr. B. Witter for her scientific support during these years, Prof. Dr. S. Waffenschmidt and Prof. Dr. S. Korsching for the valuable scientific suggestions.

I also want to thank Dr. C. Köhler for his help with the stereological tools, Dr. D. Gündisch for her advice in the evaluation of the binding assay results, C. Hoffman for the electron microscopy, Prof. Dr. K. Schomäker and Dr. T. Fischer for allowing the use of the facilities at the Department of Nuclear Medicine and for their suggestions, Dr. B. Penke for providing the A β ₃₁₋₃₄ peptide, Dr. P. Seubert for the gift of the 12E8 antibody, Dr. A. Delacourte for the AD2 antibody and Dr. J. Lindstrom for the mAb 306.

A big thank also goes to Maja Dinekov for precious technical advice.

ERKLÄRUNG

Ich versichere, dass ich die von mir vorgelegte Dissertation selbständig angefertigt habe, die benutzten Quellen und Hilfsmittel vollständig angegeben und die Stellen der Arbeit - einschließlich Tabellen, Karten und Abbildungen -, die anderen Werken im Wortlaut oder dem Sinn nach entnommen sind, in jedem Einzelfall als Entlehnung kenntlich gemacht habe; dass diese Dissertation noch keiner anderen Fakultät oder Universität zur Prüfung vorgelegen hat; dass sie - abgesehen von unten angegebenen Teilpublikationen - noch nicht veröffentlicht worden ist sowie, dass ich eine solche Veröffentlichung vor Abschluss des Promotionsverfahren nicht vornehmen werde. Die Bestimmungen dieser Promotionsordnung sind mir bekannt. Die von mir vorgelegte Dissertation ist von Prof. Dr. Hannsjörg Schröder betreut worden.

CURRICULUM VITAE

Name	Enzo Lain	
Date and place of birth	21 October 1973, Vicenza (ITA)	
Nationality	Italian	
1979 - 1984	Primary school "G. Zanella" in Trissino, Vicenza (ITA)	
1984 - 1987	Secondary school "A. Fogazzaro" in Trissino, Vicenza (ITA)	
1987 - 1992	High school "V.E.M. Marzotto" in Valdagno, Vicenza (ITA) Diploma (Maturità) in Industrial Chemistry	
1993 - 1999	University of Padua (ITA) Degree in Pharmaceutical Chemistry and Technology	
2000 - 2004	Scientific co-worker at the Institute II of Anatomy - Neuroanatomy - University of Cologne (group of Prof. Dr. H. Schröder) Enrolled in a Ph.D. program of the Faculty of Sciences, University of Cologne, since 2002	